The Spatiotemporal Dynamics of Neural Activity in the Neocortex during Waking and Sleep in Mice

Nanyi Cui

Linacre College

University of Oxford

Michaelmas 2017

Thesis submitted for the degree of

Doctor of Philosophy

The Spatiotemporal Dynamics of Neural Activity in the Neocortex during Waking and Sleep in Mice

Nanyi Cui, Linacre College

Michaelmas 2017

Abstract

Sleep is a non-homogenous physiological and behavioural state, which is regulated at many distinct levels, some of which are the focus of this project. The first objective of this project was to investigate cortical EEG dynamics at vigilance state transitions. The experiments have been carried out in adult male C57BL/6 mice, implanted with EEG screws and electromyography (EMG) wires. The main novel finding was that following REM sleep episodes, cortical activity during the initial NREM sleep was desynchronised as compared to NREM sleep episodes following waking. This was manifested in reduced number and amplitude of EEG slow waves and increased incidence of isolated slow waves. The second objective was to investigate how spatiotemporal dynamics of cortical activity during waking and sleep is affected by ongoing behaviour and preceding experience. In these experiments, animals, implanted with EEG electrodes and micro-wire arrays for recording neuronal activity, were recorded during running on a wheel and during subsequent sleep. The result revealed that voluntary wheel running in free-moving mice is associated with a substantial reduction in firing rates among large subpopulation of cortical neurons. The third objective was to address circuit mechanisms of specific brain oscillations in sleep and waking, and their relevance for normal behaviour and disease. Experiments have been carried out in Blind-drunk mice (point mutation in *Snap-25* gene), which are a newly established mouse model relevant for schizophrenia. The results confirmed previous findings of a circadian phenotype in Blind-drunk mice, and for the first time characterised their sleep electrophysiology. In conclusion, this work provides novel insights into the effects of preceding behaviour, state and specific waking experience on spatiotemporal dynamics of cortical activity during sleep. Understanding spatio-temporal dynamics of brain activity during sleep is essential for elucidating the mechanisms of sleep regulation and the role of sleep in health and pathology. (word count: ~ 28000)

Acknowledgements

I would like to express deep gratitude to my supervisors, Dr Vlad V. Vyazovskiy and Dr Peter Oliver, for providing me the opportunity to take on this project, and for their patience, guidance and kind support throughout my DPhil study. I am grateful for the great help from Dr Louise Upton, Dr Ed Mann and Dr Dennis Kaetzel when I was first setting up my experiments. I was very fortunate to have worked with great colleagues in our lab, Laura McKillop, Dr Simon Fisher, Dr Tomoko Yamagata and Mathilde Guillaumin, without whose help I could not complete my project. I also thank Ms Sarah Noujaim for her continuous support. Finally, I thank my family for always being supportive.

Declaration

The results of Chapter 3 were published as "Cui, N., McKillop, L. E., Fisher, S. P., Oliver, P. L. & Vyazovskiy, V. V. Long-term history and immediate preceding state affect EEG slow wave characteristics at NREM sleep onset in C57BL/6 mice. *Arch. Ital. Biol.* **152**, 156–168 (2014)". The results of Chapter 4 were published as part of "Fisher, S. P. *et al*. Stereotypic wheel running decreases cortical activity in mice. *Nat. Commun.* **7**, 13138 (2016)" that I co-first authored with Dr Fisher, and the published results are included in this thesis with Dr Fisher's and Dr Vyazovskiy's agreement. Published materials included in parts of this thesis were authored and produced by myself. Mice (Bdr mutants and wild-type littermates) used in Chapter 5 were provided by Dr Peter Oliver.

Contents list

CHAPTER 1: GENERAL INTRODUCTION ..... - 5 -

1.1 Electrophysiological Characteristics of Sleep and Wakefulness ..... - 5 -

1.1.1 Electroencephalography, Electrooculography and Electromyography, and their significance in defining vigilance states ..... - 5 -

1.1.2 Slow Oscillations ..... - 6 -

1.1.3 Slow Waves ..... - 10 -

1.1.4 Theta Waves ..... - 11 -

1.2 Neuromodulation of Cortical States ..... - 13 -

1.3 Sleep Homeostasis ..... - 17 -

1.4 Aims of this Thesis ..... - 20 -

CHAPTER 2: MATERIALS AND METHODS ..... - 21 -

2.1 Animals and Recording Conditions ..... - 21 -

2.2 Surgical Procedures ..... - 22 -

2.2.1 Implantation of EEG Screws in Cortex ..... - 22 -

2.2.2 Implantation of Multi-wire Arrays in Cortex ..... - 23 -

2.3 Signal Acquisition – Sampling and Online Filtering ..... - 24 -

2.4 Sleep Deprivation Methods ..... - 24 -

2.5 Histology ..... - 25 -

2.6 Pre-processing Acquired Data ..... - 26 -

2.6.1 Resampling and Offline Filtering ..... - 26 -

2.6.2 Scoring EEG Recordings ..... - 26 -

2.6.3 Spikesorting ..... - 27 -

2.7 Detection of slow waves and OFF periods ..... - 29 -

2.8 Statistical analysis ..... - 30 -

CHAPTER 3: CORTICAL DYNAMICS AT STATE TRANSITIONS: EFFECTS OF PRECEDING HISTORY ..... - 32 -

3.1 Introduction ..... - 32 -

3.2 Methods ..... - 35 -

3.3 Results ..... - 36 -

3.3.1 Sleep-Wake Distribution and the EEG Spectral Analysis ..... - 36 -

3.3.2 Effects of Time of Day on Slow Waves ..... - 38 -

3.3.3 Immediate Preceding History Affects the Dynamics of Slow Waves ..... - 42 -

3.4 Discussion ..... - 46 -

CHAPTER 4: EFFECTS OF SPECIFIC WAKING BEHAVIOUR ON CORTICAL ACTIVITY..... - 50 -

4.1 Introduction ..... - 50 -
4.2 Methods ..... - 52 -
4.3 Results ..... - 55 -
4.3.1 Cortical RUN on and RUN off neurons during spontaneous wheel running ..... - 55 -
4.3.2 Stereotypic running decreases cortical firing rates ..... - 62 -
4.3.3 Running prevents wake-dependent increases in firing rates ..... - 72 -
4.4 Discussion ..... - 75 -

CHAPTER 5: CIRCUIT MECHANISMS OF BRAIN OSCILLATIONS IN SLEEP AND WAKING AND RELEVANCE TO DISEASE ..... - 79 -

5.1 Introduction ..... - 79 -
5.2 Methods ..... - 86 -
5.3 Results ..... - 88 -
5.3.1 24-hour sleep/wake distribution and EEG spectral analysis ..... - 88 -
5.3.2 Characterising 'Burst' activity ..... - 94 -
5.3.3 Sleep Deprivation experiments on Bdr/+ and wild-type mice ..... - 97 -
5.4 Discussion ..... - 101 -

CHAPTER 6: GENERAL DISCUSSION AND CONCLUSION ..... - 111 -

6.1 Summary of Findings ..... - 111 -
6.2 Concluding Remarks ..... - 116 -

REFERENCES ..... - 119 -

Chapter 1: General Introduction

1.1 Electrophysiological Characteristics of Sleep and Wakefulness

1.1.1 Electroencephalography, Electrooculography and Electromyography, and their significance in defining vigilance states

Electroencephalography (EEG) is an electrophysiological monitoring method to record electrical activity of the cortex. Voltage readings are taken by placing electrodes on the scalp, or placed epidurally, with respect to a reference electrode least physiologically related to the recording electrodes. Fluctuations in EEG recordings, and in Local Field Potential (LFP) recorded with much smaller electrodes in the brain, are the result of net changes in the extracellular field potential, that all transmembrane currents contribute to. Neuronal activities that mediate transmembrane movement of cations and anions include synaptic activities which entails neurotransmitters acting on excitatory and inhibitory receptors respectively (Buzsaki, Anastassiou, and Koch 2012). Electrooculography (EOG) and Electromyography (EMG) are both measurements of the electrical signals produced by muscle activities of eye and body respectively.

Historically, vigilance states were defined based on observations of animal behavioural state and arousal threshold. In 1875 Richard Caton, a physician in Liverpool, presented findings about electrical phenomena of exposed cerebral hemispheres of rabbits and monkeys (Caton 1875), which marked the beginning of EEG studies in living animals. Fast forward 60 years, in 1937, Alfred Lee Loomis et al. described and separated different EEG features into five levels, representing the spectrum from wakefulness to deep sleep (Davis et al. 1937). In 1953, Aserinsky and Kleitman described Rapid Eye Movement sleep

(REMs) by studying details of human adults' EMG, EOG and EEG (Aserinsky and Kleitman 1953). The *AASM*[1] *Manual for the Scoring of Sleep and Associated Events* was published in 2007 by the AASM Visual Scoring Task Force who revised the scoring system of human at that time adding arousals, respiratory, cardiac, and movement events into consideration. Therefore, reliable determination of vigilance states requires EEG recordings and behavioural context of the recording obtained. Vigilance states can repeatedly transition between wakefulness, NREM sleep and REM sleep. The advance in physiological signals acquisition tools allowed sleep researchers to identify more precisely which vigilance state a brain was in at any given time. I will introduce in the following sections some electrophysiological hallmarks of vigilance states and their relevance to sleep and waking.

1.1.2 Slow Oscillations

Intracellular recordings in the mammalian cortex and other brain regions, such as the thalamus, striatum and the cerebellum, display rhythmic electrophysiological signals characterised by large amplitude and low frequency (< 1 Hz) oscillations (Metherate, Cox, and Ashe 1992; Steriade, Nunez, and Amzica 1993b; Crunelli and Hughes 2010; Halassa et al. 2014; Slezia et al. 2011; Fogerson and Huguenard 2016; Herrera et al. 2016; Sellers et al. 2015; Ros et al. 2009). These neuronal activities are named slow oscillations (SO), and they represent synchronised transitions between active (depolarising UP) states and silent (hyperpolarising DOWN) states. In the cortex, UP states are associated with sustained membrane potential depolarisation in single pyramidal neurons and enhanced firing at the network level, while DOWN states are characterised by membrane hyperpolarisation and

[1] AASM stands for American Academy of Sleep Medicine.

reduced circuit firing (Vyazovskiy et al. 2009; Steriade, Nunez, and Amzica 1993a; Contreras and Steriade 1995). The underlying mechanisms of cortical UP and DOWN state transitions and global slow oscillation remain unanswered and continuously debated. Regarding UP state generation, one school of thought is that slow oscillations can be generated exclusively in the neocortex (Sanchez-Vives and McCormick 2000), therefore UP states are also generated in the cortex. There have been accumulating evidence that cortical layer V is critical in the initiation of UP states. Current source density analysis of slow oscillations indicates a dominant source in deeper cortical layers (Amzica and Steriade 1998a). Multiunit activity recordings in cat neocortex showed UP states are first apparent and most prominently expressed in layer V (Sanchez-Vives and McCormick 2000). It was shown that optogenetic stimulation of subpopulation of layer V pyramidal neurons generated and maintained network UP states, also interestingly optogenetic inhibition of same types of layer V neurons attenuated spontaneous activity *in vivo* (Beltramo et al. 2013). Moreover, the same authors showed in contrast that light activation and inhibition of layer II/III pyramidal neurons had modest effects on spontaneous slow activity (Beltramo et al. 2013). Extending from layer specificity, a subset of in layer V intrinsically bursting (~0.2 – 2 Hz) pyramidal neurons were reported to drive network slow oscillations in a 'pacemaker' fashion while being resistant to excitatory or inhibitory inputs (Lorincz et al. 2015). Another school of thought is that UP state initiation relies on stochastic, spike-independent transmitter release, based on indirect evidence from intracellular recordings during slow oscillation (Chauvette, Volgushev, and Timofeev 2010a). In this scenario, spontaneous action potential-independent excitatory synaptic potentials (i.e. miniature EPSPs (Fatt and Katz 1952)) temporally summate in a critical number of layer V pyramidal neurons,

sufficient to driving these neurons to spike. These few depolarised neurons are then enough to tip the cortical network towards UP state (Neske 2016).

Evidence for a few mechanisms underlying UP to DOWN state transition have been found, and they point to either activity-dependent hyperpolarising conductances or enhanced activity of inhibitory interneurons (or synaptic depression of excitatory synapses) towards the end of the UP state. The concept of activity-dependent K^+ conductances playing a role in UP state termination originated from Steriade et al. who first characterised slow oscillation, and stemmed from the observation of long-lasting afterhyperpolarisations (AHPs) in pyramidal neurons following UP states (Steriade, Nunez, and Amzica 1993b). In the follow-up experiment, Steriade et al. showed that by stimulating brainstem nuclei originating cholinergic projections to cortex UP-DOWN transitions were abolished (Steriade, Amzica, and Nunez 1993). This result suggested Ca^{2+}-dependent K+ (KCa^{2+}) conductances play an important role in UP state termination since the KCa^{2+} channels are blocked by acetylcholine via muscarinic receptors, which is one of many effects acetylecholine has including inhibiting other K channels. Similar functionality of voltage-dependent K_{NA} conductances in UP state termination has been suggested since these conductances cause activity-dependent slow AHPs in cortical neurons, which are also blocked by acetylcholine (Sanchez-Vives, Nowak, and McCormick 2000). Furthermore, activation of activity-dependent K^+ conductances during UP states in the pyramidal neurons would decrease their excitability and firing rates, and result in average disfacilitation in the cortical network that leads to UP state termination. Disfacilitation can also result from short-term synaptic depression (Thomson and Deuchars 1994), and the causal relationship between synaptic depression and disfacilitation was strengthened by the observation that input resistance of neurons during slow oscillation was lowest at UP

state initiation and highest at UP state termination (Contreras, Timofeev, and Steriade 1996). The role of inhibitory inputs in UP state termination has been studied too, and although it has been suggested that both excitatory and inhibitory synaptic inputs decrease during the UP state (Shu, Hasenstaub, and McCormick 2003) indicating less of a role by inhibition, specific inhibitory receptors have been shown to play different roles. By blocking $GABA_A$ and $GABA_B$ receptors separately, it was posited that $GABA_B$ receptor-mediated inhibition could synaptically control UP-DOWN state transition across cortical circuits synchronously, and $GABA_A$ receptor-mediated inhibition control the duration and spike rate and synchrony of UP state (Mann, Kohl, and Paulsen 2009).

The role of thalamus in regulating cortical slow oscillation has been emphasised after slow oscillation's first descriptions. Steriade et al., after observing phasic burst-firing of thalamocortical neurons at the onset of UP state that preceded cortical neuronal firing by a few tens of miliseconds, proposed that thalamocortical neurons could regulate UP state initiation and play a role in slow oscillation synchronisation (Contreras and Steriade 1995; Amzica and Steriade 1995). In a recent thalamectomy study, where cortical slow oscillation was continuously recorded before and after thalamic lesion, the authors found that in the first 12 hours after lesion slow oscillation frequency remained significantly lower than 30 hours after lesion when slow oscillation frequency was comparable to pre-lesion state (Lemieux et al. 2014). This result shows that thalamus is important in the full expression of slow oscillation. The hippocampus has also been shown to be involved during cortical slow oscillation. Specifically, hippocampal CA1 neurons' spiking activity was increased during medial entorhinal cortical (layer III) slow oscillation, which was locked to neocortical slow oscillation with a short delay (Hahn et al. 2012).

1.1.3 Slow Waves

EEG slow waves, or cortical delta waves (0.5 – 4 Hz), are the main phenomenon of deep non-rapid eye movement (NREM) sleep, or slow-wave sleep (SWS). In contrast to low-voltage, fast frequency EEG observed during wakefulness, EEG slow waves of NREM sleep shows high-voltage and low-frequency characteristics. Cortical slow waves reflect the interaction of distinct neural activities within corticothalamic network, and at the EEG level take the shape of polymorphic waves. Within the delta frequency band, there are three distinct neuronal oscillations in terms of their sites of genesis and their electrophysiology. Slow oscillations, as previously introduced, for one contribute to the polymorphic slow waves. Secondly, intrinsic delta oscillations in cortical neurons can arise during the depolarising component of slow oscillation (Amzica and Steriade 1998b). Thirdly, thalamocortical neurons have the ability to generate a clock-like oscillation in the 1-4 Hz frequency range, the mechanism of which relies on the interplay between the low-threshold transient Ca^{2+} current and the hyperpolarisation-activated cation current (McCormick and Pape 1990; Amzica and Steriade 1998c). As the cortex transitions from waking to sleep, the occurrence of DOWN states in cortical and thalamocortical neurons together gives rise to EEG or LFP slow waves. Although the underlying mechanism of how slow waves are mediated among cortical neurons in the intact brain remains elusive, it was suggested that slow waves may arise from change in the excitability of a neuronal network (Vyazovskiy and Harris 2013). It was hypothesised that after a period of sustained UP states, a build-up of synaptic depression and intrinsic hyperpolarisation reduce network excitability to stop recurrent synaptic activity and to allow for cellular maintenance. Due to the extensive recurrent circuitry of the cortex, this requires the local population to enter OFF periods synchronously, manifesting the electroencephalographical slow waves. EEG

slow waves is widely believed to be the most important index to quantify homeostatic sleep propensity. Changes in the prevalence and amplitude of EEG slow waves quantified by Fourier transform as EEG delta power, also called slow wave activity (SWA), reliably follow the sleep-wake distribution (Tobler and Borbely 1986; Dijk et al. 1987). At the beginning of NREM sleep, SWA is high, and decreases with the duration of time spent asleep. The declining trend of SWA during NREM sleep is thought to reflect the homeostatic decline of sleep propensity. Following an extended episode of wakefulness, SWA in the subsequent NREM sleep is high, and the amplitude of SWA depends on the duration of prior wakefulness (Achermann and Borbely 2003).

1.1.4 Theta Waves

Theta waves (4 – 9 Hz) are low-amplitude rhythmic patterns of neural activity most commonly observed in the hippocampus, the neocortex and entorhinal cortex. In REM sleep, cortical theta activity is more synchronised than in certain waking behaviours (such as exploration, active task performance and quiet wakefulness), and is accompanied with total loss of postural muscle tone. The muscle atonia during REM sleep was shown to require both $GABA_A$ and $GABA_B$ mediated inhibition of motoneurons (Peever 2011), and muscle atonia was triggered by cholinergic activation in the pontine reticular formation (Mitler and Dement 1974). However, the eye movements during REM sleep are proposed to be controlled under a different mechanism that involves the abducens, the lateral geniculate nucleus and oculomotor system. Cholinergic activation by microinjections of carbachol in the caudal pons was shown to induce oculomotor phenomena similar to eye movements during REM sleep (Marquez-Ruiz and Escudero 2010). The desynchronised EEG pattern occurring during REM sleep is represented by the time course of relative amplitude

values of higher frequencies (5 – 16 Hz) that oscillate reciprocally with SWA. Cortical theta activity during REM sleep is thought to be strongly linked to hippocampal theta activity (Sirota et al. 2008). In the same study, multisite recordings from the cortex and hippocampus in anaesthetised rats showed that theta activities from those regions co-varied in both frequency and magnitude. Furthermore, Sirota and colleagues demonstrated that the magnitude of cortical theta power is correlated with the anatomical distance from the hippocampus suggesting that theta activity in the neocortex is dominated by currents that are volume-conducted from the hippocampus. On the other hand, neocortical generation of theta oscillations was also implicated in human EEG studies during cognitive tasks, where changes in cortical theta activity was closely related to the timing of task events (Caplan et al. 2003; Kahana et al. 1999). Additionally, it was reported that prefrontal cortical theta activity was different in frequency from hippocampal theta activity (Siapas, Lubenov, and Wilson 2005), and various *in vitro* studies showed neocortical slices under pharmacological manipulations can exhibit theta-frequency oscillations (Silva, Amitai, and Connors 1991; Bao and Wu 2003). It is difficult to disintegrate locally generated cortical theta activity from volume-conducted hippocampal theta activity when both are oscillating at same frequency. Current source density studies have indicated entorhinal cortex afferents drive theta-related firing in hippocampus CA1 (Brankack, Stewart, and Fox 1993), and have also showed highly layer specific theta phase and coherence in the hippocampus which suggest that many hippocampal layers generate theta current dipoles (Montgomery, Betancur, and Buzsáki 2009). An *in vitro* current source density analysis in rat neocortical slices under pharmacological conditions revealed large-amplitude current sinks and sources in layers II/III and layer V, respectively (Lukatch and MacIver 1997). However, this study cannot answer the crucial question of whether there are neocortically

generated theta rhythms, and no direct evidence for or against this question has been found yet. Extensive research has been trying to understand hippocampo-neocortical theta coupling, and what are the potential mechanisms which facilitate theta coupling. The first model posited that there is an independent pacemaker that orchestrate theta oscillation coupling, possibly in the septal complex (Petsche and Stumpf 1962), and/or in basal forebrain (Lee et al. 2005). The second proposed mechanism for theta coupling entails the utilisation of the entorhinal cortex and the prefrontal cortex by way of their widespread reciprocal connections with various neocortical regions (Groenewegen and Uylings 2000; Thierry et al. 2000). The third possibility is that the class of sparse long-range hippocampal projections to distant neocortical regions brings about hippocamo-neocortical coordination (Cenquizca and Swanson 2007; Jones and Wilson 2005). Thus, theta oscillations in the neocortex may arise locally and/or phase-synchronise with hippocampus via the above three pathways.

1.2 Neuromodulation of Cortical States

The brain switches between waking and sleep to facilitate different functions associated with each state. For example, learning and memory are putative brain functions associated with slow wave sleep (Marshall et al. 2006; Vyazovskiy et al. 2011), while selective attention and sensory information processing are associated with wakefulness (Harris and Thiele 2011). Several key subcortical regions are known to be necessary and sufficient to enable global state switching (see Illus. 1). From brainstem, the ascending reticular activating system projects to the thalamus, hypothalamus and basal forebrain which are important for maintaining wakefulness (Moruzzi and Magoun 1949; Jones and

Yang 1985). The ascending activating system consists of locus coeruleus (noradrenergic), dorsal raphe nucleus (serotonergic), and tuberomammillary nucleus (histaminergic). Optogenetic stimulation of the noradrenergic neurons in locus coeruleus has been shown to cause an immediate transition from sleep to wakefulness (Carter et al. 2010). Antihistamine drugs are known to promote sleep, and lesion of the histamine neurons induces hypersomnia (Monti 1993). Serotonin receptor agonists enhance wakefulness, whereas serotonin receptor antagonists increase sleep (Dugovic, Wauquier, and Janssen 1989). The cholinergic neurons in the brainstem are located in the pedunculopontine tegmental and lateral dorsal tegmental nuclei, and they project extensively to the thalamus, hypothalamus, and basal forebrain (Steriade et al. 1988; Jones and Cuello 1989). These cholinergic neurons fire at higher rates during wakefulness (Steriade et al. 1990). Another crucial subcortical structure involved in brain state regulation is the lateral hypothalamus, which contains orexin/hypocretin neurons. Orexin neurons have high activity during wakefulness and low activity during sleep (Lee, Hassani, and Jones 2005; Mileykovskiy, Kiyashchenko, and Siegel 2005). Optogenetic stimulation of orexin neurons has also been demonstrated to induce wakefulness (Adamantidis et al. 2007). Cholinergic neurons in the basal forebrain have similar functions as in the brainstem, and provide main source of cholinergic input to cortex (Zaborszky et al. 1999). Ventrolateral preoptic area contains sleep-promoting GABAergic neurons, and they are more active during sleep than wakefulness (Sherin et al. 1996). GABAergic neurons innervate cortex along with the basal forebrain (Henny and Jones 2008), and project to hypothalamus and brainstem (Gritti, Mainville, and Jones 1994). Therefore, the long-range connections between ventrolateral preoptic area and the ascending arousal system form a reciprocal inhibition, and together with the mutual inhibition between GABAergic and cholinergic neurons within forebrain

and preoptic area, act as a sleep-wake switch (Lee and Dan 2012). It is believed that the thalamus serves as a major gateway through which the neuromodulatory inputs regulate cortical function. Thalamic neurons are highly connected with cortical neurons. Furthermore, the prefrontal cortical neurons provide strong descending inputs to the neuromodulatory circuits in the basal forebrain (Golmayo, Nunez, and Zaborszky 2003) and brainstem (Jodo and Aston-Jones 1997). Thus, global state transition could be mediated by the activation of thalamic neurons or neuromodulatory circuits. Lastly, the suprachiasmatic nucleus (SCN) in the hypothalamus tightly controls sleep in synchronisation with the circadian rhythms by receiving inputs from the optic nerves (Mistlberger 2005).

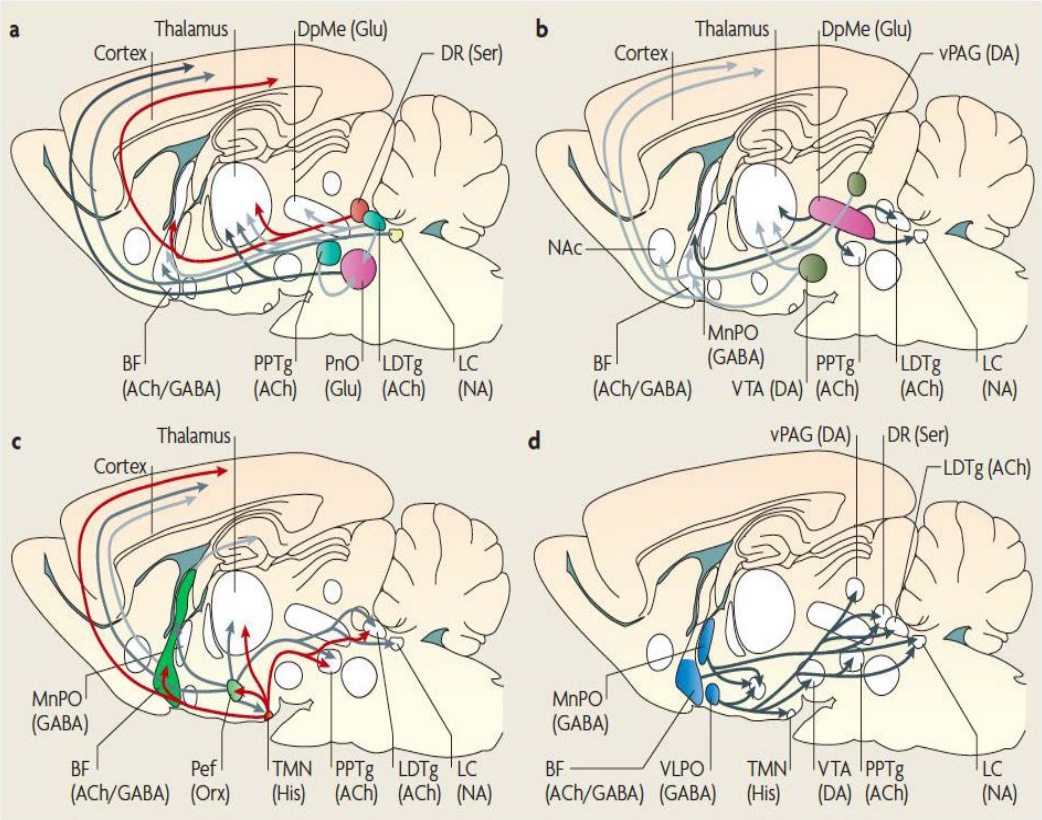


Illustration 1, parasagittal section of rat brain. ***a****. shows arousal nuclei in the pons.* ***b****. shows arousal nuclei in the midbrain.* ***c****. shows arousal nuclei in the hypothalamus and basal*

*forebrain. **d**. shows sleep-promoting pathways. Adopted from Franks NP, Nature Review Neuroscience, 2008 (Franks 2008)*

Taken the vast topographical organisational of projections from arousal centres to the cortex, it is possible to hypothesise if the locality aspect of sleep emergence arises from the specificity of topographical organisation of projections from arousal centres. Despite the proposed uniform physiologic effects throughout the brain of the abovementioned arousal centres, evidence have shown heterogeneity in the target projection locations from subgroups of the arousal centres. For example, in rats, subgroups of locus coeruleus were shown to project to orbitofrontal, medial prefrontal, anterior cingulate and motor cortices using retrograde tracers, and these subgroups of LC cells innervating specific sub-regions of the prefrontal cortex are electrophysiologically distinct from those terminating in motor cortex (Chandler, Gao, and Waterhouse 2014). Using genetic fate mapping tool, different subgroups of serotonin neurons were shown to innervate individual target area in the forebrain, e.g. prefrontal and parietal cortices with fine (< 1 μm in diameter) varicosities (Bang et al. 2012). As stated in the previous paragraph, although basal forebrain is one of the main pathways through which the cholinergic, serotonergic and noradrenergic projections pass together, Zaborszky et al. have revealed that the extent of overlap between basal forebrain populations projection to specific frontal and posterior cortical targets depends on the strength of intracortical projections (Zaborszky et al. 2015). It has been established that cortically projecting neurons from the basal forebrain comprise cholinergic, GABAergic, and glutamatergic neurons, and these subtypes of neurons could affect specific cortical cell populations in a complex manner (Hassani et al. 2009). Although more evidence is needed to test the relationship between the topographical organisation

of projections from arousal centres and local slow wave emergence, at this stage current knowledge at least suggests that this hypothesis is worth investigating.

1.3 Sleep Homeostasis

The concept of homeostasis was first introduced, by Claude Bernard, as the property of a system to maintain its internal environment stable and constant allowing an organism to function optimally over a range of environmental conditions. Homeostatic regulation is composed of three essential parts: a sensor that measures the control variable, an integrator that compares the measure to a set point and an effector that renormalizes the variable from deviated level. The same concept can be applied to sleep, except we are still not certain what functions sleep fulfils, what the 'integrator' is, how 'sensor' measures sleep, nor what the 'set point' is. However, researchers have identified one of the variables, i.e. slow wave activity, which reliably model sleep-wake distribution. Homeostatic sleep pressure, or sleep propensity, accumulates during wakefulness and decreases during sleep. This is reflected by the effects of spontaneous waking episode durations (Franken, Chollet, and Tafti 2001), and by performing sleep deprivation studies (Vienne et al. 2010). Most of the variance in EEG delta power can be attributed to sleep-wake distribution, suggesting that SWA as a homeostatically controlled variable related to NREM sleep. Not only EEG delta power but also NREM sleep duration is likely to be homeostatically regulated, as NREM sleep duration tends to increase after extended period of wakefulness. However, sleep duration depends upon homeostatic control as well as circadian phase. As proposed in the Two-Process model, the circadian rhythm is the other main factor that determines sleep-wake distribution (Borbely 1982; Daan, Beersma, and Borbely 1984). As previously

introduced, SCN in the hypothalamus tightly controls sleep-wake behaviour in accordance with circadian rhythm. The SCN, considered to be the 'master clock' in the brain, receives input from the optic nerves which provides information about circadian time to SCN. The received time information is then processed to aid the underlying intrinsically timed clock genes *period* (*per*) and *cryptochrome* (*cry*) expression for time adjustments in the SCN (Nakamura et al. 2008). Per and Cry protein syntheses are activated by BMAL1/CLOCK dimers, but Per and Cry proteins themselves inhibit BMAL1/CLOCK activity, forming an intracellular transcription-translation feedback loop with a roughly 24-hour periodicity (Takahashi et al. 2008). The interaction between homeostatic and circadian processes closely model the duration, the quality and the quantity of sleep, and allows for alertness through the day when sleep need is increasing and for sleep through the night when sleep need is decreasing. The question of what the underlying cellular pathways or network mechanisms are that regulate sleep homeostasis remains elusive.

There are cumulative evidence suggesting that sleep can be initiated in a local use-dependent manner (Aton et al. 2009; Krueger et al. 2008; Tononi and Cirelli 2006; Vyazovskiy et al. 2011). It was argued that an inherent fundamental premise of sleep regulatory circuitry is the sole regulator, and that neuromodulatory circuits impose sleep on the brain, therefore sleep is initiated by these circuits (Krueger 2012). The sleep regulatory circuit paradigm lacks the explanation for the mechanisms underlying impaired performance associated with prolonged wakefulness, sleep inertia and sleep need. In contrast, the local use-dependent sleep theory addresses these issues to the extent that it is easy to envisage how deficits could arise if local areas of the brain were asleep while other areas were awake (Krueger et al. 2008; Vyazovskiy et al. 2011). An unresolved question is how processes occurring at cellular level, such as UP and DOWN states can be

reconciled with the phenomena occurring at the level of the whole brain, for instance the global slow waves, and the disconnection with the outside world. It was hypothesized that global sleep state facilitates the occurrence of OFF periods, a transient network silence among neuronal assembly, at the level of single cells that could make the process of cellular maintenance during periods of reduced synaptic input more efficient (Vyazovskiy and Harris 2013). It was found that across sleep period, initially global slow wave oscillations, typical for early sleep, gradually break down into sparsely distributed local slow waves (Vyazovskiy and Tobler 2005). This notion supported the theory in that as neurons obtain necessary rest they resume firing, and progressively smaller neuronal population engage in locally synchronised DOWN states only. In other words, global OFF periods, typical for early deep sleep, seem to be much more efficient in providing favourable conditions for cellular rest.

1.4 Aims of this Thesis

1.4.1 To investigate cortical dynamics at state transitions: effects of long-term and immediate preceding history. When NREM sleep episodes terminate, the brain transitions either into wake or REM sleep. The NREM-REM-NREM sleep cycle repeats itself several times before waking up. What is the dynamics of slow waves within each NREM sleep episode at these state transitions at local and global scale? To address this, I examined the spatiotemporal dynamics of EEG slow waves in NREM sleep from two cortical derivations, frontal and occipital regions) in adult male C57BL/6 mice.

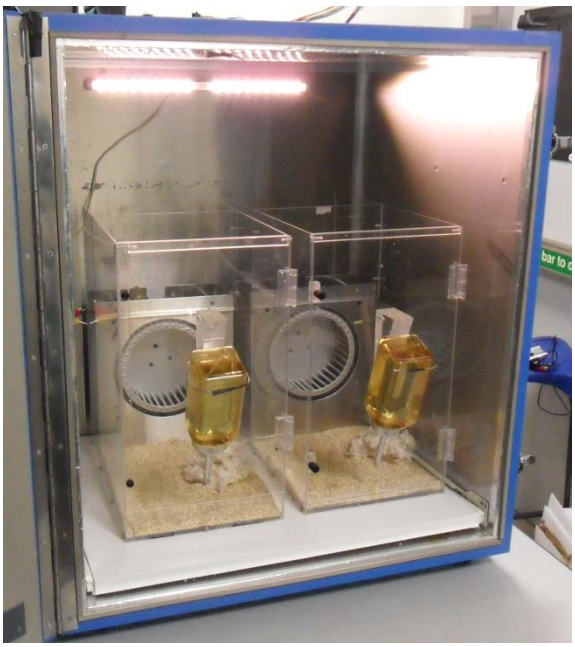
1.4.2 To investigate local spatiotemporal dynamics of cortical activity during ongoing behaviour and subsequent sleep. To address this, I investigated effects of wheel running behaviour and sleep deprivation on cortical dynamics in C57BL/6 mice, recording EEG epidurally and multi-unit activity extracellularly in either the motor cortex or the somatosensory cortex *in vivo*.

1.4.3 To investigate and characterise cortical dynamic changes and sleep phenotype of mouse model with synaptic dysfunction, and their relevance to disease. To address this, I examined the Blind-drunk mice, an animal model of Schizophrenia with a point mutation in the SNAP-25 gene resulting in disrupted synaptic activity, and compared their electrophysiological and behavioural phenotypes with wild-type controls.

Chapter 2: Materials and Methods

2.1 Animals and Recording Conditions

The experiments carried out during the course of my DPhil project were performed in adult male C57Bl/6J mice (Harlan UK Ltd, United Kingdom) aged 18 - 30 weeks old and in 18 – 24 weeks old adult mutant Blind-drunk mice (Bdr/+) and their age matched wild-type mice (+/+). During recording sessions, mice were individually housed in custom-made plexiglass cages (20.3 x 32 x 35 cm) with free access to running wheels (Campden Instruments, Loughborough, UK, 20 x 23 cm, wheel diameter 14 cm, bars spaced 1 cm apart) under a 12:12 hour light-dark cycle (lights on 9am). Mice were single housed in sound-attenuated Faraday chambers (Campden Instrument, Loughborough, UK, up to two cages per chamber, shown below) and mice were habituated to both the running wheel and recording cable for a minimum of four days before the recording began. Room temperature and relative humidity were maintained at 20 ± 1 °C and 60 ± 10 %, respectively. Food and water were provided *ad libitum*.



2.2 Surgical Procedures

All procedures were performed in accordance with the Animal (Scientific Procedures) Act 1986 under a UK Home Office Project Licence and were in accordance with Oxford University institutional guidelines.

2.2.1 Implantation of EEG Screws in Cortex

The animals underwent cranial surgery to implant custom made EEG/EMG headmounts, which were composed of stainless steel screw electrodes (shaft diameter 0.86 mm, InterFocus Ltd, Cambridge, UK), soldered to an 8-pin surface mount connector (8415-SM, Pinnacle Technology Inc, Kansas, USA). Surgical procedures were carried out under isoflurane anaesthesia (3 - 5 % for induction, 1 - 2 % for maintenance) using aseptic surgical techniques. Throughout the surgical procedure animals were head fixed using a stereotaxic frame (David Kopf Instruments, California, USA) and Viscotears liquid gel (Alcon Laboratories Limited, Hemel Hempstead, UK) was applied at regular intervals to protect the eyes. An incision was made along the midline of the head and the skull was thoroughly cleaned with 3 % hydrogen peroxide followed by saline. A high-speed drill (carbon burr drill bits, 0.7 mm, InterFocus Ltd, Cambridge, UK) was used to drill holes in the skull and screws were implanted epidurally over the frontal (motor area, M1, anteroposterior (AP) +2 mm, mediolateral (ML) 2 mm) and occipital (visual area, V1, AP -3.5 to 4 mm, ML +2.5 mm) cortical regions. Additional epidural screws were implanted over the cerebellum to act as a reference and contralaterally to the frontal screw to stabilize the head implant. Two single stranded, stainless steel wires were inserted either side of the nuchal muscle to record electromyography (EMG). All screws and the headmount wires were secured using dental cement (Associated Dental Products Ltd, Swindon, UK). Overall, this provided two

EEG channels (frontal vs cerebellum and occipital vs cerebellum) and one EMG channel. All animals were administered saline (100 µl per 20 g body weight, s.c.) and were maintained on thermal support throughout surgery and for the immediate hours following. Analgesics were administered preoperatively (Metacam 1 - 2 mg per 1 kg body weight, s.c., meloxicam, Boehringer Ingelheim Ltd, Bracknell, UK) and also orally together with mashed chow for at least three post-operative days. A minimum of two-week recovery period was permitted prior to cabling the animals for recording.

2.2.2 Implantation of Multi-wire Arrays in Cortex

Animals in which I recorded multi-unit activity (MUA) from underwent similar surgical procedure to that of EEG screws implantation, but with the additional implantation of a single polyimide-insulated tungsten micro-wire array (Tucker-Davis Technologies Inc, Alachua, FL, USA). The arrays consisted of 16 - channels (2 rows each of 8 wires) with properties as follows: wire diameter 33 µm, electrode spacing 250 µm, row separation L - R: 375 µm, tip angle 45 degrees. A 1 x 2 mm craniotomy was made using a high-speed drill (carbon burr drill bits, 0.7 mm, InterFocus Ltd, Cambridge, UK) in the region of interest, with the midpoint of the craniotomy relative to bregma as follows: M1: anteroposterior (AP) +1.5 to 2 mm, mediolateral (ML) 2 mm; somatosensory cortex: AP -1 mm, ML 3.25 mm. The dura was dissected using a 25 gauge needle and saline was applied to the cranial opening to keep the exposed brain moist. In most cases, removal of the dura did not cause bleeding (when bleeding occurred, it was stopped with gelfoam soaked in sterile saline). The electrode array was advanced into the brain until both rows of the array were at the level of cortical layer 5 (M1: 0.7 to 0.8 mm below the pial surface, SCx: 0.5 to 0.6 mm). A two-component silicon gel (KwikSil; World Precision Instruments, FL, USA) was used to seal

the craniotomy and protect the surface of the brain from dental acrylic. After 5 to 10 minutes, required for the gel to polymerise, dental acrylic was applied to fix the array to the skull.

2.3 Signal Acquisition – Sampling and Online Filtering

Data acquisition was performed using the MultiNeurophysiology Recording System (TDT, Alachua FL, USA). EEG, LFP and EMG data were collected at a sampling frequency of 256.9 Hz and amplified (PZ5 NeuroDigitizer pre-amplifier, TDT Alachua FL, USA). MUA data were filtered between frequency range of 300 Hz to 5 kHz, and MUA data are stored at sampling rate of 763 Hz. A manual threshold of -25 μV is set to detect spikes cross below this level, which are then sampled at 25 kHz to store spike waveforms. The spike waveforms stored include 46 samples (0.48ms before and 1.36ms after the threshold crossing), which are then subject to spikesorting. I programmed custom virtual circuits on TDT software platform to accommodate simultaneous recording of two-channel EEG, one-channel EMG, 16-channel LFP, 16-channel MUA signals and one-channel wheel running activity for each animal, up to four animals at any time. I also programmed cross-platform (TDT x visual discrimination task) data acquisition for synchronised recording of electrophysiological signals and digital behavioural task outputs.

2.4 Sleep Deprivation Methods

The following protocols were followed for all sleep deprivation method. After mice recovered from surgery and habituated to the recording cable and home cage, mice were left undisturbed except for daily general inspection to establish Baseline day recording. Baseline day is selected with some criteria: mice are showing entrainment to the circadian

phase reflected from hypnograms and wheel running behaviour, and recorded data are free from artifacts. After a stable Baseline day recording, animals were recorded during six-hour period of continuous wakefulness starting at light onset. During this time, the animals were spontaneously awake and their behaviour as well as their polysomnographic recordings were under constant visual observation. Sleep was prevented by providing the animals regularly with novel objects because this method mimics naturalistic conditions of wakefulness, is effective, ethologically relevant, and does not appear to stress the animals (Palchykova et al. 2006; Tobler and Borbely 1986; Vyazovskiy et al. 2007). All mice were well habituated to the experimenter and to the exposure to the novel objects prior to the experiment. Novel objects included nesting and bedding material from other cages, wooden blocks, small rubber balls, plastic, metallic, wooden, or paper boxes and tubes of different shape and colour. SD was performed in the animal's home cage, where they had access to running wheels.

2.5 Histology

Upon completion of the experiments, mice were injected with pentobarbital (1 – 2 ml) and transcardially perfused with 0.9 % saline followed by 4 % paraformaldehyde solution. Brains were sectioned using a freezing Microtome (Leica, Germany) to produce 50µm coronal slices of the motor cortex. Sections were mounted on slides and subjected to cresyl-violet (Nissl) staining. Microwire arrays were coated with a thin layer of DiI fluorescent dye (DiIC18(3), Invitrogen) to facilitate subsequent localization (Magill et al. 2006).

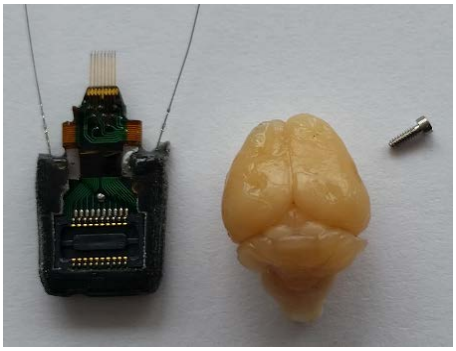


Illustration showing the Multi-wire array (on the left) and EEG screw (on the right), compared to a hardened mouse brain (in the middle) showing vaguely implantation marks.

2.6 Pre-processing Acquired Data

2.6.1 Resampling and Offline Filtering

Data were resampled offline at a sampling rate of 256 Hz. Signal conversion was performed using custom-written Matlab (The MathWorks Inc, Natic, MA, USA) scripts and was then transformed into European Data Format using open source Neurotraces software (www.neurotraces.com). Spike waveform data were collected continuously at sampling frequency of 25 kHz, and LFP signals are computed from recordings from the same electrodes filtered between 0.1 Hz – 300 Hz.

2.6.2 Scoring EEG Recordings

Frontal and occipital EEG continuous recordings were scored offline through visual inspection of consecutive 4-second epochs. The EEG scoring software (SleepSign, Kissei Comtec Co, Nagano, Japan) displays also multi-unit activities recorded by multi-wire arrays, the EMG signals from neck muscles and wheel running activity from a wheel installed in mice's home cages, all in a synchronous manner. Diurnal entrainment was verified by analysis of wheel-running activity over several days to ensure these had fully normalised

prior to commencing experiments. For each mouse, an undisturbed spontaneous 24-hour recording beginning at lights-on was selected for vigilance state and analysis. Vigilance states were classified as waking (low voltage, high frequency EEG with a high level or phasic EMG activity), NREM sleep (presence of slow waves, a signal of a high amplitude and low frequency), REM sleep (low voltage, high frequency EEG with a low level of EMG activity) or Burst (high frequency, high amplitude EEG high-voltage spindle-like). Care was taken to eliminate epochs contaminated by eating, drinking or gross movements resulting in artifacts in at least one of the two EEG derivations or in any of the multi-unit activity channels.

2.6.3 Spikesorting

Online spike sorting was performed primarily to eliminate artifactual waveforms caused by electrical or mechanical noise. This was performed with OpenEx software (TDT), by manually applying an amplitude threshold for online spike detection. Whenever the recorded voltage exceeded this predefined threshold (at least -25 µV), a segment of 46 samples (0.48 ms before, 1.36 ms after the threshold crossing) was extracted and stored for later use, together with the corresponding time stamps. Firstly, an artifacts removal procedure was implemented to eliminate remaining artifactual waveforms and to facilitate subsequent clustering. Typical spurious spike waveforms included waveforms which were likely the result of a combination of several spikes from different neurons occurring concurrently and preventing their reliable classification. After removal of the artifactual spikes, principal components were computed using principal component analysis (PCA) on a segment of the spike waveform between the 5^{th} and the 35^{th} time sample, because this is the segment that contains the initial negative peak after threshold crossing and

subsequent afterhyperpolarisation, and is therefore more informative about the overall spike waveform. In PCA an orthogonal linear transformation of the original data is performed, through singular value decomposition of the data matrix (Jolliffe 2002). After performing PCA, each spike between samples 5 and 35 was thus described by 31 variables, each being a linear combination of the original sampling values. Each PC corresponds to an eigenvalue and an eigenvector from the singular value decomposition of the data matrix. The first PC is associated with the eigenvector on the direction of maximal variance of the dataset, and so on in decreasing order for the remaining PCs. The ratio between each eigenvalue and the sum of all eigenvalues represents the ratio of the total variance described by a single PC.

Clustering was performed based on the k-means algorithm (Hartigan 1975). This is a partitioning method that aims to divide *n* observations into *k* clusters in which each observation belongs to the cluster with the nearest mean, serving as a prototype of the cluster. There are several k-means algorithms available which are based on different ways to proceed through the iterations. I used the k-means function in Matlab, which was implemented according to Lloyd's algorithm (Lloyd 1982). In particular, it chooses *k* initial cluster centres (centroid) through an initialisation step, and then computes point-to-cluster-centroid Euclidean distances of all observations to each centroid. Based on the distance, each observation is assigned to the cluster with the closest centroid. As a next step, the algorithm computes the average of the observations in each cluster to obtain *k* new centroid locations. Finally, it repeats previous steps until cluster assignments do not change, or the maximum number of iterations is reached. This approach requires the user to a priori select the number of clusters. Based on visual inspection, it was found unlikely that more than 5 distinct waveforms were present in the same MUA channel, and

so the procedure has been performed with *k*=2, 3, 4, 5. For each case, several features were extracted within each cluster and were used to validate the quality of clustering and to select the best outcome of the clustering procedure within each animal and recording channel. These were the average spike waveform with standard deviation, inter-spike interval distribution, the time course of peak-to-peak amplitude, the time course of firing rates and the autocorellogram of the corresponding spike trains. All selected clusters were screened and visually classified according to their signal to noise ratio, waveshape of the action potential, stability of the amplitude across time and inter-spike interval (ISI) distribution histogram (criterion for ISI > 2ms). It should be emphasised that based on recording and sorting technique used it cannot be excluded that two or more neurons having identical spike waveform shapes, amplitude and firing properties are present simultaneously on the same channel.

2.7 Detection of slow waves and OFF periods

Individual slow waves were detected and analysed during sleep and wake. Slow waves were detected as previously described in (Vyazovskiy et al. 2011). In NREM sleep, slow waves were detected by band-pass filtering LFP signal between 0.5 – 4 Hz, and in wake between 2 – 6 Hz using inbuilt Matlab function *filtfilt* applying a Chebyshev Type II filter design. Waves in both sleep and wake were detected as positive deflections of filtered signal between two consecutive negative deflections below the zero-crossing points. First, local minima and maxima are calculated using second derivative of the signal. Then, a single slow wave is defined as the signal between two consecutive local minima. The amplitude of a slow wave is the peak-to-trough amplitude of the wave. Only waves with the peak amplitude larger than the median amplitude across all detected waves within the same

vigilance state were included. During sleep, the first rising slope of wave (from the first negative peak to the maximal positive peak) is thought to correspond to the DOWN state of the slow wave oscillations, whereas the second slope (from the maximal positive peak to the second negative peak) roughly corresponds to the UP state (Vyazovskiy et al. 2009) (shown below). Average MUA firing rates triggered by LFP waves were computed as previously described (Destexhe, Contreras, and Steriade 1999; Haider et al. 2006; Ji and Wilson 2007; Vyazovskiy et al. 2009). OFF periods are defined based on LFP and MUA, where spiking activity during a single LFP wave reduces to below 20% of mean of the one-second window centred at the peak of LFP wave.

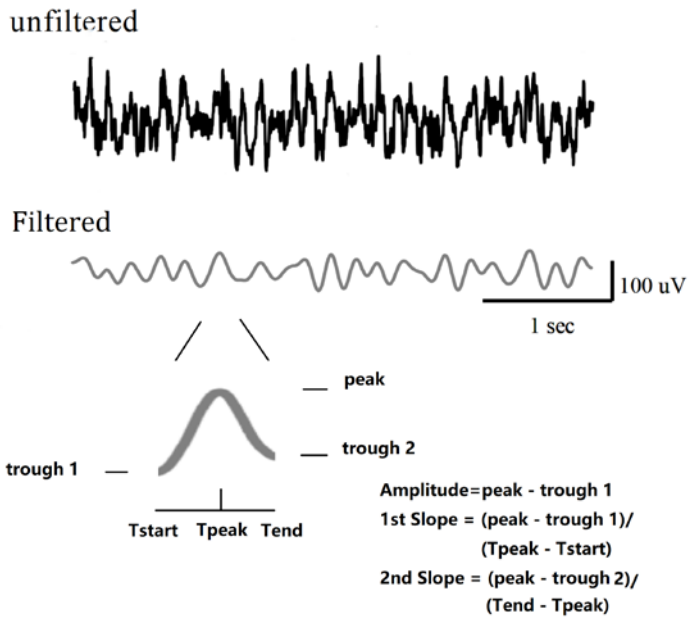


Illustration of how individual slow wave is defined and its parameters calculated.

2.8 Statistical analysis

All statistical analyses were performed in Matlab© (The MathWorks Inc., Natick, Massachusetts, USA) or SigmaPlot© (Systat Software Inc., San Jose, California, USA), and all values reported are mean ± SEM. ANOVAs were used to detect statistically significant

effects for within-subject (e.g. within the same cortical area) comparisons (e.g. running wheel speed or acceleration on firing rates, because running speed or acceleration are discretised rather than continuous). Two-tailed paired t-tests were used for comparisons between two groups (e.g. two cortical regions, day vs night, or sleep vs wake). The assumptions for using ANOVA and two-tailed t-tests are that the variables are normally distributed. In addition, I also employed a normalisation procedure by expressing some of the variables in relative terms (as % of the mean value across all artifact free epochs during the recording period). I have done this in those cases where interindividual variability of absolute values is not relevant for the effects observed, instead relative magnitude of the effects may be useful. Normalisation of values in this manner is a widely used approach and therefore facilitates comparison between studies, where relative values are reported.

Chapter 3: Cortical Dynamics at State Transitions: Effects of Preceding History

3.1 Introduction

Animals spontaneously exhibit a sequence of distinct states of vigilance in their daily behaviour throughout their lifespan (McCarley and Hobson 1975; Fort, Bassetti, and Luppi 2009; Mignot 2008). Sleep is an active and dynamic physiological and behavioural state consisting of interchanging periods of NREM sleep, or slow-wave sleep (SWS), and REM sleep. Similarly, waking is a complex biological process, varying on a timescale of hours to even seconds from the largely dissociated state of drowsy wakefulness to alert attentive vigilance.

The vigilance states of sleep and wakefulness alternate in sequences that are governed by preceding sleep-wake history and the circadian clock (Tobler 2005). Transitions between waking and sleep are heterogeneous and are characterised by varying temporal dynamics and synchronies of brain activity across regions (Buchsbaum et al. 1982; Wright, Badia, and Wauquier 1995; De Gennaro et al. 2001). During the transitioning from waking to sleep, the EEG progressively shifts from low-voltage fast-frequency activity, to a rhythmic synchronised pattern of high amplitude slow wave oscillations in which neurons alternate between active UP states and silent DOWN states (Steriade, Timofeev, and Grenier 2001). Further spatio-temporal complexity of cortical activity during sleep is manifested by regular transitions of NREM to REM sleep and gradual changes in EEG slow wave activity (SWA), a well-established physiological correlate of sleep homeostasis (Achermann et al. 1993). Levels of SWA during sleep are positively correlated to the

duration and intensity of preceding waking and dissipate during ensuing sleep (Tobler and Borbely 1986; Vyazovskiy et al. 2006). Recent studies have suggested that changes in SWA arise from alternations at the level of individual EEG or LFP slow waves. Specifically, under elevated sleep pressure, slow wave characteristics such as the amplitude, incidence and duration change systematically (Mistlberger, Bergmann, and Rechtschaffen 1987; Geering et al. 1993; Vyazovskiy et al. 2009; Hajnik, Toth, and Detari 2013). It has been proposed that an essential determinant of the homeostatic increase in SWA is elevated cortical network synchrony, which is reflected by the slope of individual slow waves (Riedner et al. 2007; Vyazovskiy et al. 2007; Vyazovskiy et al. 2009). One possible mechanism for this is that neuronal synchrony increase as a result of net increase in the strength of cortico-cortical connections during wakefulness, and decreases during sleep (Tononi and Cirelli 2006).

In addition to these temporal changes, there is significant regional specificity of SWA across cortical areas that varies with sleep state and EEG frequency. In humans, this includes a frontal predominance of SWA, evident during baseline (Werth, Achermann, and Borbely 1996) and following sleep deprivation (Rusterholz and Achermann 2011). Similarly in rodents SWA is greater and exhibits faster dynamics in frontal relative to the more posterior regions after sleep deprivation (Schwierin et al. 1999; Huber, Deboer, and Tobler 2000; Vyazovskiy, Borbely, and Tobler 2002). At NREM sleep initiation, SWA and spindle activity increase progressively in humans and rodents (Vyazovskiy, Achermann, et al. 2004; Aeschbach et al. 1996), and pronounced regional differences in the EEG dynamics at sleep onset have been found in humans (De Gennaro et al. 2001; Magnin et al. 2010; Sarasso et al. 2014). The activity of the brain during sleep is also influenced by the preceding type of activity and sleep/wake state. In support of this, local activation of specific cortical areas

during wakefulness results in elevated delta power in the same cortical region during subsequent sleep (Kattler, Dijk, and Borbely 1994). Further evidence from human subjects (Huber et al. 2006; Krueger and Tononi 2011; Murphy et al. 2011) and animal models (Lancel, van Riezen, and Glatt 1992; Schwierin et al. 1999; Huber, Deboer, and Tobler 2000; Vyazovskiy, Borbely, and Tobler 2000) indicates that SWA and recovery from sleep loss are regional processes.

Notably, the levels of SWA are not only determined by a long-term preceding history, but also change systematically on a much faster time scale, such as within individual sleep episodes, suggesting that immediate preceding history is important. For example, a positive correlation has been identified between the length of NREM sleep bouts and the duration of prior REM sleep episodes (Benington and Heller 1994b). Within individual sleep episode, it was found that SWA decreased gradually, reaching a plateau, which could be described by a saturating exponential function that was relatively independent of both time of day and NREM bout duration (Trachsel, Tobler, and Borbely 1988, 1989). A recent human study using high density EEG provided evidence for the occurrence of two distinct categories of slow waves during the transition to sleep based on a variety of properties including their origin, spatio-temporal profile, and amplitude (Siclari et al. 2014). The authors hypothesized that initially upon falling asleep there is a global subcortico-cortical synchronisation process that is followed by more local, cortico-cortical processes.

In this chapter, I will describe experiments that aimed to examine the spatio-temporal dynamics of EEG slow waves in NREM sleep from two cortical derivations (frontal

and occipital regions) during the initial minutes of individual sleep episodes in adult male C57BL/6 mice.

3.2 Methods

The experiments were performed in adult male C57BL/6J mice (n = 9) (see **Section 2.1 Animals and Recording Conditions**). Mice underwent surgical procedures described in **Section 2.2.1 Implantation of EEG screws in Cortex** for EEG recording in the frontal and occipital lobe.

Experimental setup and signal pre-processing are described in **Section 2.3 *In Vivo* Electrophysiology Recording Setup** and **Section 2.6 Pre-processing Acquired Data**. Vigilance states (Fig. 3.1a) were classified as Waking, NREM sleep or REM sleep. Epochs contaminated by artifacts in at least one of the two derivations were removed from analysis (3.6 ± 0.7 % of total recording time). The onset of NREM sleep episodes was defined by the first occurrence of slow waves in at least one of the two EEG channels, and disappearance of phasic EMG activity recorded from the nuchal muscle. NREM sleep episodes were defined as periods consisting mostly of epochs scored as NREM sleep (on average 94.5 ± 0.5 %), allowing for interruptions of up to a maximum of 16 seconds (brief awakenings, which were not included in the spectral and slow-wave analyses), and preceded and followed by consolidated periods of waking or REM sleep. Only NREM sleep episodes longer than 3 minutes were included in the analyses. In total 8.9 ± 0.5 hour of NREM sleep contributed to the analyses which consisted of 78.7 ± 3.4 NREM episodes per 24 hours per animal, lasting on average 7.2 ± 0.4 minutes. NREM episodes were further subdivided according to whether they were preceded by at least 40 seconds of waking or at least 24 seconds of REM sleep.

3.3 Results

3.3.1 Sleep-Wake Distribution and the EEG Spectral Analysis

First, I calculated the overall dynamics of sleep and waking over the light and the dark period in the data set contributing to this study (Fig. 3.1). Representative 8-second traces of frontal and occipital EEGs and EMG for Wake, NREM and REM sleep are depicted in Fig 3.1a. All mice were strongly entrained to the 12:12 hour L-D cycle, as shown by the predominant occurrence of wheel running activity and episodes of continuous wakefulness during the dark period and sleep during the light phase (Fig. 3.1b, c & e). EEG SWA showed a consistent decreasing trend across the light period, during the habitual sleep period in both the frontal and the occipital derivation (Fig. 3.1b and 3.1d). The initial values of SWA, during the first 1 hour after light onset, expressed relative to the 24-hour mean in NREM sleep, were higher in the frontal EEG, as compared to the occipital derivation, albeit not significantly ($p = 0.234$, paired t-test). However, during the dark period, SWA during dark hours 15, 16, 18, 19 and 21, corresponding to sleep following prolonged waking episodes, was significantly higher in the frontal derivation ($p < 0.05$, paired t-test). To investigate which of the characteristics of individual slow waves reflect these changes in “global” SWA, I calculated the time course of EEG slow wave incidence, duration, amplitude and slopes. I found that in both derivations EEG slow waves were overall more frequent and were highest in amplitude during the first 1-2 hour of the light period. Slow wave incidence decreased across the 12-hour light period, from the first to the last hour, on average by 19.6 % in the frontal and 21.3 % in the occipital derivation ($p = 0.01$ and 0.009 respectively, paired t-test). In contrast, the decrease in slow wave amplitude was less pronounced, although it was still statistically significant (frontal: 11.3 %, $p = 0.003$, occipital = 8.7 %, $p =$

0.0002). Notably, slow wave duration, defined as the time from the start to the end of a slow wave remained constant, as reflected in the absence of a significant change from the beginning to the end of the light period ($p = 0.28$ and $p = 0.9$ for the frontal and the occipital derivation respectively). However, slow wave slopes showed a decline during the light period, with the steepest slopes found at the onset of the light phase, progressively becoming shallower. This change reached a statistical tendency level for the frontal derivation (1^{st} and 2^{nd} slopes: decline by 9.9 %, $p = 0.06$ and 10.2 %, $p = 0.08$, respectively), and was significant in the occipital derivation (1^{st} and 2^{nd} slopes: decline by 14.1 %, $p = 0.005$ and 10.3 %, $p = 0.009$). Thus, the overall magnitude of change within the light period was largest for slow wave incidence, followed by slope changes and slow wave amplitude. This suggests that a higher incidence of large-amplitude slow waves together with steeper slopes contribute the most to homeostatic changes in SWA in mice.

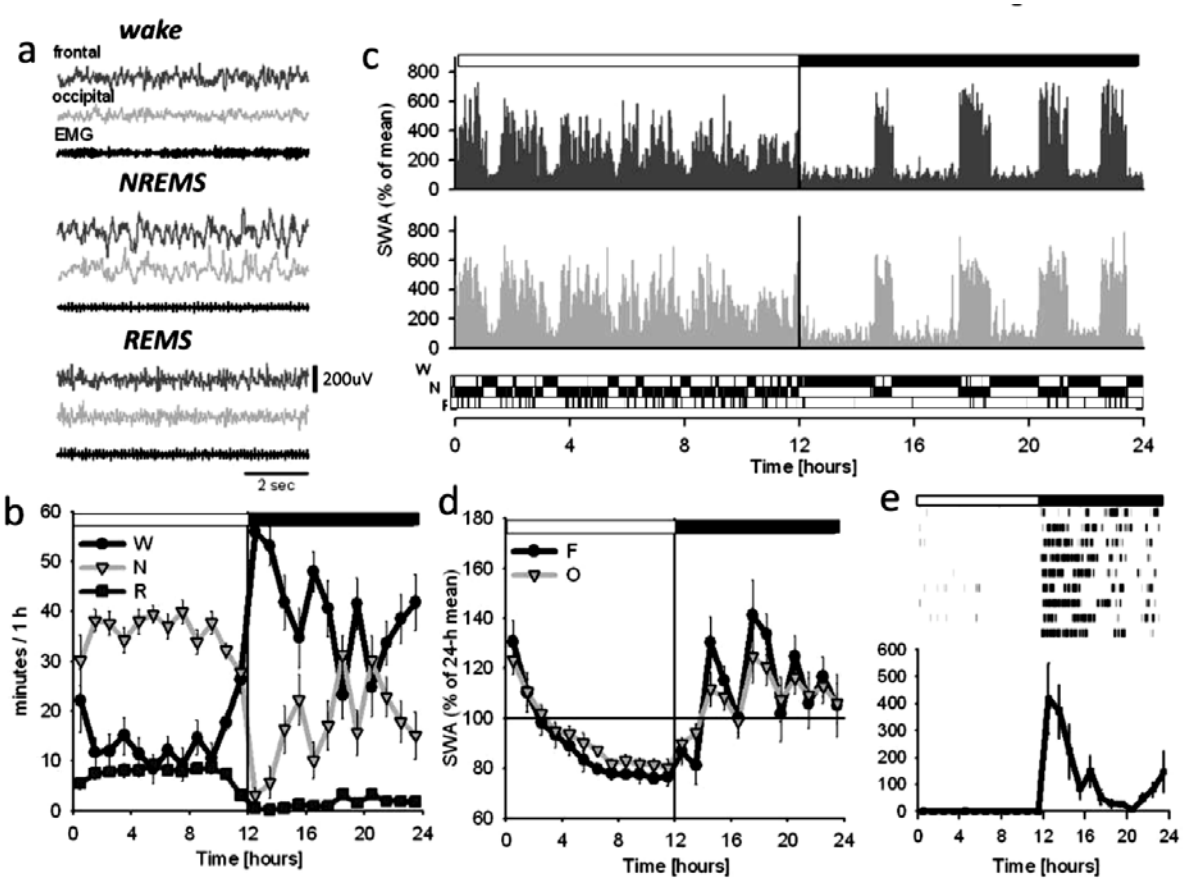


Figure 3.1, Sleep architecture and the EEG over 24 hours. *a) representative raw EEG (frontal and occipital) and EMG traces for wake (top), NREM sleep (middle) and REM sleep (bottom); b) time course of waking (W), NREM sleep (N) and REM sleep (R) over 24 hour expressed in minutes per hour; Mean values (n = 9, SEM). c) time course of EEG SWA (0.5-4 Hz) over 24 hour expressed as percentage of daily mean (1-min values) in one individual mouse (top: frontal, bottom: occipital). The hypnogram is shown below. d) Time course of NREM sleep SWA over 24 hours. Mean of 2-hour values (n = 9, SEM). e) Top: Running wheel (RW) - activity over 24 hours for each of the nine mice during 24-h period included in analysis; bottom: average profile of RW-activity (n = 9, mean values, SEM).*

3.3.2 Effects of Time of Day on Slow Waves

It is well established that SWA is not stable within an episode, but changes substantially from sleep onset to awakening or during a transition into REM sleep on a time scale of several minutes (Trachsel, Tobler, and Borbely 1989; Vyazovskiy, Achermann, et al. 2004). On the other hand, SWA and the parameters of individual slow waves change across the 24-hour period. To address the interaction between these slow and fast time scales, I

calculated the evolution of various slow wave parameters for the first 3 min after the initiation of individual NREM sleep episodes. Overall, within individual NREM sleep episodes, the incidence of slow waves increased by approximately 30 % throughout the first 3 minutes in the frontal derivation, while in the occipital derivation the increase attained maximal values, which were about 15 % above the initial 16-second value, after approximately 1 minute ($p < 0.0001$, repeated measures ANOVA for both F and O). The amplitude and slopes of individual slow waves similarly increased, albeit at a slower rate (Frontal - amplitude: 21.6 %, 1st slope: 14.3 %, 2nd slope: 19.1 %; Occipital - amplitude: 13.6 %, slope 1st: 9.5 %, slope 2nd: 8.2 %). Repeated measures ANOVA for all these variables revealed significant changes ($p < 0.0001$) in both derivations. In contrast, average slow wave duration changed only marginally across the first 3 min after NREM sleep initiation (by 6.0 and 6.8 % in the frontal and occipital derivation respectively), although the change was also significant ($p < 0.001$). Interestingly, while slow wave amplitude kept increasing throughout the first three minutes of a NREM sleep episode in both the frontal and the occipital derivation, slow wave slopes in the occipital derivation reached a maximal point earlier (~ 2.1 minutes after sleep onset). This result suggested that different aspects of local and global network activity underlying the generation and synchronization of slow waves change at a different rate following the onset of sleep episode. This hypothesis was supported by the observation that at the very beginning of NREM sleep episodes, slow waves in the frontal and occipital derivation often occurred in isolation, as quantified by initially longer latencies between consecutive slow waves in the two regions (66.1 % above the values later in the episode, $p < 0.001$, repeated measures ANOVA).

To investigate the dynamics of slow waves on a short time scale as a function of long-term preceding history or time of day, I calculated the time course of slow wave

parameters within consecutive 4-hour intervals across 24-hour (Fig. 3.2). Preceding sleep-wake history and/or time of day substantially affected the dynamics of slow wave parameters during the initial NREM sleep episode. Specifically, both the initial values of slow wave incidence, duration, amplitude and slopes, as well as the maximal values attained during the episode changed across 24-hour (Fig. 3.2). Unexpectedly, results show that slow wave incidence was initially lower during the first 3-hour of the light period (Fig. 3.2a), but, although slow waves were less frequent, they had a similar duration and had higher amplitudes to begin with, as compared to subsequent 4-h intervals in the light period (Fig. 3.2b, c). At the same time, in both derivations, slow wave slopes were initially steeper during the light period, and, following a decline, increased again during the dark period (Fig. 3.2d, e), suggesting that local network synchronization is sensitive both to the timing within individual NREM episode and preceding long-term history. Interestingly, the initial latencies between consecutive slow waves in the F and O derivations showed a U-shaped curve across 24-hour, reaching highest values during the intervals when physiological sleep pressure was high – at the beginning of the light period and in the second part of the dark phase. Overall, these data together reveal a complex temporal scale of slow wave dynamics that change drastically immediately after entering into NREM sleep and change throughout 24-hour period.

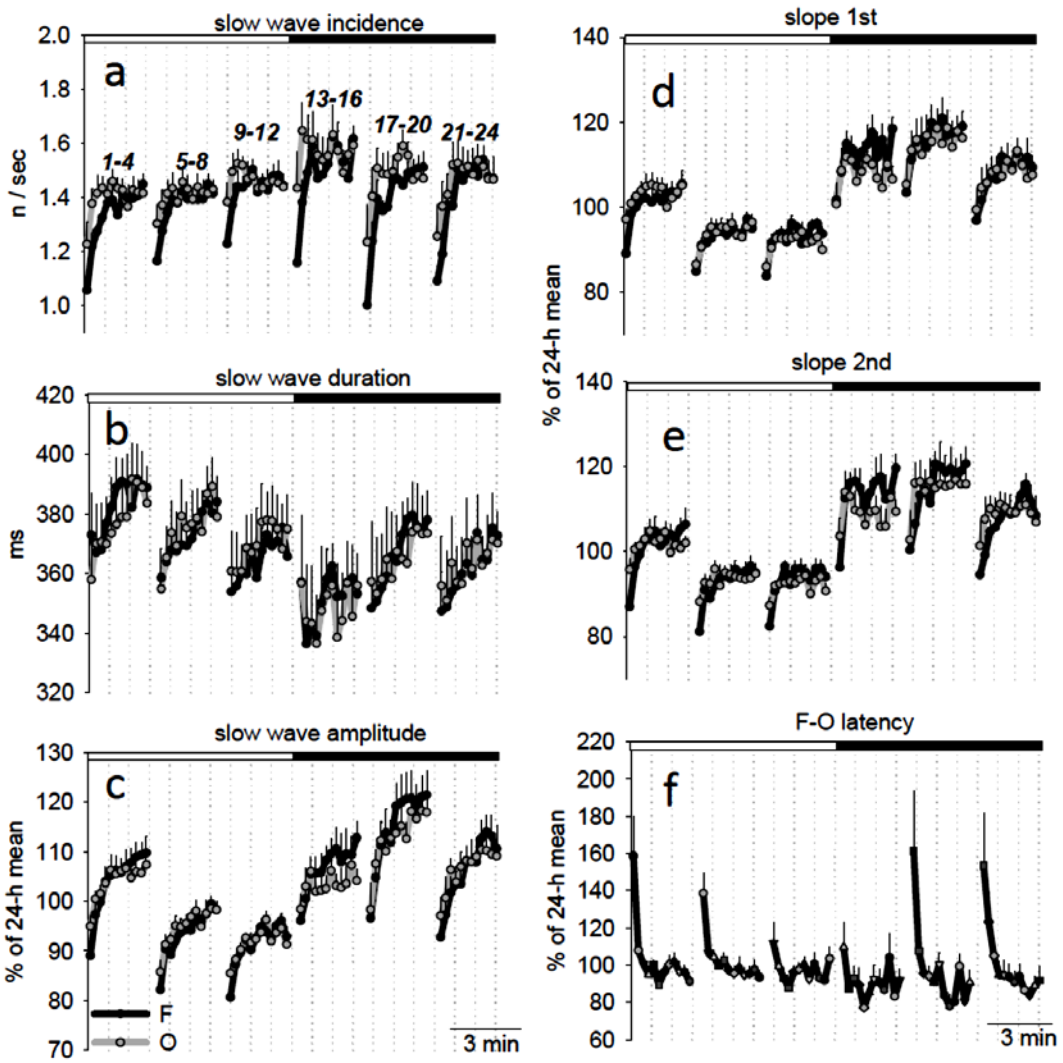


Figure 3.2, Characteristics of EEG slow waves during the first 3 minutes after sleep onset across 24 hour. *Each of the slow wave parameters was computed over all NREM sleep episodes > 3 min occurring within consecutive 4-hour intervals (e.g., first interval corresponds to hours 1 to 4 after light onset, second interval: hours 5 to 8 etc.). a) slow wave incidence; b) slow wave duration; c) slow wave amplitude; d) slope 1st; e) slope 2nd; f) F-O latency, defined as the time between consecutive slow waves occurring in the frontal (F) and in the occipital (O) derivation. c-f expressed as percentage of 24-hour mean across all NREM sleep episodes; Mean values are plotted in 16-second bins (SEM), n = 9 mice.*

3.3.3 Immediate Preceding History Affects the Dynamics of Slow Waves

The polyphasic nature of sleep patterns in mice provides an opportunity to analyse NREM sleep episodes following both waking and REM sleep. Fig. 3.3a shows typical transitions from waking (W-N) and REM sleep (R-N) to NREM sleep. On average, both the number and the duration of NREM sleep episodes were comparable between episodes occurring after waking and REM sleep (Fig. 3.3b). It should be noted, however, that R-N episodes were more frequent during the light period as compared to the dark period, while W-N transitions were equally distributed across 24-hour (Fig. 3.3c). The EMG profile at 1 min before and 1 min after NREM sleep episode initiation is shown on Fig. 3.3d. For W-N transitions, EMG activity begins to decline approximately 20 sec prior to sleep onset, and remains at a stable low level from the first epoch scored as NREM. REM sleep is in most cases followed by a brief awakening, and so a transient surge of EMG activity was observed, followed by an immediate reduction of EMG activity to previous levels (Fig. 3.3d). Immediately after the transition into NREM sleep, EEG SWA began to rise in both derivations at a similar rate, and reached approximately 200% of pre-NREM sleep levels within 1 min (Fig. 3.3e).

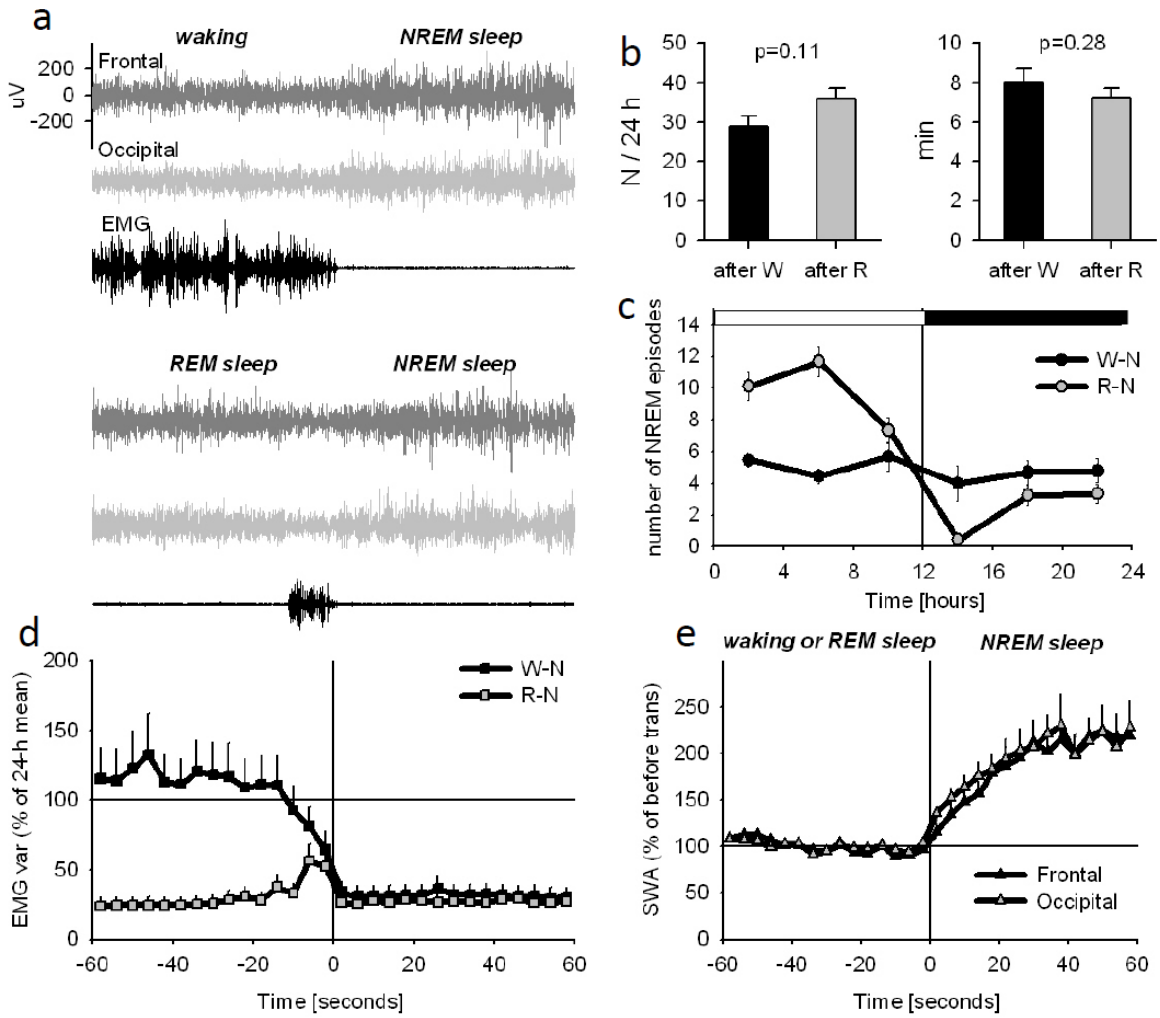


***Figure 3.3**, **NREM transitions and the effect of immediate preceding history.** a) representative raw EEG (frontal and occipital) and EMG traces for a typical waking to NREM transition (W-N, top) and REM to NREM transition (R-N, bottom); b) number of NREM episodes per 24 hour and episode duration is shown for both episodes occurring after waking and after REM sleep; c) distribution of NREM episodes over 24 hours for W-N and R-N transitions; d) The profile of EMG variance of 1 minute before the initiation of NREM sleep episode and the first minute after NREM sleep episode onset, expressed as a percentage of 24-hour mean for both W-N and R-N transitions; e) average profile of EEG SWA (0.5 - 4 Hz) of 1 minute before the initiation of a NREM sleep episode and the first minute after NREM sleep episode initiation for all transitions (from waking and/or REM), separately shown for the frontal and occipital cortical derivations. Panels b-e: mean values (SEM), n = 9 mice.*

To investigate the effects of immediate preceding history on the dynamics of cortical activity, all NREM sleep episodes longer than 3 min were subdivided into those which transitioned from a prolonged waking episode or REM sleep (typically followed with a brief awakening < 16 seconds). Intriguingly, immediate preceding history also had a noticeable influence on the dynamics of slow wave parameters. Specifically, while the incidence of slow waves reached roughly similar levels during NREM episodes after waking or REM sleep, the values were substantially lower initially after REM sleep, especially in the frontal derivation, and showed a more prominent increase (Fig. 3.4). The magnitude of change of slow wave incidence within the first 3 minutes after NREM sleep episode onset after waking was 19.1 % and 8.0 % for the F and the O derivation, respectively, while the corresponding increases after REM sleep reached 44.4 % and 24.6 %. This was also the case for slow wave amplitude, although the difference was less prominent (after W vs R: frontal, 16.5 vs 26.5 %, occipital: 7.1 vs 20.1 %). Consistently, both the 1st and the 2nd slopes also started from substantially lower values after REM sleep, as compared to waking, and increased more rapidly. They also remained at a consistently lower level throughout the first 3 minutes of the episode (1st slope: frontal, 8.9 vs 21.1 %, occipital: 6.1 vs 15.9 %; 2nd slope: frontal, 13.0 vs 25.0 %, occipital: 5.2 vs 14.6 %) if was preceded by REM sleep. To address whether this result may be confounded by the time of day, I made this computation separately for the light and the dark period, as well as for the first and the last 4 or 6 hours of the light phase, the results of which were similar in all cases.

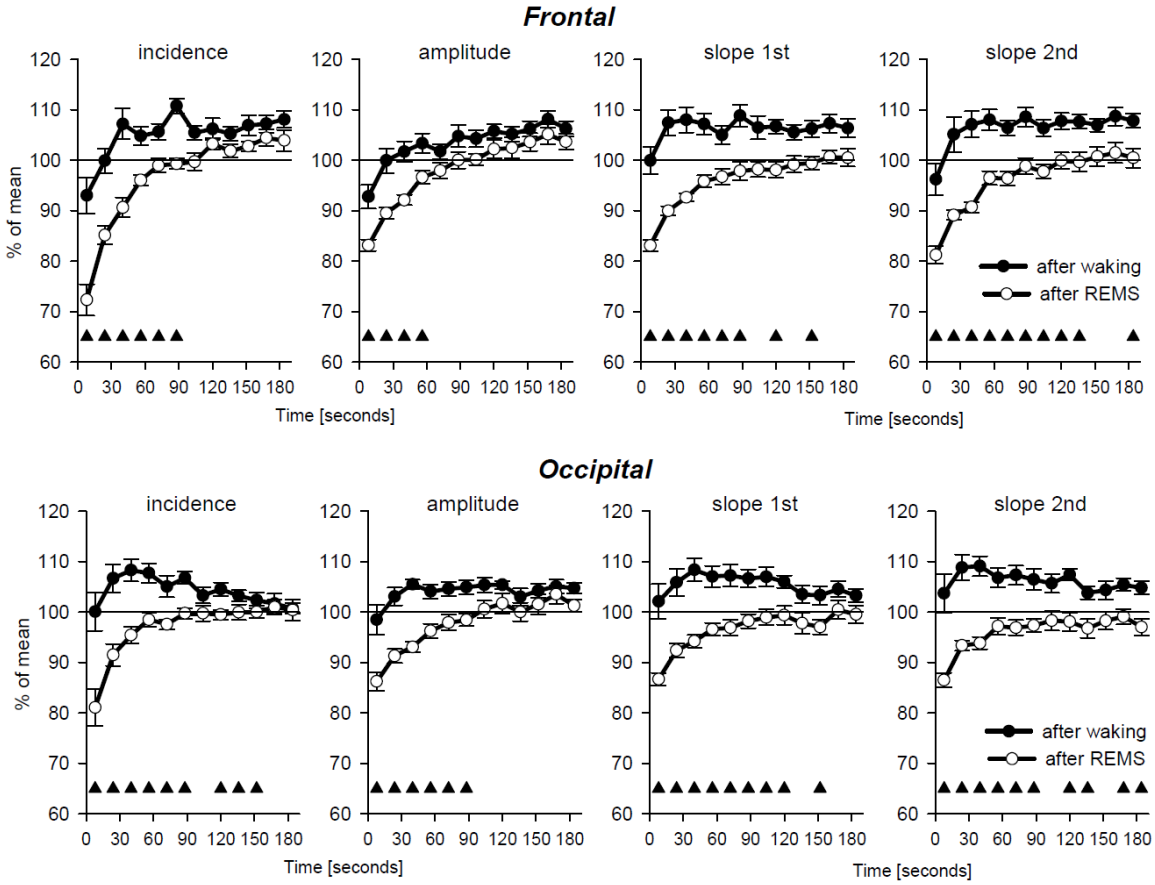


Figure 3.4, Immediate preceding history affects the dynamics of cortical slow waves. *All NREM sleep episodes longer than 3 minutes were subdivided into those that transitioned from a prolonged waking episode or after REM sleep (in most cases including a brief awakening). Slow wave incidence, amplitude, slope 1st and slope 2nd for transitions after waking and REM are shown, separately for the frontal and occipital derivations. Mean values (SEM, n = 9) are shown for 16-second bins. Triangles below the curves depict 16-second bins, where the difference between the episodes after waking and after REM sleep was significant (p < 0.05, paired t-test).*

3.4 Discussion

In this study, I have characterized the spatio-temporal dynamics of individual EEG slow waves during the first minutes of spontaneous NREM sleep episodes in adult male C57BL/6 mice. These results highlight a complex picture, where both time of day, as well as immediate preceding state history play a significant role. The main findings were: the changes of EEG spectral power in the slow-wave range (SWA) on a global scale across 24-h are accounted for by more frequent slow waves with higher amplitude and steeper slopes. Within individual NREM sleep episodes high physiological sleep pressure is mostly reflected in slow waves of higher amplitude and steeper slopes. Finally, in addition to the preceding long-term history and intra-episodic dynamics, the parameters of individual slow waves are strongly influenced by immediate preceding states. Specifically, the main novel finding of this study was that following REM sleep episodes, NREM sleep initiates in a more desynchronized, or local, fashion, compared to NREM sleep episodes following waking. It has been suggested that sleep emerges at the level of local neuronal populations as a direct consequence of fine synaptic modifications and local changes in neuronal connectivity arising from specific preceding waking activities (Krueger and Tononi 2011). While local neuronal populations seem to be capable of independently generating sleep-like patterns of activity (Sirota and Buzsaki 2005), a significant proportion of normal physiological sleep is global, as manifested in behaviour and a large-scale synchrony of sleep slow waves (Massimini et al. 2004; Nir et al. 2011; Vyazovskiy et al. 2011). However, specific cellular and network mechanisms responsible for the occurrence of local sleep and its subsequent progression into a global deep sleep state remain unclear (Vyazovskiy and Harris 2013). Another view is that cortical sleep is regulated in a top-down fashion such that subcortical

neuromodulatory influences precipitate global sleep transitions (Saper, Scammell, and Lu 2005). In a recent study where LFPs were recorded from several subcortical centres concomitant with the cortical EEG (in a fronto-parietal configuration), it was found that subcortical changes preceded the power shifts in the cortical EEG (Baker et al. 2014). The shifts in global-local coordination of neuronal activity at the initiation of a sleep episode are not yet understood, and elucidating the cortical dynamics considering both long-term and immediate preceding history may provide important insights. Previously, several studies have demonstrated that SWA is initially lower and then builds up during the course of a sleep episode in both humans and rodents (Trachsel, Tobler, and Borbely 1988, 1989; Aeschbach et al. 1996; Vyazovskiy, Achermann, et al. 2004). Such alterations can be accounted for by a combination of the change in slow wave incidence, slow wave amplitude and slow wave slopes. The slow wave incidence reflects the tendency of the network to enter generalised silence, and in addition, opposing process takes place, which forces the network to resume activity, that in turn prevents sustained periods of neuronal silence (Vyazovskiy et al. 2013; Vyazovskiy et al. 2017). The EEG slow wave amplitude across a 24 hour period is finely modelled by the Sleep Homeostatic Process of the Two Process model (Borbely 1982) when transformed into EEG power spectrum as Slow Wave Activity, which suggest the slow wave amplitude reflects sleep pressure. It has been shown in rats that the amplitude of slow waves is determined mainly by the duration of generalised network silence (Vyazovskiy et al. 2007; Vyazovskiy et al. 2009; Vyazovskiy et al. 2013). Since the positivity in EEG signal corresponds to the down state of cortical neurons as recorded intracellularly, and to the suppression of spiking activity as recorded extracellularly, suggesting that the rising slope (1st slope) corresponds to the network synchrony of transitioning from a period of elevated activity to generalised silent states,

and the descending (2nd slope) corresponds to the network synchrony of transitioning from generalised silent state into enhanced network activity (Vyazovskiy et al. 2009; Steriade, Nunez, and Amzica 1993a; Amzica and Steriade 1998b). One the caveats of this study is that the parameters of slow waves are not independent of each other, specifically amplitude and the slow wave slopes. Yet, because the parameters are not totally dependent, it may still be useful to look at them in different circumstances in the future experiments such as sleep deprivation experiments. In this study, results show that all these variables change gradually within the first 3 min after sleep onset, albeit at different rates. While this finding does not rule out the influence of subcortical neuromodulation, it suggests that local cortical network dynamics also play a role. Specifically, the fact that slow wave characteristics change differently with respect to each derivation within the first minutes after sleep onset is difficult to reconcile with the global top-down switch of the cortex between different states. Another possibility, which needs to be investigated further is that subcortical regions indeed provide a stable signal dictating when to switch between global stages, but local cortical areas may be in a different state of "responsiveness" to such influences, resulting in some areas lagging others. While the mechanisms underlying the different levels of "responsiveness" are unclear, it cannot be excluded that they are of cortical origin, and are modulated by long-term and short-term preceding history of local activity. One of the novel observations in this study was that REM sleep seems to consistently lead to a breakdown of large-scale cortical synchronisation, as reflected in measures such as a less frequent occurrence of slow waves, a reduction in their amplitude and slope, and prolonged latencies between consecutive frontal and occipital slow waves. While the mechanisms and functional significance of such a re-setting of brain state after

individual REM sleep episodes remains to be investigated, it may be an essential feature of physiological sleep regulation (Vyazovskiy and Delogu 2014).

The interaction of long-term and immediate preceding history with respect to slow wave characteristics during the initial NREM sleep points to the effects of neuromodulators, as well as the remaining trace that the preceding state leaves on the circuits. There is evidence that early intense sleep, such as after sleep deprivation, is characterized by increased global synchrony, manifested in a higher proportion of global slow wave events, steeper slow wave slopes, higher incidence of high-amplitude slow waves and increased network synchronisation (Vyazovskiy et al. 2007; Vyazovskiy et al. 2009; Vyazovskiy et al. 2013). These results suggest that the picture is more complicated, and immediate state history also plays a significant role. Recently, it was found, that while immediate awakening is associated with lower firing rates and more frequent OFF periods, possibly underlying sleep inertia, this effect was mostly pronounced after awakening from REM sleep (Vyazovskiy and Delogu 2014).

Chapter 4: Effects of Specific Waking Behaviour on Cortical Activity

4.1 Introduction

The duration, timing and architecture of waking and sleep are regulated by many factors including circadian influence and preceding sleep-wake history, the homeostatic process. The Two Process model (Borbely 1982) argues that sleep propensity increases as wakefulness lasts, as reflected in the levels of electroencephalogram (EEG) slow wave activity (SWA, 0.5-4 Hz) during subsequent non-rapid eye movement (NREM) sleep (Dijk, Beersma, and Daan 1987). Sleep slow waves emerge within thalamo-cortical networks (Timofeev 2013; Crunelli and Hughes 2009) and have been proposed to contribute in cellular restoration, information processing and synaptic renormalisation (Rasch and Born 2013; Vyazovskiy and Harris 2013). Recent evidence suggested that sleep has properties of an activity-dependent process, whereby it is initiated at the level of local neuronal networks which were more active during waking, and progressively encompasses larger brain territories, before eventually precipitating global behavioural sleep (Krueger et al. 2008; Kattler, Dijk, and Borbely 1994; Vyazovskiy, Welker, et al. 2004; Vyazovskiy and Tobler 2008). Consistently, sleep deprivation has been associated with a progressive increase in local “sleep-like” activities in the cortex during waking (Vyazovskiy et al. 2011). Another view proposes that global sleep-wake switching is initiated from subcortical areas, which integrate external and internal information including the time of day, immediate and long term preceding history of activity and metabolic requirements (Saper et al. 2010).

It has been postulated that neuronal firing rates undergo continuous homeostatic regulation, ensuring stability in the circuits function (Turrigiano 1999). The evidence for

firing rate homeostasis in vivo raises an important question about the role of behaviour and brain state in the dynamics of this process (Hengen et al. 2013; Vyazovskiy et al. 2009; Grosmark et al. 2012). The hypothesis that waking and sleep have opposing effects on neuronal excitability or synaptic strength has so far yielded conflicting evidence (Vyazovskiy et al. 2009; Vyazovskiy et al. 2008; Chauvette, Seigneur, and Timofeev 2012; Durkin and Aton 2015; Aton et al. 2014). Evidence supporting synaptic potentiation during wake and synaptic depression during sleep: Cortical firing rate is higher after sustained wakefulness, whereas after sustained sleep firing rate decreased, Vyazovskiy et al. 2009. GluR1-containing AMPA receptor levels are high during wakefulness and low during sleep, and changes in phosphorylation states of AMPARs, CamKII and GSK3β are consistent with synaptic potentiation and depression in wake and sleep respectively Vyazovskiy et al. 2008. Evidence supporting synaptic potentiation during sleep: Somatosensory evoked potentials during wake were enhanced after slow-wave sleep compared to previous wake episode Chauvette et al. 2012. V1 synaptic potentiation response associated with shift in orientation preference occurs only after sleep, Aton et al. 2014. Firing rate response to visual stimuli were unchanged across wake, but were enhanced across post-stimulus sleep Durkin & Aton 2015.This suggests that other factors need to be taken into account, such as circadian time or behavioural state, and new models are required to address these discrepancies. One possibility is that those waking experiences or behaviours, which do not entail a generalized increase in cortical activity, may be associated with a slower rate of accumulation of “global” sleep need.

In this study, colleagues and I performed continuous recordings of cortical neuronal activity from two cortical regions in mice given free access to running wheels. It has been shown previously, that spontaneous running is associated with distinct changes in the

architecture and distribution of vigilance states across 24 h, and leads to regional changes in waking and sleep EEG (Edgar et al. 1991; Gu et al. 2015; Vyazovskiy and Tobler 2012; Vyazovskiy et al. 2006). Two regions – the primary motor cortex (M1) and the somatosensory field (SCx) investigated in this study have been widely studied with respect to sleep and wake regulatory mechanisms, and regional changes in the dynamics of EEG markers of sleep need have been found, during both acute and chronic sleep deprivation (Cui et al. 2014; Leemburg et al. 2010; Vyazovskiy, Welker, et al. 2004; Vyazovskiy et al. 2002; Huber, Deboer, and Tobler 2000). However, despite running wheel activity being widely used in circadian neurobiology, it remains unknown whether this behaviour is associated with changes in cortical neuronal activity, both in relation to running characteristics per se, as well as with respect to dynamic changes in local cortical excitability during continuous periods of spontaneous running.

4.2 Methods

Experimental animals. In total n = 16 adult male C57BL/6J mice, were used in this study (mean age 27.9 ± 0.6 weeks old at the time of the experiment). All the animals were subdivided into two experimental groups, according to whether the microwire array was implanted in the motor cortex (M1) or somatosensory somatosensory field (SCx). In several animals (n=5) more than one recording day has been analysed with the intention to ensure stability and reproducibility of results (1-3 days per animal). Subsequently, to prevent bias in selecting a specific day in the final analyses, for those animals where more than one day was analysed, the data were averaged between days prior to calculating means between animals. The same surgical procedures are used for EEG screw and microwire array implantation as described in **Section 2.2 Surgical Procedures** in **Chapter 2 Materials and**

Methods. In a subset of animals, in which the microwire array was implanted in M1 (n = 9), sleep deprivation (SD) was performed as described in **Section 2.4 Sleep Deprivation methods**.

In this study, stereotypic wheel running behaviour of C57BL/6J mice was the main subject of investigation. Running wheel activity (RW) is a widely used behavioural assay, utilizing the well-established fact that mice have a spontaneous tendency to run. In this study animals had free access to running wheels (Campden Instruments, Loughborough, UK, wheel diameter 14 cm, bars spaced 1.11 cm apart inclusive of bars), and mice were given 15.3 ± 2.1 days to habituate to wheels prior to the analysed electrophysiological data in dark periods. There were no significant differences in the duration of the habituation to the wheel between the groups of animals (unpaired t-test: M1 vs SCx, p=0.21).

The wheels were custom made for tethered animals, and did not prevent the animals from running *ad libitum*. Each running wheel was fitted with a digital counter (Campden Instruments) which uses an infra-red (IR) emitter/receiver to detect each rung passing the IR beam as the wheel rotates. Running wheel activity was recorded with a high temporal resolution (one full wheel revolution consists of 38 individually detected rung counts, thus 10 counts per second corresponds to 10.11 cm/sec) within the same system used to record electrophysiological signals. This facilitates to achieve a precise synchrony between instantaneous changes in electrophysiological signals/behaviour and RW activity/speed. The wheel counter output is a 5 V TTL pulse (0 V with no output), that triggers an edge detector in the TDT acquisition system, and in turn creates a time stamp that is stored for each wheel count. For most analyses, RW activity was analysed in 1-sec epochs that were grouped based on the number of counts within the 1-sec epochs. The average running speed for those epochs with at least 1 count was 9.6 ± 0.6 counts per

second. Since the number of 1-sec epochs with progressively higher numbers of counts decreased progressively, I also used progressively wider ranges for the bins (0; 1; 2-3; 4-7; 8-11; 12-32), to obtain a sufficiently high yet reliable number of counts within each speed category (Fig. 4.1). Since the number of 1-sec epochs for non-running waking was much larger than the number of epochs with RW activity, some analyses were repeated on a randomly chosen subset of non-running epochs matching the number of epochs with RW activity, which did not alter the results.

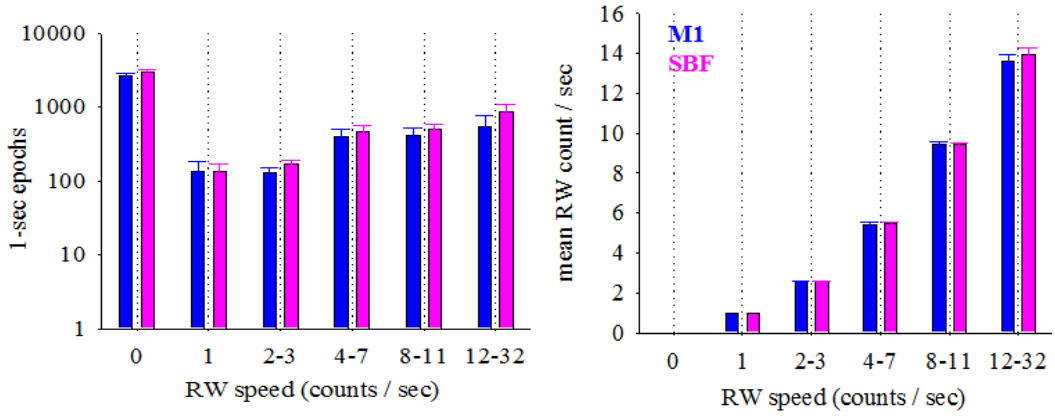


Figure 4.1, ***Left***, *the total number of 1-sec epochs with and without running which contributed to this study shown for the experiments where cortical firing rates were investigated in M1 and SCx. All epochs were grouped as a function of increasing running speed.* ***Right***, *the corresponding average values of RW speed (counts / sec). Mean values, SEM, n=11 mice (M1), n = 5 mice (SCx).*

Two animals in the motor cortex implanted group were excluded from specific data analyses where the effects of RW speed were calculated, due to a low temporal resolution of RW-activity recordings (one for technical reasons and the other because an individual mouse never attained high speed running). Therefore, only n=9 mice contributed to these mean values. For the analyses depicted in Fig. 4.13, neuronal firing rates were calculated during epochs in which the animals either accelerated on a wheel, ran steadily or

decelerated. This analysis has been performed on a 1-sec basis, focusing on those epochs with at least 4 RW counts. Acceleration-deceleration index (ADI) was obtained by calculating mean second derivative of the time series for each 1-sec epoch, and subsequently grouped epochs according to ADI into ten 10% percentiles prior to calculating averages between animals.

$$\text{ADI for each putative single unit} = histogram((\sum_{i}^{n\ epochs} RW_i'') \div n\ , 10\ bins)$$

4.3 Results

4.3.1 Cortical RUN on and RUN off neurons during spontaneous wheel running

In the first experiment, continuous multiunit activity (MUA) from layer 5 of the motor cortex (Fig. 4.2a) and EEG recordings were performed in n = 11 mice which had free access to the running wheel in their home cages. All animals were habituated to the wheel for 15.3 ± 2.1 days prior to the dark period used in the analyses, and used it extensively during the experimental night, having run spontaneously on average more than 800 meters within the 12-h period (868.7 ± 161 m, Fig. 4.2b). In every animal, several prolonged waking periods dominated by running wheel (RW) activity were observed during the dark period, interspersed by naps of various durations. As typically observed, during waking epochs with wheel running (wRUN), EEG was dominated by theta-activity (6-9 Hz), which was substantially lower when the animals did not run (nwRUN, Fig. 4.2c).

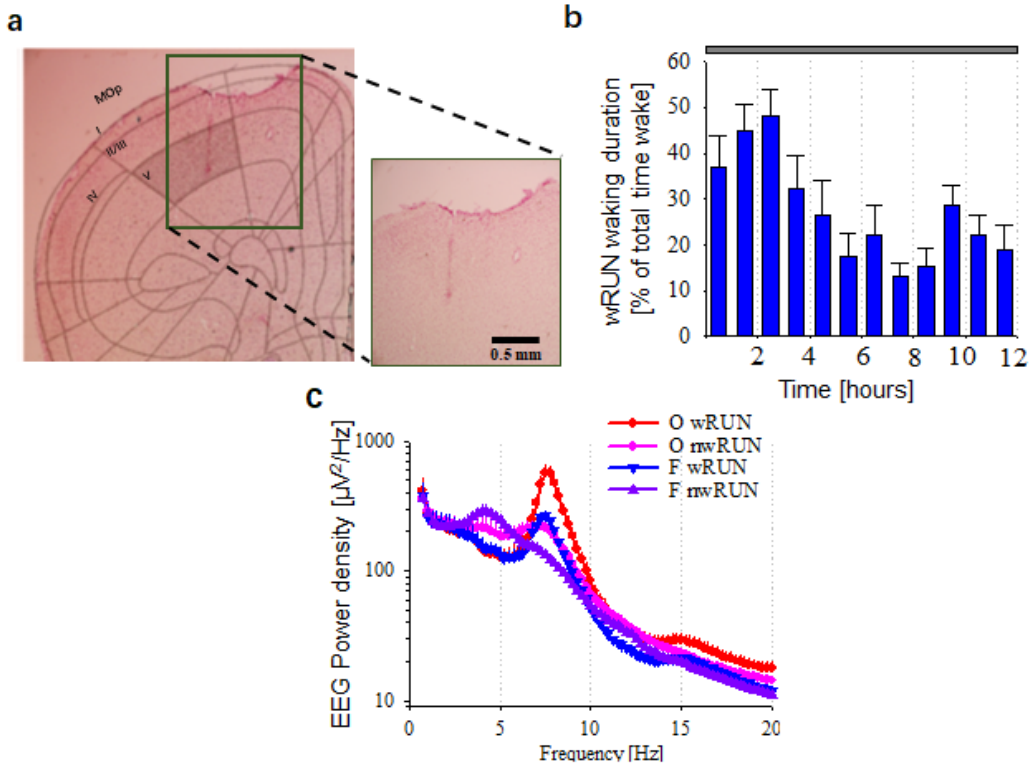


Figure 4.2, *a) Representative histological verification (Nissl staining) of the electrode location in M1 (one single tract is shown with an overlay of an anatomical reference adapted from the Allen Mouse Brain Atlas). b) Average profile of running-wheel (RW) activity during the experimental night. The amount of waking spent running in animals implanted in the motor cortex (M1, n=11) Mean values, SEM. c) EEG power spectral density during running (wRUN) and non-running (nwRUN) waking shown for the frontal (F) and occipital (O) EEG signals. Note the increase EEG power at ~7 Hz during running in both derivations. Mean values, SEM (n=11 mice).*

During NREM sleep, cortical LFP recorded from M1 was dominated by high-amplitude positive slow waves, associated with a brief generalized reduction of MUA (OFF-periods) across all or most of the electrodes within the 16-channel array (Fig. 4.3a). In contrast, during waking there was a prominent dissociation between the activities of putative individual neurons depending on animal's behaviour (Fig. 4.3b).

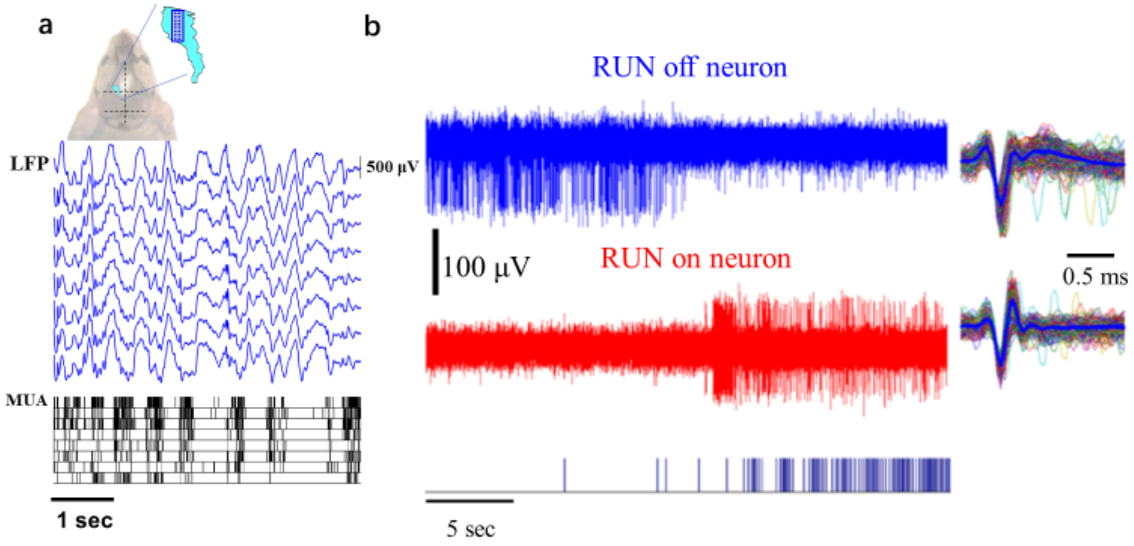


Figure 4.3, *a) Schematic representation of the position of the primary motor cortex (M1, blue area drawn with reference to Paxinos & Franklin, 2001) shown on the dorsal surface of the mouse head, and the position of the 16-ch microwire array above M1 (dots indicate the position of individual wires within the array). Traces on the right: top, representative local field potentials (LFP) recorded during NREM sleep from one row of microwires; bottom, raster plot of multiunit activity (MUA, each vertical line represents a spike) recorded from the same wires. Note the close temporal relationship between positive LFP waves and periods of generalised neuronal silence. d) Two MUA traces recorded from M1 in the same animal with corresponding RW-activity (bottom, each vertical bar represents a single wheel rung count). Corresponding waveforms of the action potentials recorded extracellularly are shown on the right.*

Specifically, all recorded animals had individual neurons which slowed down substantially or ceased firing altogether during intense running on the wheel (RUN off neurons, Fig. 4.4a). Overall, cortical neuronal activity was on average 25.0 ± 9.3% lower during wRUN compared to nwRUN waking and NREM sleep (repeated measures ANOVA, factor 'vigilance/behavioural state', $F(2,18)=17,23$, $p=0.0001$, 3 states, Fig. 4.4b). Although a larger population of recorded neurons were RUN off neurons, and overall cortical activity decreased during running, putative single units were highly variable with respect to

running behaviour (Fig. 4.3b, 4.4a). Among recorded neurons, ones that increased firing during running (RUN on neurons) were occasionally observed. Notably, most neurons did not only change firing rate when the animals ran, but exhibited varying relationship to running speed (Fig. 4.5), and on average resulted in a significant inverse correlation to running speed ($F(5,53) = 8,61$, 6 run speed categories, 9 mice, $p < 0.001$, ANOVA for repeated measures, factor 'running speed').

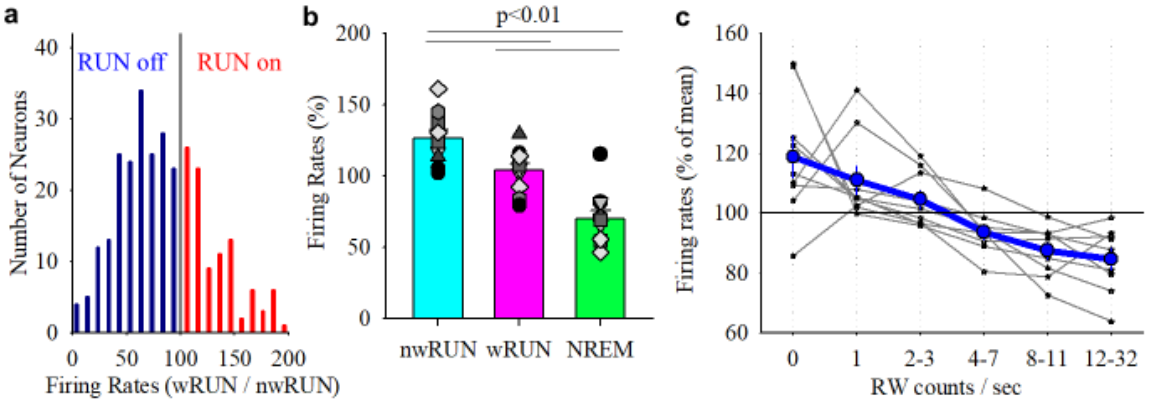


Figure 4.4, *a) The distribution of all putative single units recorded in n=11 mice as a function of the ratio of their average firing rates (FR) during running (wRUN) and non-running waking (nwRUN). Note that a smaller proportion of neurons increase firing during wheel running (red, RUN on neurons), while the majority decrease FR during running (blue, RUN off neurons). b) Average FR in M1 during nwRUN waking, wRUN waking and NREM sleep. Mean values, SEM, n=11 (individual mice: grey symbols). Significant differences between vigilance states are depicted above the bars (obtained by two-tailed paired t-test following significant one-way ANOVA). c) FR in M1 shown as function of running speed. Thick lines: mean values, SEM, n=9 mice. Values from individual animals are shown as thin line plots.*

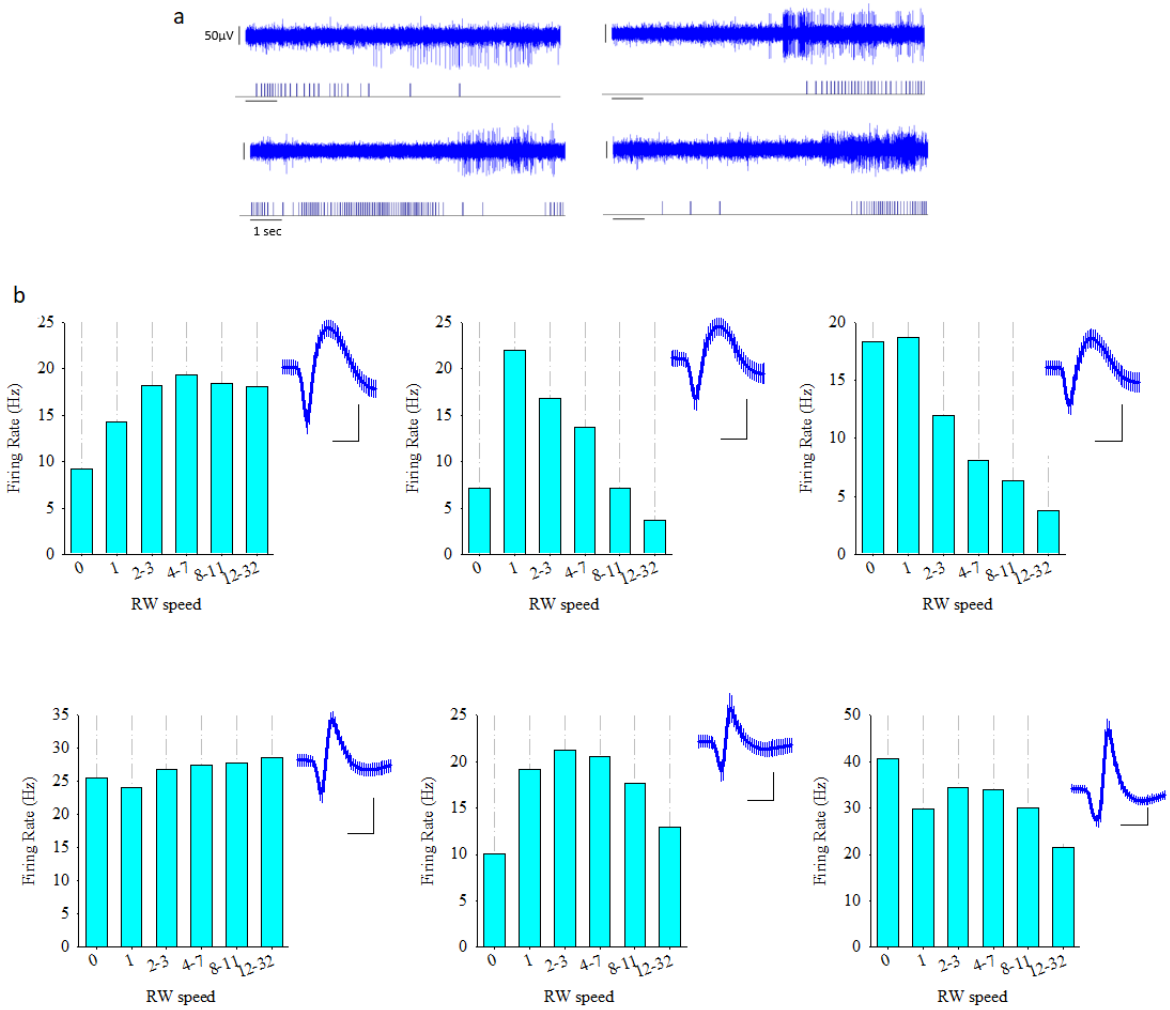


***Figure 4.5**, a) Individual representative examples depicting the effect of voluntary running on cortical neuronal activity in M1. Four neurons are shown recorded from M1 together with corresponding running wheel (RW)-activity (each bar represents a single wheel rung count). The two examples on the left depict cases when multiunit activity (MUA) decreases specifically during running. The two examples on the right show traces, where MUA increases immediately before running onset and is maintained during running. b) Individual examples of single putative neurons recorded in M1 (six in total, taken from different animals) showing the average spike waveform (± standard deviation) and the change in average firing rates as a function of running speed. Scale bars: vertical: 50µV, horizontal: 0.5 ms. Note that individual neurons in M1 were variable with respect to their firing as a function of running speed.*

Next, to investigate if spontaneous wheel running behaviour affects neuronal firing rates in another cortical area, implantation of micro-wire arrays was performed in the somatosensory cortex (SCx) to record MUA (Fig. 4.6a, b). Visual inspection of data did not find individual neurons in SCx that stopped firing during running as observed in some cases in M1, but most neurons also changed substantially their firing activity during running. Similar to M1, considerable variability was observed between putative individual neurons with respect to their relationship with running behaviour (Fig. 4.6c), and on average neuronal firing rates in the SCx also showed an inverse correlation to running speed (Fig. 4.6e, $F(5,29) = 19{,}42$, 6 run speed categories, 5 mice, $p < 0.001$, ANOVA for repeated measures, factor 'running speed').

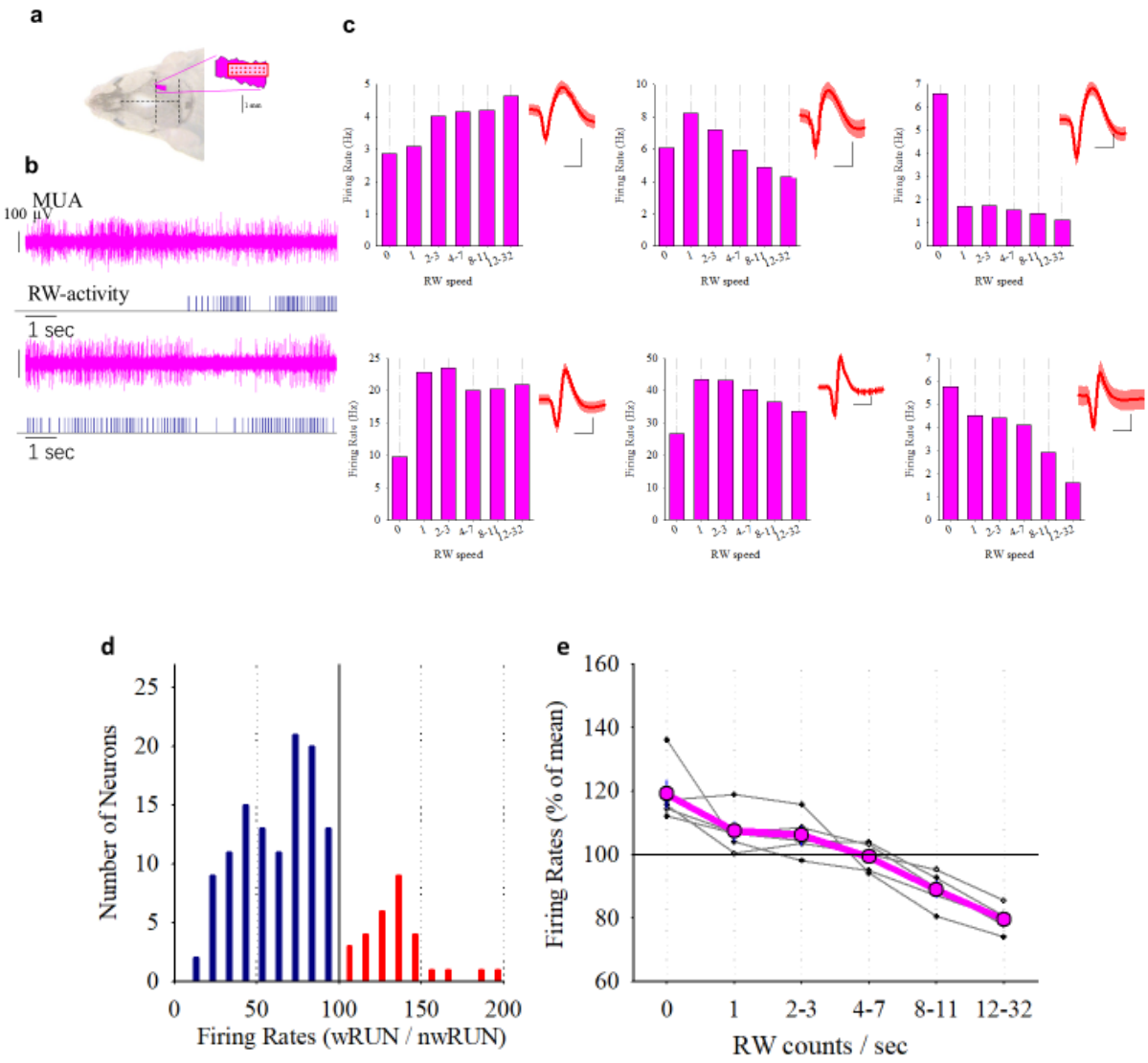


***Figure 4.6**, a) Schematic representation of the position of the 16-ch microwire array shown relative to the barrel cortex (drawn in reference to Paxinos & Franklin, 2001) shown on the dorsal surface of the mouse head (dots indicate the position of individual wires within the array). b) Individual representative examples depicting multiunit activity (MUA) in SCx during wheel running. Corresponding running wheel (RW)-activity is shown below each trace (each vertical bar represents a single wheel rung count). c) Individual examples of putative single neurons (six in total, taken from different animals) showing the average spike waveform (±standard deviation) and the change in their average firing rates as a function of running wheel speed. Scale bars: vertical: 50µV, horizontal: 0.5 ms. Note that individual neurons in SCx were variable with respect to their firing rates as a function of running speed. d) The distribution of all putative single units recorded in SCx (in n=5 mice) as a function of the ratio of their average firing rates (FR) during running (wRUN) and non-running waking (nwRUN). Note that a smaller proportion of neurons increase FR during running (red), while the majority decrease spiking activity (blue). e) FR in SCx shown as a function of running speed (count/sec). Thick lines: mean values, SEM, n=5 mice. Values from individual animals are shown as thin line plots.*

4.3.2 Stereotypic running decreases cortical firing rates

During mice's spontaneous wheel running activity, frequently there were brief pauses in running and fluctuations in running speed, irrespective of running bout length. It is well known that the mode of activity of cortical circuits is particularly critical during purposeful movement, which entails continual bidirectional communication between motor and somatosensory regions (Brown and Marsden 2001; Saleem et al. 2013; Zagha et al. 2013), as compared to automatic stereotypic locomotion, which largely relies on subcortical pathways (Marder and Bucher 2001). In this experiment, striking changes were observed in the firing activity of the motor cortex depending on the pattern and nature of running behaviour, such as during initial acceleration, during steady constant running and during brief pauses in RW activity (Fig. 4.7a). Most putative single units had a 'preferred' frequency of firing, which was affected substantially by wheel running behaviour (Fig. 4.8b). To investigate this aspect in more detail, a running acceleration / deceleration index (ADI, explained in **Chapter 4.2 Methods** section) was calculated based upon the timing of individual RW counts within 1-sec epochs. For most analysed epochs, the average ADI was low representing negligible ac-/deceleration within an epoch representing stereotypic steady running, although abrupt fluctuations in running speed during a consolidated running bout were frequently encountered (Fig. 4.8a). Firing rates appeared to follow a quadratic correlation to the ADI in both the M1 and the SCx (M1: $F(9,89)=6.31$, $p=1.5427e-006$, SCx: $F(9,49)=13.9$, $p=2.5696e-009$). Specifically, firing rates were on average 20-30% lower during epochs with steady running, as compared to epochs with rapid acceleration or deceleration (Fig. 4.8c). The relationship between firing rates and ADI were investigated separately for RUN on and RUN off neurons, and the results revealed that during steady

running firing rates were lower in both regions (Fig. 4.9).

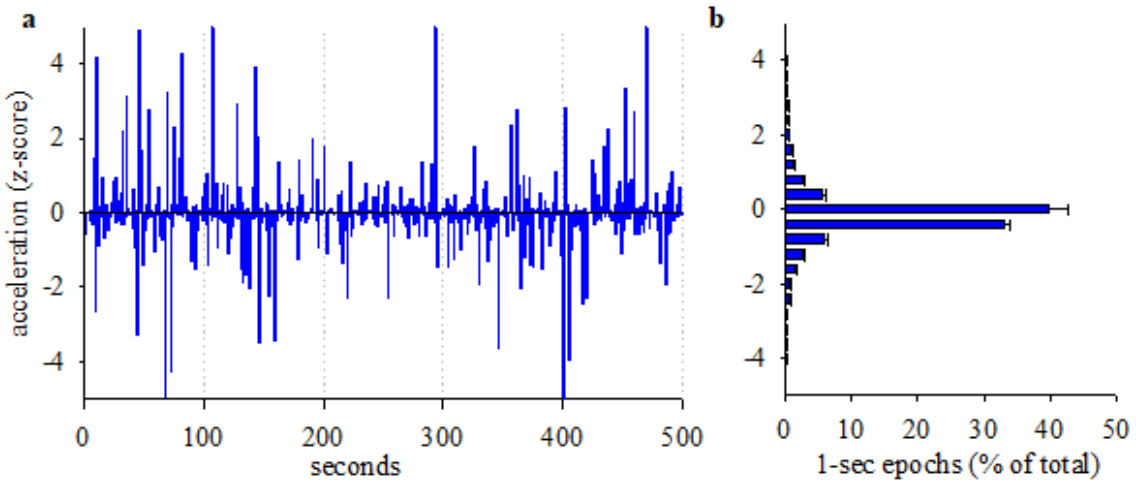


***Figure 4.7**, **The pattern of wheel running.** a) The distribution of 1-sec epochs with wheel acceleration (negative values) or deceleration (positive values) within a representative bout of running. b) Distribution of 1-sec epochs as a function of wheel acceleration and deceleration (z-score). Note that during most epochs, running is stereotypic as manifested in a relatively constant speed, although in a subset of epochs rapid changes in running speed are apparent. Mean values, n=9 mice.*

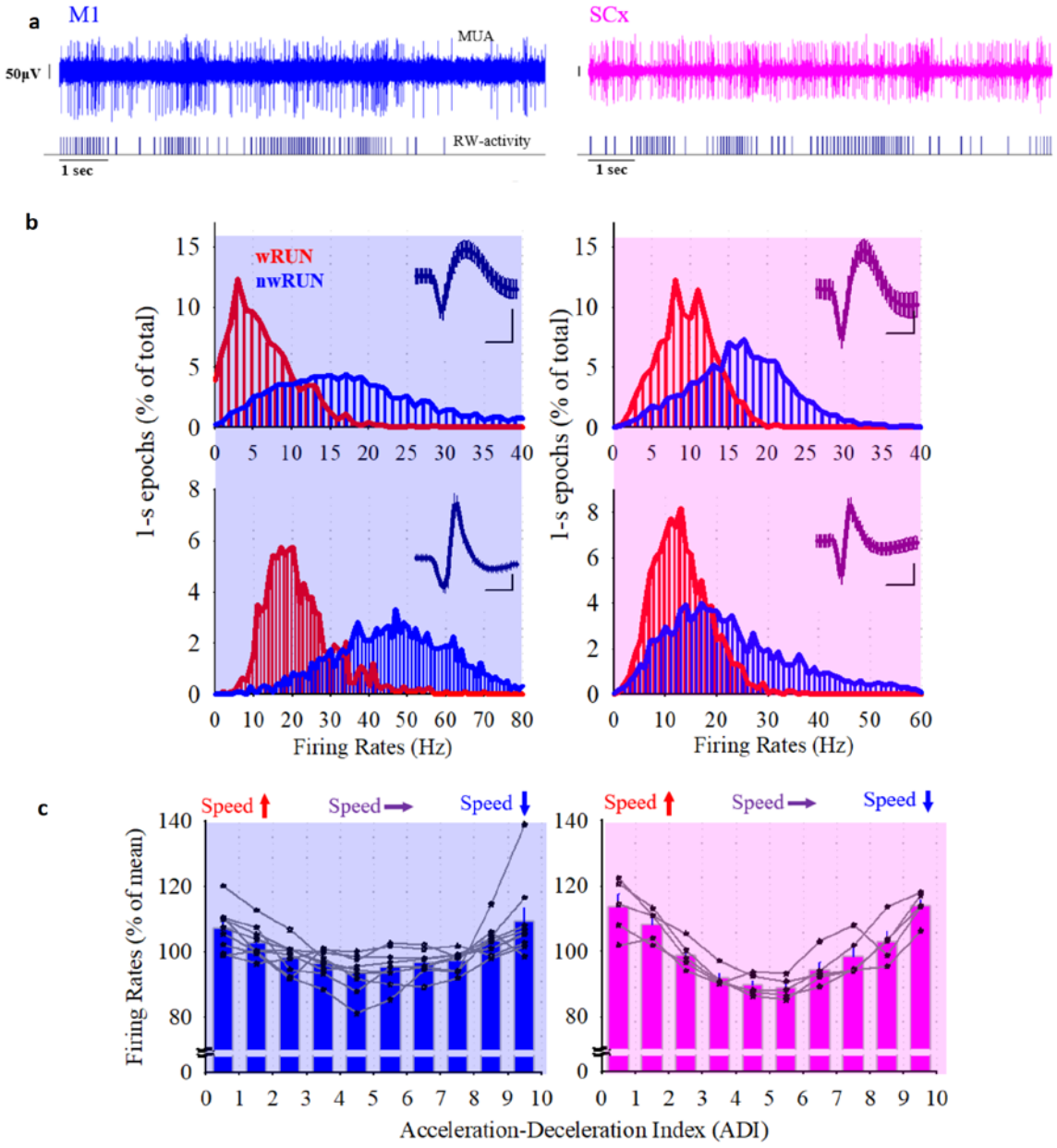


***Figure 4.8**, a) Individual examples depicting cortical firing rates (FR) in the motor cortex (M1) modulated by running wheel behaviour. From top to bottom: MUA recorded in one representative channel of the 16-channel array, and running-wheel (RW)-activity (each vertical bar represents a single wheel rung count). b) The distribution of 1-sec epochs as a function of firing rates during wRUN and nwRUN waking. Four individual putative single units are shown. Blue background relates to data recorded in M1, pink background relates to data recorded in SCx Insets: corresponding spike wave shapes. c) Cortical FR in M1 (blue) and SCx (pink) shown as a function of the wheel acceleration-deceleration index. All 1-sec epochs were subdivided into ten 10-percentiles, each consisting of the same number of epochs. These were sorted as a function of the change in wheel running speed within an epoch from fast acceleration to fast deceleration (schematically shown as arrows above), and corresponding average FR were calculated prior to averaging between animals. Mean values, SEM, M1: n=9 mice, SCx: n=5. Mean values are shown as bar plots, the individual values from individual animals are shown as thin line plots.*

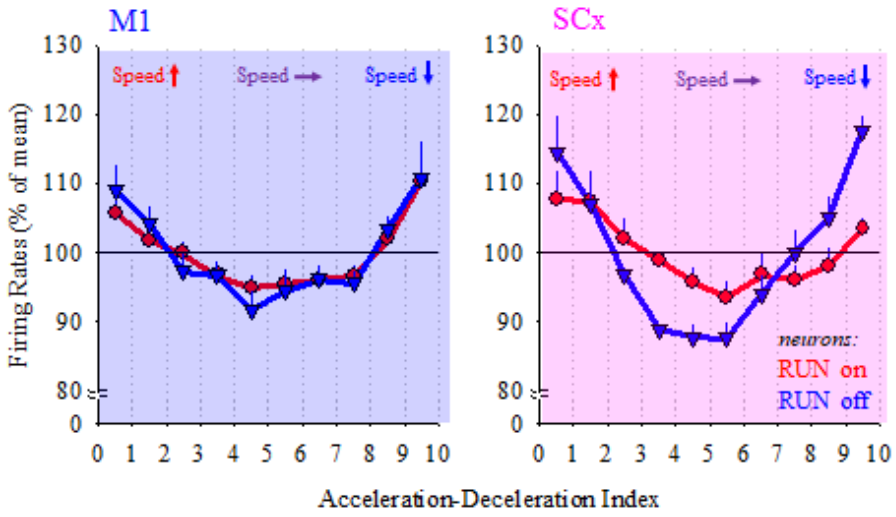


Figure 4.9, The relationship between spontaneous acceleration and deceleration while running on the wheel and cortical firing rates*. All 1-sec epochs were subdivided into ten 10-percentiles, each consisting of the same number of epochs. These were sorted as a function of the change in wheel speed within an epoch from fast acceleration to fast deceleration (schematically shown as arrows above), and corresponding population firing rates were calculated prior to averaging between animals (M1: n=9 mice, SCx: n=5 mice, mean values, SEM). Corresponding statistics are as follows: M1: RUN on, F(9,89)=3.18, p=0.0027; RUN off, F(9,89)=4.1, p=0.0003; SCx: RUN on, F(9,49)=2.49, p=0.03, RUN off, F(9,49)=13.0, p=6.3261e-009. ANOVA for all tests, factor 'ADI'.*

The next question to address was to investigate if the observed relationship between firing rates and running behaviour would persist under different conditions such as time of day, lighting condition and presented with novel objects. To address this, mice were sleep deprived for 6 hours starting at light onset by continuously providing them with novel objects. As typical for C57BL/6 mice, they spent most of their time exploring the objects, and they would also often choose to run on the wheel, with in general, an even distribution of running across the 6-h period of sleep deprivation (F(5,53)=1.24, 6 hours, 9 mice, p=0.31, ANOVA for repeated measures, factor '1-h interval', Fig. 4.10a,b), which suggests that the animals have a high tendency to run even when physiological sleep pressure is high, and at a time of day when they do not normally run. Like under normal

laboratory recording conditions, in all individual animals again exhibited cases of putative neurons decreasing spiking substantially during running (Fig. 4.10c), and on average, firing rates decreased with increasing running speed in all animals (Fig. 4.10d).

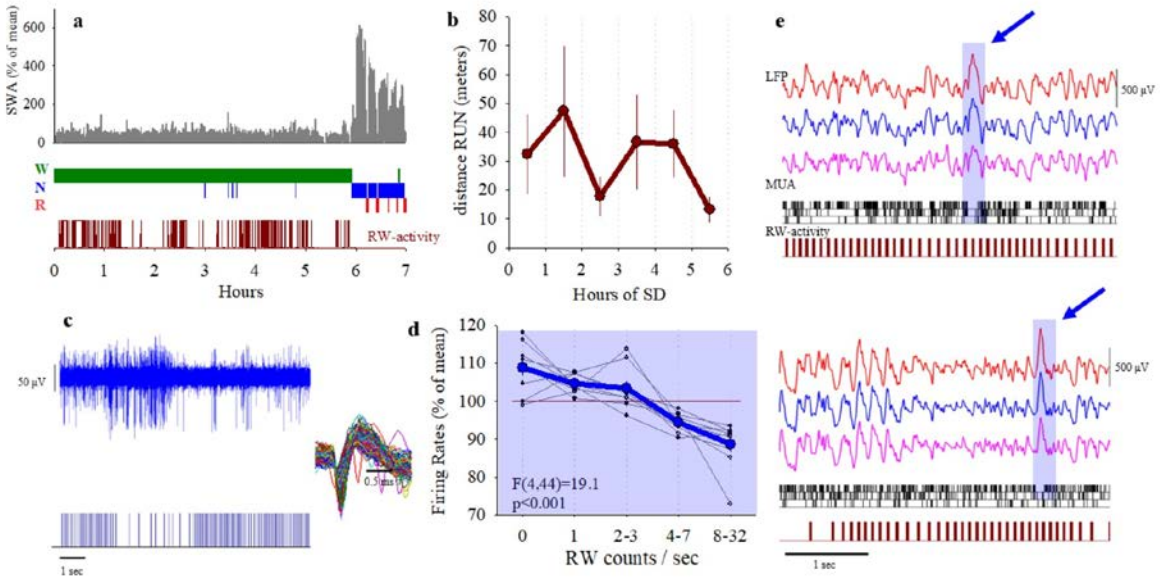


Figure 4.10, Cortical neuronal activity in M1 during wheel running during sleep deprivation. *a) Individual profile of EEG slow-wave activity (SWA, EEG power between 0.5-4.0 Hz) recorded in the frontal cortex, running-wheel (RW) activity and the distribution of sleep-wake stages (W= wakefulness, N = NREM sleep, R= REM sleep) across 6-h of sleep deprivation (SD) and subsequent 1 hour of sleep in one representative mouse. b) Time course of RW activity represented as distance run per hour during 6-h SD. Mean values, SEM, n=9 mice, each bar represents a single wheel rung count. c) Individual representative example depicting the change in cortical neuronal activity as a function of voluntary wheel running. Top: multiunit activity (MUA) trace recorded from M1 together with corresponding RW-activity (bottom), in the same animal. Corresponding waveforms of the action potentials recorded extracellularly from these channels are shown on the right. d) Average cortical firing rates in M1 shown as a function of running speed (x-axis). Thick lines: mean values, SEM, n=9 mice. Values from individual animals are shown as thin line plots. e) Two representative examples of 'sleep-like' LFP/OFF periods (arrows) in M1 occurring during high speed running during sleep deprivation. Top: local field potentials (LFP) recorded concomitantly in three channels of the 16-channel microwire array. Corresponding MUA is shown below as a raster (each bar is an individual spike). Bottom: corresponding RW-activity. Note that a positive LFP wave is accompanied with reduced MUA.*

State-dependent changes in cortical activity are caused by many underlying mechanisms, including intrinsic properties of individual neurons, local and global neuromodulation, active inhibition and disfacilitation, as well as connectivity within the network (Connors and Gutnick 1990; Rudolph et al. 2007; Zagha and McCormick 2014; Okun et al. 2015; Lemieux et al. 2014). Raw data showed occurrence of isolated brief (~100–200 ms) periods of reduced neuronal spiking that corresponded to positive, large and slow fluctuations in the LFP, even during wheel running in both M1 and SCx (Fig. 4.11a,d and Fig. 4.10e). Next, since individual neurons' firing rates are modulated by running behaviour, I investigated the pattern of their spiketrains of each epoch. The distribution of inter-spike intervals (ISIs) during wRUN and nwRUN waking was calculated for each putative single unit. Shorter ISIs were more predominant among RUN off neurons (Fig. 4.11c,f) in both regions, while RUN on neurons showed a higher frequency of longer ISIs in comparison to RUN off neurons, similar to those occurring during NREM sleep (Vyazovskiy et al. 2009).

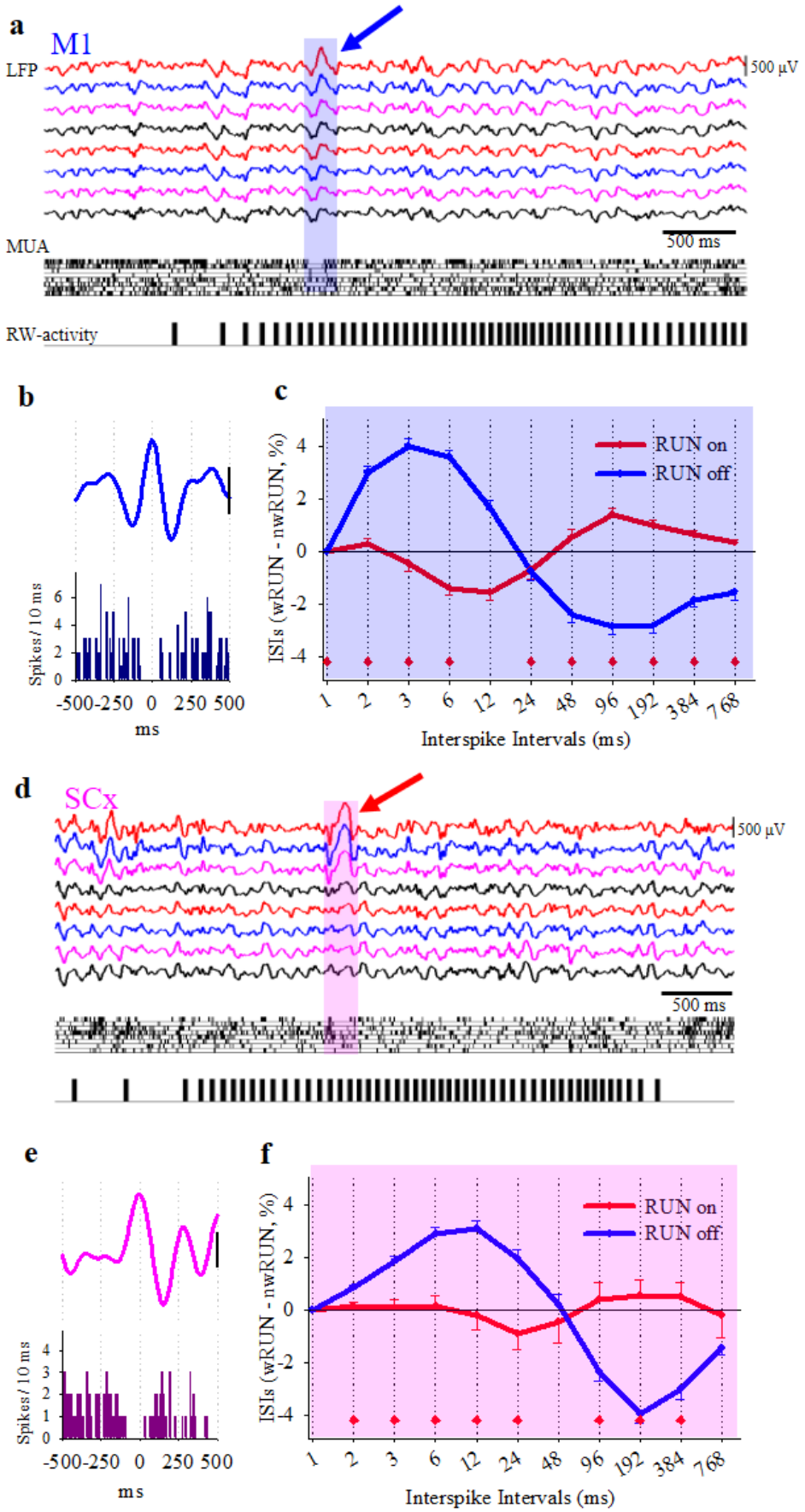

a
M1
LFP
500 µV
MUA
500 ms
RW-activity
b
Spikes / 10 ms
-500 -250 0 250 500
ms
c
RUN on
RUN off
ISIs (wRUN - nwRUN, %)
Interspike Intervals (ms)
d
SCx
500 µV
500 ms
e
Spikes / 10 ms
-500 -250 0 250 500
ms
f
RUN on
RUN off
ISIs (wRUN - nwRUN, %)
Interspike Intervals (ms)

Figure 4.11, Cortical activity during voluntary wheel running. *a) Representative example of an OFF period (arrow) recorded from the motor cortex (M1) occurring during high speed running in one individual mouse. Top traces show representative local field potentials (LFP, 0.1-100 Hz) in eight channels of the 16-channel microwire array. Middle: raster plot of multiunit activity (MUA) recorded in the same eight channels (each vertical line represents a spike). Bottom: corresponding running-wheel (RW)-activity (each bar represents a single wheel rung count). Note that a positive LFP wave is accompanied with reduced MUA in corresponding channels. b) Individual representative example of a positive LFP slow (2-6 Hz) wave recorded with one individual wire of a 16-channel microwire array during wheel running. Bar plot below shows corresponding MUA. Scale-bar: 200µV. c) The distribution of interspike intervals (ISIs) as a function of wheel running behaviour. The number of ISIs calculated as a function of logarithmically increasing ISI duration bins, plotted against lower limits of ISI duration bins. For each putative single unit ISIs were calculated during wRUN and nwRUN waking, and the difference between the two states was calculated separately for RUN on and RUN off neurons. The distribution of ISIs were normalized to the total number of ISIs in each state before subtraction. Mean values, SEM, n=9 mice (red diamonds, $p<0.05$, paired t-test). Note a relative predominance of short ISIs during running among RUN off neurons, compared to nwRUN waking and RUN on neurons. (d, e, f): the same analysis for SCx. Mean values, SEM (n=5 mice).*

The observation of clear cut OFF periods during intense running was unexpected and intriguing, as neuronal down-states are usually considered to be incompatible with active waking, when arousal-promoting neuromodulators are generally increased (Constantinople and Bruno 2011; Polack, Friedman, and Golshani 2013). Therefore, next step was to investigate the occurrence of such events in greater detail, both in relation to running, and in terms of their local occurrence. As a first step, I identified all positive LFP waves between 2-6 Hz associated with at least 20% reduction of neuronal spiking during the 200 ms window centred on the positive peak of the wave (Fig. 4.12b). The next step is to quantify the occurrence of these LFP/OFF periods across the entire 16-channel microwire array per time spent in wRUN and nwRUN waking, and found that during running

overall they occurred at a similar rate between M1 and SCx, but were somewhat more frequent during non-running waking (M1: wRUN, 0.6 ± 0.1 / sec, nwRUN: 1.04 ± 0.1 / sec, $p<0.05$; SCx: wRUN, 0.6±0.1 / sec, nwRUN: 0.87 ± 0.02 / sec, $p<0.05$). Since it was apparent that such events often encompassed only a subset of recording channels, next I calculated the occurrence of LFP waves based on individual channels. Interestingly, although in most channels recorded from M1, the occurrence of LFP/OFF periods was less frequent during wRUN waking (1.6 ± 1.4 channels all 16 recording channels), than in the somatosensory cortex about one third of channels showed more frequent LFP/OFF periods during running (34.3 % ± 7.5 of all recording channels). This suggested an interesting possibility that wheel running is associated with an occurrence of predominantly localized cortical activities.

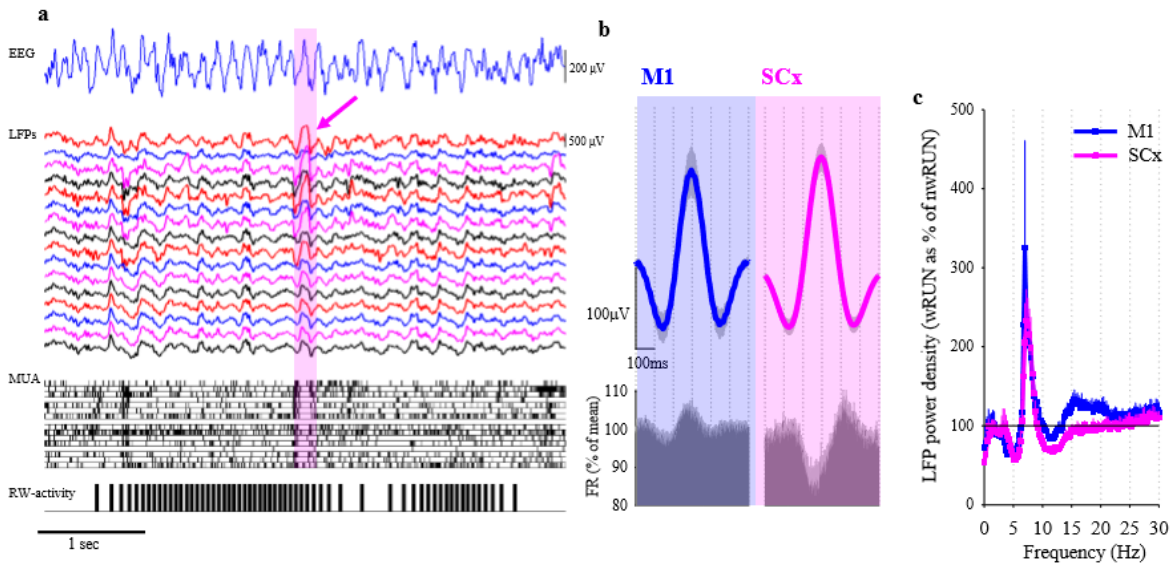


Figure 4.12, Cortical activity during voluntary wheel running. *a) Representative example of EEG, LFP and MUA in the somatosensory cortex (SCx) during high speed running. Top: EEG recorded in the occipital derivation. Note the presence of strong EEG theta-activity, typical for running. Traces below represent local field potentials (LFP) recorded concomitantly in all sixteen channels of the 16-channel microwire array. Corresponding multiunit activity (MUA) is shown below as a raster (each bar is an individual spike). Bottom: corresponding running-wheel (RW)-activity (each bar represents a single wheel rung count). Note that a positive LFP wave (arrow) is accompanied with reduced MUA across most of the 16 channels. b) Average LFP slow (2-6 Hz) wave recorded during waking, and corresponding average MUA from all recording channels in the primary motor cortex (M1) and SCx. Mean values, n=7 mice (M1) and n=5 mice (SCx), s.e.m.. Note that in both regions MUA during waking is modulated by LFP slow waves, but only a moderate reduction of firing rates is observed in the SCx in association with positive LFP wave. c) LFP spectral power density calculated for signals recorded in M1 and SCx. The spectra during running waking (wRUN) are shown as percentage of corresponding spectra during non-running (nwRUN) waking. Mean values, s.e.m. (n=7 and 5 mice for M1 and SCx recordings respectively).*

Caution was taken in making direct comparisons between this "local sleep-like" pattern of activity during running and bona fide NREM sleep because the latter is traditionally defined based on the presence of high-amplitude EEG or LFP slow waves, synchronized across larger cortical networks (Destexhe, Contreras, and Steriade 1999;

Vyazovskiy et al. 2009; Chauvette, Volgushev, and Timofeev 2010b). Typically, during active waking, slow waves are absent, although in some cases a dissociation between behaviour and cortical activity can be induced pharmacologically, such as by administration of muscimol or atropine (Vyazovskiy, Tobler, and Winsky-Sommerer 2007; Qiu, Chen, and Lu 2015). The possibility remains, however, that even in the absence of overt EEG slow-wave activity, a slow pattern could be revealed in the modulation of faster cortical activities. Indeed, visual inspection of individual EEG traces filtered in the theta-activity frequency range revealed that the amplitude of theta-waves during running was not uniform or random, but was instead characterised by a periodic waxing-waning pattern, where each theta-event consisted of several individual theta waves (Fig. 4.12a). The peak-to-peak amplitude of such theta events substantially increased as a function of running speed, on average by 30-40% (frontal: $F(4,32)=7.25$, $p=0.0003$, occipital: $F(4,32)=12.79$, $p<0.0001$), suggesting that during intense running cortical activity is organised in a periodic slow frequency pattern, of ~ 1-2 Hz, showing a surprising resemblance to the periodicity of slow network activity during NREM sleep.

4.3.3 Running prevents wake-dependent increases in firing rates

Similar to previous study (Vyazovskiy et al. 2006), the amount of running during specific waking bouts was correlated with the bout length, and when animals engaged in running behaviour waking bouts were longer (Fig. 4.13a). This observation raised a question that is would running behaviour not only instantaneously change cortical activity as a function of running speed, but also impact cortical activity on a larger timescale. To try to answer this question, firstly spontaneous waking periods lasting > 40 min were selected, and average firing rates across all recorded putative single units in the first 15 min (W1)

and the last 15 min (W2) of each period were compared (Fig. 4.13b, Fig. 4.14). Average firing rates increased significantly by ~10% from W1 to W2, in both the M1 and SCx areas (Fig. 4.13c, $P < 0.05$, paired t-test). Secondly, all waking periods were categorised into two groups (high and low amounts of RW activity), and again changes in firing rates from W1 to W2 of each period were calculated (Fig. 4.13d). Interestingly, the initial firing rates at W1 were not significantly different between low and high RW activity in M1 ('high' running: 12.0 ± 1.2 Hz, 'low' running: 12.0 ± 1.4 Hz, P=0.99).

In 'low-running' waking bouts, there was an increase in neuronal firing rates from W1 to W2 in both regions (M1: +14.7 ± 4.2%, SCx: +21.2 ± 2.0%, $P<0.005$, paired t-test, Fig. 4.13d), while the change was minimal during 'high-running' waking bouts in both M1 and SCx (Fig. 4.13d). This result suggests that the type of behaviour during a specific waking period contributes to wake-time-dependent changes in cortical firing rates. The difference in firing rates between W1 and W2 were calculated separately for RUN on and RUN off neurons (Fig. 4.13e). The results showed that RUN on and RUN off neurons followed similar firing pattern, suggesting that the behaviour-dependent change in cortical excitability may be a widespread network phenomenon.

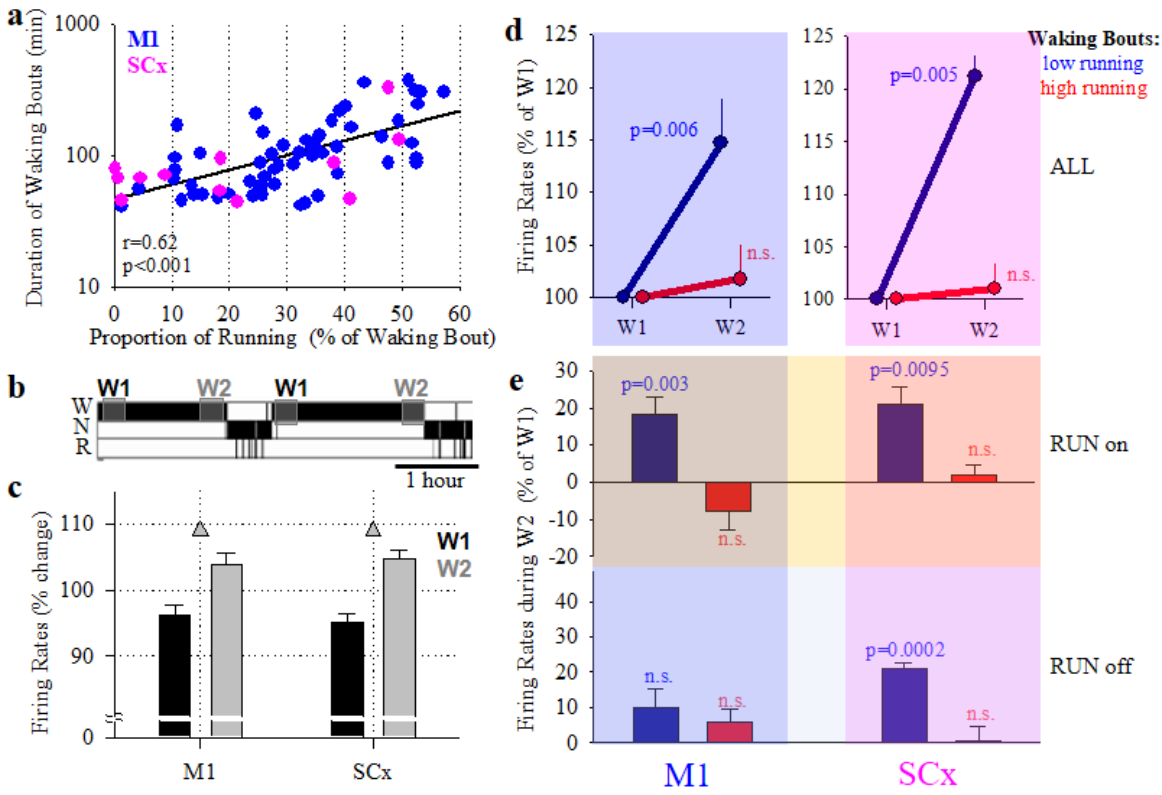


Figure 4.13, *a) The relationship between the proportion of time spent running during a period of spontaneous waking and the duration of the corresponding waking period. Each dot corresponds to an individual waking period. The data are shown separately from animals implanted in M1 (n=11) and SCx (n=5). Note that a higher proportion of running is associated with longer waking periods. b) Sleep-wake stages (W=wakefulness, N=NREM sleep, R=REM sleep) from one representative mouse showing two consolidated spontaneous waking periods. Shaded areas indicate the 15-min time intervals used for comparison between the beginning (W1) and end (W2) of waking periods >40 min. Scale bar, 1 h. c) Average firing rates (FR) during W1 and W2 represented as % of the mean value between W1 and W2 for each putative single unit. Note that on average spontaneous cortical FR increased significantly (triangles, P<0.05, paired t-test) from W1 to W2 in both M1 and SCx. Mean values, s.e.m. (n=11 and n=5 animals for M1 and SCx, respectively). d) Average FR during W1 and W2 shown separately for waking periods with a high or low amount of running (top and bottom 50% of the distribution of all waking periods, respectively = 'high'—red, and 'low'—blue). FR during W2 are shown as % of corresponding values during W1. Note that FR increased significantly only in the course of waking periods with low RW-activity. e) Average FR during W2 shown as % of W1 shown separately for RUN on neurons (top) and RUN off neurons (bottom). As in c, blue bars correspond to waking periods with low RW-activity, and red bars correspond to waking periods with high RW-activity. NS, not significant.*

4.4 Discussion

In this study changes in cortical neuronal firing rates recorded from the motor (M1) and somatosensory (SCx) cortex in freely moving mice during voluntary unrestricted running-wheel (RW) activity were analysed and reported. The results showed that wheel running behaviour modulates a subproportion of cortical neurons, leading to an overall reduction in neuronal activity in M1 and SCx specifically during high speed and/or stereotypic running. Furthermore, these data suggest that the amount and/or type of activity during waking may contribute to wake-dependent changes in firing rates in a region- and behaviour-dependent manner. Overall, these results highlight a complex relationship between locomotion and the activity of individual cortical neurons in freely-moving, non-head-restrained mice, which supports and extends previous findings (Saleem et al. 2013; Niell and Stryker 2010; Vinck et al. 2015; McGinley, David, and McCormick 2015). Recently it has been shown that a subset of neurons in the entorhinal cortex exhibit properties of “speed cells”, manifested in a positive relationship between their firing rates and running speed (Kropff et al. 2015). In contrast, the results showed that a substantial proportion of neurons across the neocortex decrease spiking activity with increasing wheel running speed. An interesting observation, however, was that even within the same area there was a vast diversity in the relationship of individual neurons to running behaviour. However, rather than merely being a correlate of running speed, the decrease in network activity reflected the type of running, such as how stereotypic the running behaviour was. Thus, these data suggest a distinct role of specific cortical circuits in locomotion which is dependent on the precise nature or form of the behaviour, for example automatic locomotion as compared to purposeful or exploratory behaviour when the animal

navigates to obtain a reward. Although each animals were recorded either in M1 or SCx, the implication of long-range connectivity of M1 and SCx is also worth noting, where motor cortex was shown to modulate somatosensory network state in a series of experiments that whisker stimulation and optogenetic excitation of M1 activates S1 in waking mice (Zagha et al. 2013). Therefore, it would be a logical next step to investigate neuronal activity in both cortical regions adopting simultaneous recording.

Contrary to expectation, namely that running acts as an "arousing" stimulus, these data revealed that cortical activity was reduced during running, at least with respect to local cortical states. The role of motivation in spontaneous wheel running remains an important issue. One view is that wheel running is an "addictive" or "rewarding" behaviour per se, and has an intrinsic reinforcement value (Belke and Pierce 2014; Belke and Wagner 2005). In rats, this was demonstrated using conditioned place preference, where prolonged access to the wheel was associated with plasticity in the mesolimbic reward circuitry, including the nucleus accumbens and the ventral tegmental area (Greenwood et al. 2011). Furthermore, it has been reported that wheel running interacts with the rewarding properties or effects of drugs of abuse (Zlebnik et al. 2014; Lacy et al. 2014), suggesting an overlap in the underlying neurophysiological mechanisms. Notably, it has recently been shown that mice have a preference towards running when given a choice between engaging in this behaviour and eating a highly palatable food, and this effect was related to dopaminergic transmission (Correa et al. 2015). At the same time, it was suggested that removing the running wheel might trigger an activation of specific brain regions implicated in motivation and reward (Rhodes, Garland, and Gammie 2003). An alternative view is that RW-activity resembles some forms of naturalistic behaviours, is elective in nature and represents a form of exercise (Meijer and Robbers 2014). Surprisingly,

we also observed that mice readily run during sleep deprivation (SD), which is unusual for at least two reasons. First, this procedure was performed during the light period, when the mice typically do not run. Second, during SD the animals were constantly provided with novel objects. However, animals did not always stop wheel running behaviour to spend time exploring novel stimuli/objects, they often chose to keep engaging in stereotypical running. While the functional significance of this behaviour remains to be determined, these data suggest that even when stereotypic running occurs outside of the usual time and setting, it has similar effects on cortical activity as during spontaneous running during the dark phase. It has been previously shown that blocking access to running wheels substantially affects the distribution of vigilance states, such that animals would fall asleep later and have less sleep altogether when they are given free access to the wheel (Vyazovskiy and Tobler 2012; Vyazovskiy et al. 2006). On the contrary, if access to wheels is restricted to specific times of day, this can phase advance rhythms of behavioural activity, heart rate and body temperature and can even improve these rhythms in mice with core circadian deficits (Power et al. 2010; Schroeder et al. 2012). RW-activity may also affect subcortical circuits relevant for the timing and architecture of vigilance states. Indeed, earlier studies reported effects of running wheel activity on the activity in the suprachiasmatic nucleus (SCN) (Yamazaki et al. 1998; Meijer et al. 1997), which raises an intriguing possibility of behavioural feedback affecting the circadian clock, which could have consequences for the timing of waking and sleep across 24h. While the functional significance of such behavioural feedback remains to be determined, it is tempting to speculate that stereotypic behaviours, such as wheel running may enable a default state, which represents a compromise between maintaining alert wakefulness while minimizing brain metabolic costs normally associated with demanding cognitive activities. Arguably,

this would confer a significant advantage, as it would not only enable animals to remain effectively “online” therefore avoiding dangers associated with a sensory disconnection during sleep, but it may in some cases be necessary for specific behaviours such as during migration or a mating season when prolongation of wakefulness is favoured ecologically (Siegel 2008; Lesku et al. 2012). We propose that this low-cost default wake state is uniquely suited to be effectively placed in the continuum between sleep and specific purposeful, goal-directed behaviours, which renders substantial adaptive flexibility with respect to changing environmental conditions, time of day and homeostatic needs.

It has been suggested that sleep or sleep-like activity represents a “default state” of cortical networks, which does not only provide benefits with respect to energy conservation, but is also essential for the maintenance of anatomical and functional connectivity among cortical and subcortical circuits (Hinard et al. 2012; Lemieux et al. 2014; Sanchez-Vives and Mattia 2014; Corner 2013). These data provide an important new angle to this notion, showing that waking behaviours consisting of repetitive stereotypic movement also share characteristics of a stable default state. We propose that an important feature of this state is that it represents waking of a “lower cost”, as manifested at the neuronal level by an attenuation of wake-dependent increases in cortical excitability. The finding that stereotypic phases of running behaviour may oppose potentially destabilising increases in neuronal excitability is intriguing as it suggests that firing rate homeostasis can, at least in part, be achieved within the awake state.

Chapter 5: Circuit Mechanisms of Brain Oscillations in Sleep and Waking and Relevance to Disease

5.1 Introduction

Schizophrenia is a debilitating psychiatric disorder that affects approximately 1 % of the world's population, and remains one of the most complex and challenging medical conditions to treat (Jablensky 2000; Whiteford et al. 2013). Schizophrenia displays a variety of positive and negative symptoms in humans. Positive symptoms include delusions, disordered thoughts and speech, and hallucinations as manifestations of psychosis. Negative symptoms include little emotion, poverty of speech, inability to experience pleasure, lack of desire to form relationships, and lack of motivation. A more important negative symptom of schizophrenia is cognitive dysfunction, and the deficits impacting cognitive dysfunction are found in various aspects: working memory, long-term memory (Kurtz et al. 2001), verbal declarative memory (Cirillo and Seidman 2003), semantic processing (Pomarol-Clotet et al. 2008), episodic memory (Goldberg et al. 2010), and learning (Kurtz et al. 2001). These symptoms are thought to be caused by a combination of genetic susceptibility and environmental factors (Ruderfer et al. 2014). Mechanistically, many hypotheses suggest that deficiencies in neurotransmitter systems contribute to schizophrenia. The dopamine hypothesis was supported indirectly by observations that pharmacologically increasing extracellular dopamine level with amphetamine can induce psychosis in humans (Bramness et al. 2012), whereas antipsychotics like reserpine that block dopamine reduce positive symptoms of schizophrenia (Walinder et al. 1976). Post-mortem studies indicated neuropathological changes in schizophrenia included both an

increase in striatal dopamine levels and an increase in D2 receptor density (Mackay et al. 1982). Animal studies have also provided evidence to support dopamine hypothesis, the elevation in presynaptic dopamine leads to its release in the absence of appropriate stimuli. Dysregulated dopamine release is thought to lead to attribution of salience to irrelevant stimuli, which is thought to account for psychotic phenomena (Bromberg-Martin, Matsumoto, and Hikosaka 2010; Fusar-Poli et al. 2013). Similarly, the glutamate hypothesis was supported by the observations that schizophrenia was associated with reduced NMDA receptor subunit (R1) in the frontal cortex (Sokolov 1998), and the administration of glutamate antagonists in healthy subjects induced psychosis (Morgan and Curran 2006). The third hypothesis incorporates the first two hypotheses and proposed that general deficits in synaptic function are the underlying cause of schizophrenia (Johnson, Oliver, and Davies 2008); This 'synaptic' hypothesis posited that if presynaptic abnormalities in the neurotransmitter exocytic machinery are altered in schizophrenia, it could yield problems with dopaminergic and glutamatergic signalling, synapse function, and neural development resembling symptoms of schizophrenia (Ramos-Miguel et al. 2015a). Neurotransmitter release involves dynamic molecular machinery of interactions of multiple proteins that dock the neurotransmitter-containing vesicle to the plasma membrane at the release site and mediate membrane fusion. The core *S*oluble N-ethylmaleimide-sensitive factor (NSF) *A*ttachment protein *RE*ceptor (SNARE) complex plays a crucial role in the docking and merging of vesicle to cell membrane. Neuronal SNARE complexes are composed typically of vesicle SNARE synaptobrevin (or vesicle-associated membrane protein, VAMP) and the target SNARE proteins syntaxin and synaptosomal-associated protein 25 (SNAP-25) (Sudhof and Rothman 2009) (See Illus. 2). In response to calcium influx, the SNARE proteins embedded in the synaptic vesicle membrane and cell

membrane form a *trans*-complex that involves zippering of the four helical SNARE complexes (i.e. synaptobrevin, SNAP-25 and syntaxin). Zippering of *trans*-SNARE complexes forces the fusing membranes into proximity. Fully opening the fusion pore requires other facilitating and accessory proteins such as Munc18-1 and complexins. The gradual fusion pore expansion transforms the initial *trans*-SNARE complexes into *cis*-SNARE complexes, which are disassembled by the NSF and SNAP ATPase, and the vesicles are recycled and reused (Sudhof 2013).

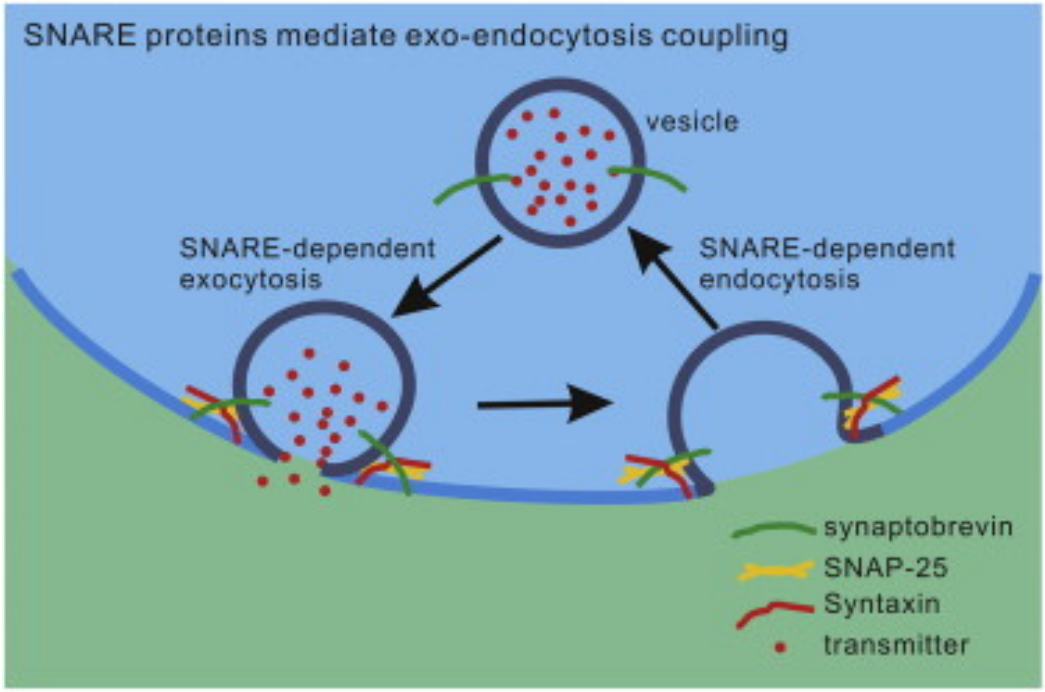


Illustration 2, Adopted from Xu et al. Cell Reports 2013 (Xu et al. 2013)

Therefore, due to the fundamental nature of the SNARE complex in neurotransmission, several psychiatric disease models are based on gene-targeted mouse mutants for SNARE complex proteins. Human biochemical and protein expression data link SNAP-25 protein to a range of psychiatric conditions including schizophrenia. In particular, a significant reduction in SNAP-25 immunoreactivity have been described in the hippocampus of patients with schizophrenia (Thompson, Egbufoama, and Vawter 2003).

SNAP-25 is a cytosolic protein and contributes with two α-helices to the coiled-coiled structure that holds the core fusion *trans*-SNARE complex together (Sutton et al. 1998). There are two variant forms of *Snap-25* gene expression, SNAP-25a and SNAP-25b (Bark 1993). The SNAP-25a protein appears to represent a developmentally earlier and minor isoform, whereas the SNAP-25b protein is the dominant variant in adult brain. Complete knockout of the *Snap-25* gene in mice resulted in death at birth of homozygous mutants, in which not any SNAP-25 isoform gene expression was detected (Washbourne et al. 2001). In a rescuing experiment using viral introduction and overexpression of SNAP-25a or SNAP-25b in embryonic *Snap-25* null mutant chromaffin cells, it was demonstrated that SNAP-25b had a greater ability than SNAP-25a to maintain a larger pool of vesicles in a fusion-ready state in turn achieving fast Ca^{2+}-triggered exocytosis (Sørensen et al. 2003). The fact that SNAP-25 isoforms control late steps prior to fusion by regulating the size of different vesicle pools explains partly biological importance of signalling cells to express SNAP-25a/b in required ratio at different developmental stage. Heterozygous *Snap-25* knockout mice were reported to develop cognitive deficits and cortical hyperexcitability (Corradini et al. 2014), and they only have 50% of normal SNAP-25 expression levels (Washbourne et al. 2001). There have also been efforts to engineer single-gene knockout mutants for synaptobrevin, and the result was similar that homozygous synaptobrevin 2 knockout mice also died at birth, and little phenotypical difference between heterozygous form and wild-type littermates were reported (Schoch et al. 2001). Two additional mouse models relevant to SNARE complex are the complexin I and complexin II knockout mice (Reim et al. 2001). Complexin expression has been found to be altered in the brain of schizophrenic patients, and it was reported that complexin I knockout mice are ataxic and complexin II knockout mice show progressive cognitive and motor deficits (Glynn, Bortnick, and Morton 2003;

Glynn et al. 2005). A recent polyacrylamide gel electrophoresis study in post-mortem sample of orbito-frontal cortex in schizophrenic patients found ~45% increase of SNARE heterotrimer (syntaxin+SNAP-25+synaptobrevin, 150 kDa) and ~65% increase of SNARE-Complexin1 (200 kDa), and 37% decrease in SNAP25-synaptobrevin dimer (70 kDa) and 24% decrease in Complexin I containing oligomers (550 kDa) (Ramos-Miguel et al. 2015b). These alterations indicate enhanced cortical SNARE protein-protein interactions in schizophrenia, putatively due to the increased binding affinity for complexins and/or Munc18-1 (Ramos-Miguel et al. 2015b).

In this chapter, I will focus on the blind drunk (Bdr) mouse model (Oliver and Davies 2009; Jeans et al. 2007), named after its distinctive ataxic gait, which contains a dominant point (T to C) mutation in codon 67 of *Snap-25b* isoform (I67T) resulting in an increased binding affinity for syntaxin within the core SNARE complex which hinder rapid disassembly of SNARE complex and prevent the normal recycling of synaptic vesicles (Jeans et al. 2007). Interestingly, a human patient with neurological problems, including generalised atypical polyspike and wave discharges in EEG, developmental problems in language and intellectual skills and ataxic gait (Shen et al. 2014), has since been identified with a mutation at the same amino-acid position in SNAP-25B (I67N). These clinical symptoms of EEG and ataxic gait resembled similarities in the preliminary analysis to Bdr mutant mice. *In vitro* electrophysiology of intercostal endplate cells of this patient showed that synaptic response to acetylcholine, i.e. endplate potential, was slightly reduced, but acetylcholine quanta showed huge variability sometimes even higher acetylcholine quanta than healthy control group (Shen et al. 2014). Mutant SNAP-25B transfected bovine chromaffin cell exocytosis occurred at a much slower rate and vesicle release generated lower-amplitude spikes than wild-type cells in *in silico* amperometry study (Shen et al. 2014). Thus, altered

spontaneous and depolarisation-evoked exocytosis changes the amplitude of cortical neurotransmission. Like ataxia observed in Bdr mice, the human patient also exhibited difficulties in standing and walking. Another similarity is that the mutation in Bdr also decreased the frequency of the miniature excitatory postsynaptic current in cortical brain slices by 30% of wild-type (Jeans et al. 2007). Bdr mice showed significantly impaired prepulse (90 db) inhibition of acoustic startle (110 db) response, and impaired sensorimotor gating, both important schizophrenia endophenotypes (Jeans et al. 2007). Therefore, blind-drunk mouse is a useful model linking aberrant neurotransmission to behaviour.

Schizophrenic patients have often been shown to have irregularities in sleep and circadian rhythms such as higher variation in day-to-day sleep onset and termination (Wulff et al. 2012). Total sleep time and sleep latency are also reported to be longer in schizophrenic patients than controls (Wulff et al. 2012). There are several rodent models that resemble sleep and circadian phenotypes observed in schizophrenic patients. For example, in the schizophrenic mouse model group II metabotropic glutamate receptors mGlu2 and mGlu3 double knockout mice (Grm2/3$^{-/-}$) showed increased wheel-running activity fragmentation and reduced total activity levels under 12-12 hour light-dark cycle, but no phase change in circadian rhythm was observed (Pritchett et al. 2015). Other schizophrenia related animal models also showed circadian abnormalities. For example, duplications of vasoactive intestinal peptide receptor 2 (Vipr2) were reported to be related to prominently increased risk for schizophrenia in a genome-wide association study (Vacic et al. 2011). Under 12-12 hour dark-dark cycle, in some Vipr2 knockout mice fragmented activity rhythms with ultradian components were observed, while some became completely arrhythmic (Hughes et al. 2004; Hughes and Piggins 2008). Vipr2 is involved in

cyclic adenosine monophosphate (cAMP) signalling and activation of cAMP-dependent protein kinase A, which in turn modulates NMDA receptor mediated synaptic transmission in the hippocampus (Yang et al. 2009), an important structure for REM sleep theta activity.

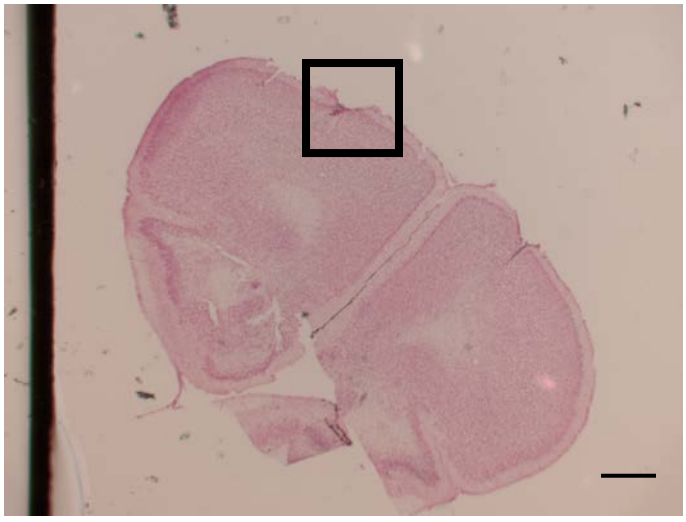
Blind drunk mice, show a reduced amplitude of rest-activity rhythmicity, and exhibited a phase advance in 24-hour rhythms of plasma corticosterone in the suprachiasmatic nucleus (SCN) under normal 12-12 hour light-dark cycle (Oliver et al. 2012). The same authors also reported that Per2: Luciferase expression in the SCN was not affected possibly ruling out a scenario where the core clock is dysfunctional. While the input pathway to the core clock remains intact in Bdr mice (Oliver et al. 2012), this phase advancement and reduced night activity may point to a common cause which resulted in disturbed sleep patterns similarly seen in schizophrenic patients. Not much evidence was collected beyond Oliver et al. in establishing a full account of sleep phenotypes in blind-drunk mutants. In this chapter, I investigated the circadian, sleep and electrophysiological phenotypes of Bdr mutants, for the first time using chronic behavior recording (wheel running activity) and chronic electrophysiology, and for the first time their behavioural and physiological response to sleep deprivation experiments. Since the original Bdr* mutants are reported to show ataxic gaits which would disable animals' wheel running behaviour, I adopted Bdr mutants back-crossed with C57BL/6 mice over six generations (details in Methods section) to elevate this confounding effect.

5.2 Methods

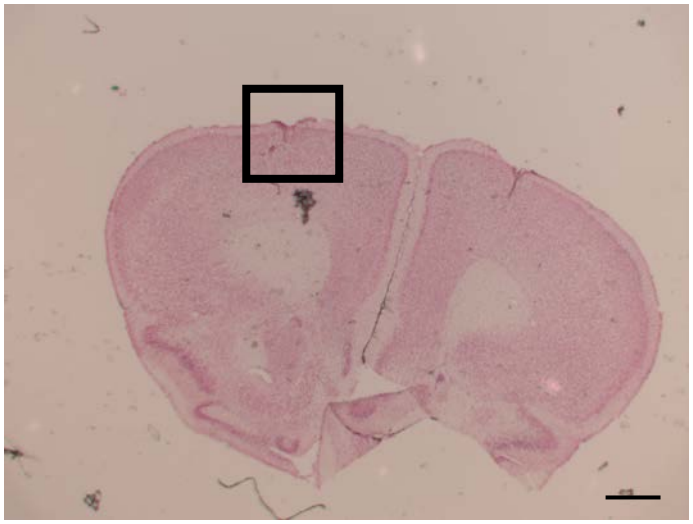
Animals. Male Bdr mutants (Bdr/+) were originally maintained on a C3H/HeH background. For this study, Bdr mice were backcrossed to C57BL/6 over six generations to generate mutant and wild-type littermates (+/+) to assist in data comparisons between new data in this project and other data generated in the group that has been based on the same C57BL/6 genetic background. In addition, C3H/HeH strain contains an endogenous mutation (rd) that causes retinal degeneration and precludes behavioural tasks that require visual acuity.

Circadian rhythm analysis. Wheel running activity was sampled at 256 Hz, and fitted to a 24-hour rhythmicity, the power of which was calculated using Matlab inbuilt function *periodogram()*.

Surgery procedures, histology, analysis of electrophysiological recording, sleep deprivation protocol and statistical analysis are as described in **Chapter 2 General Methods.**



Slice number 1



Slice number 6

*Illustrations showing two brain slices of a Bdr/+ mouse showing traces left by EEG screw implantation (**Black**). Nissl staining. Scale bar = 1 mm.*

5.3 Results

5.3.1 24-hour sleep/wake distribution and EEG spectral analysis

First, I examined the overall dynamics of sleep and waking over the 24 hours of baseline day for Bdr/+ and +/+ mice. All electrophysiological recording started two weeks after recovery from surgery. All mice were entrained to the 12:12 hour Light-Dark cycle after recovery from surgery as shown by the predominant occurrence of wheel-running activity during the dark period (Fig. 5.1a). However, Bdr/+ mice exhibited less running wheel activity than their wild-type counterparts (Fig. 5.1a). In support of this, the total time Bdr/+ mice spent in wakefulness during dark period was significantly less than wild-type mice (Fig. 5.3b and 5.3c, and summarised in Table 1, Bdr vs wild-type Baseline day 13-24 h dark phase, mean values of NREMS time as percentages of total recording time. Difference = 29.206 %, $t = 4.469$, $P < 0.001$, unpaired two-tailed t-test). Next, I examined if the preceding sleep history affected the vigilance states in the dark period. The amount of NREM sleep of Bdr/+ and wild-type mice in the preceding light period were not significantly different (Table 1, $P > 0.05$, unpaired two-tailed t-test), but Bdr/+ mice had less REM sleep (Table 1, Bdr vs wild-type Baseline day 1st – 12th h light phase, mean values of REMS time as percentage of total recording time. Difference = - 4.289 %, $t = - 3.069$, $P < 0.05$, unpaired two-tailed t-test). Combining wheel running activity data in both light and dark periods, Bdr/+ mice showed higher percentage of light period activity (Fig. 5.1b, Difference = 10.2%, $t = 2.584$, $P < 0.05$, unpaired two-tailed t-test). To investigate the difference in the circadian rhythmicity of running behaviour between Bdr/+ and +/+ mice, I plotted wheel count periodogram one Baseline days using Welch's method (Welch 1967) (sampling frequency = 256 Hz, over 24 hours).

Table 1, Time spent in vigilance state in +/+ wild-type mice and Bdr/+ mice

		+/+			**Bdr/+**	
Unit [%]	Waking	NREMS	REMS	Waking	NREMS	REMS
Baseline						
Light						
1-6 h	26.4 ± 2.3	63.5 ± 2.4	9.3 ± 0.5*	30.4 ± 2.4	63.6 ± 2.3	5.7 ± 0.8
7-12 h	28.0 ± 2.2	59.5 ± 1.8	11.5 ± 0.9*	33.4 ± 5.8	59.5 ± 5.0	6.5 ± 1.5
0-12 h	27.2 ± 2.1	61.5 ± 2.0	10.4 ± 0.6*	31.9 ± 3.4	61.5 ± 2.9	6.1 ± 1.1
Dark						
13-18 h	88.0 ± 6.5*	10.7 ± 5.8	0.9 ± 0.6	54.8 ± 7.6	42.0 ± 7.0*	2.9 ± 0.7
19-24 h	72.4 ± 5.6**	24.7 ± 5.0	2.4 ± 0.6	43.6 ± 3.6	51.8 ± 3.2**	4.2 ± 0.6
13-24 h	79.8 ± 5.1**	17.7 ± 4.4	1.7 ± 0.5	45.0 ± 5.0	46.9 ± 4.3**	3.6 ± 0.6
Sleep Deprivation						
0-6 h	99.8 ± 0.1	0.2 ± 0.1	0.0 ± 0.0	99.3 ± 0.3	0.6 ± 0.3	0.0 ± 0.0
Recovery						
7-12 h	18.5 ± 1.1	69.0 ± 1.2	12.1± 0.6**	21.7 ± 1.9	71.3 ± 2.3	6.6 ± 0.6
13-18 h	81.2 ± 6.5*	16.0 ± 5.5	2.7 ± 1.0	54.3 ± 5.6	40.8 ± 5.1*	4.6 ± 0.7
19-24 h	57.6 ± 8.5	36.6 ± 7.3	5.6 ± 1.3	51.4 ± 4.7	43.5 ± 3.5	4.6 ± 1.2

Table 1, *Mean values ± S.E.M. of waking, NREM sleep and REM sleep expressed as percentage of recording time for +/+ (n = 6) and Bdr/+ (n = 8) for 6 - h intervals, and the 12 – h light and dark period during baseline, 6 – h sleep deprivation and the following recovery period. Sleep deprivation began at light onset. ** P < 0.001; * P < 0.05, two-tailed t-test between genotypes. Asterisks(*) next to numbers indicates significantly larger mean values than that of genotype counterpart's.*

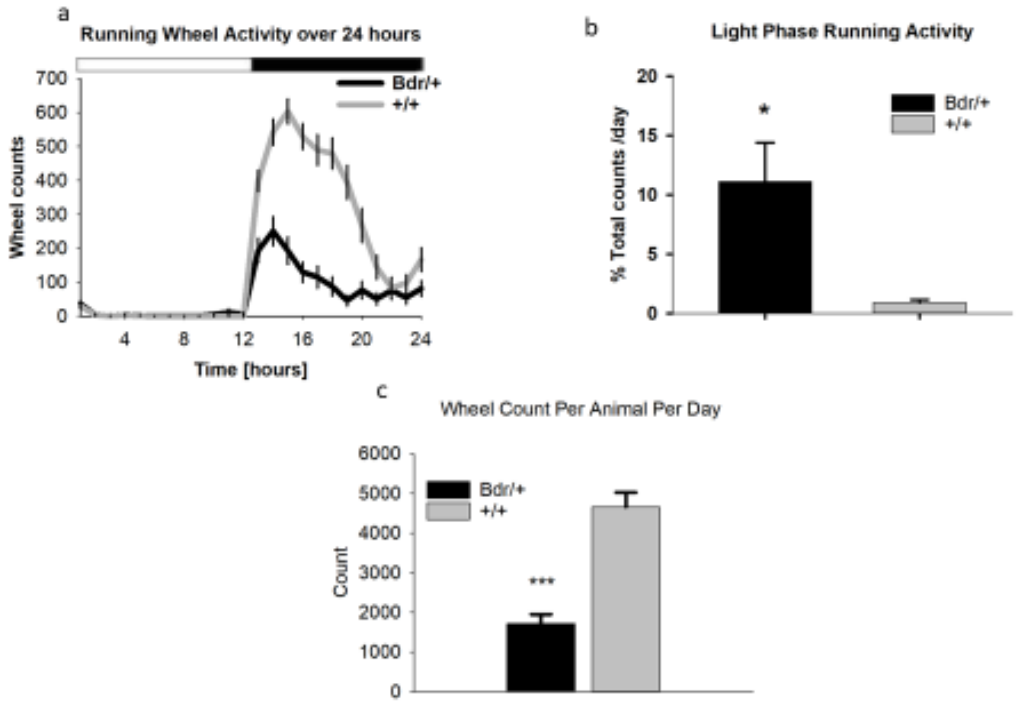


Figure 5.1, *a) Mean values of 24 – hour wheel running activity of Bdr/+ (n = 8) and +/+ mice (n = 6). White-black horizontal bar indicates light and dark period in the home cage. b) Mean percentage of running activity in the light phase with respect to 24 – hour period, and asterisk(*) indicate P < 0.05 between genotypes (unpaired t-test). c) Mean running wheel count (distance measure) run by Bdr/+ and +/+ mice. asterisk(***) indicate P < 0.001. All error bars are S.E.M.*

Fig. 5.2c illustrates an example of 24-hour SWA timecourse of a Bdr/+ mouse on a Baseline day. The majority of Bdr/+ mice (7 out of 8) showed similar SWA timecourse to this example, and the remaining Bdr/+ mouse showed SWA timecourse similar to that of a wild-type mouse as in Fig. 5.2b. 12 - hour SWA of wild-type (Fig. 5.3a) showed a consistent decreasing trend across the light period, whereas SWA of Bdr/+ showed a flatter decreasing trend with inconsistencies during 9^{th} to 12^{th} hour. Graphical representation of Table 1 (Fig. 5.3b and 5.3c) again shows expected activeness during dark period by wild-type mice, and reduced activity in the same period for Bdr/+ mice.

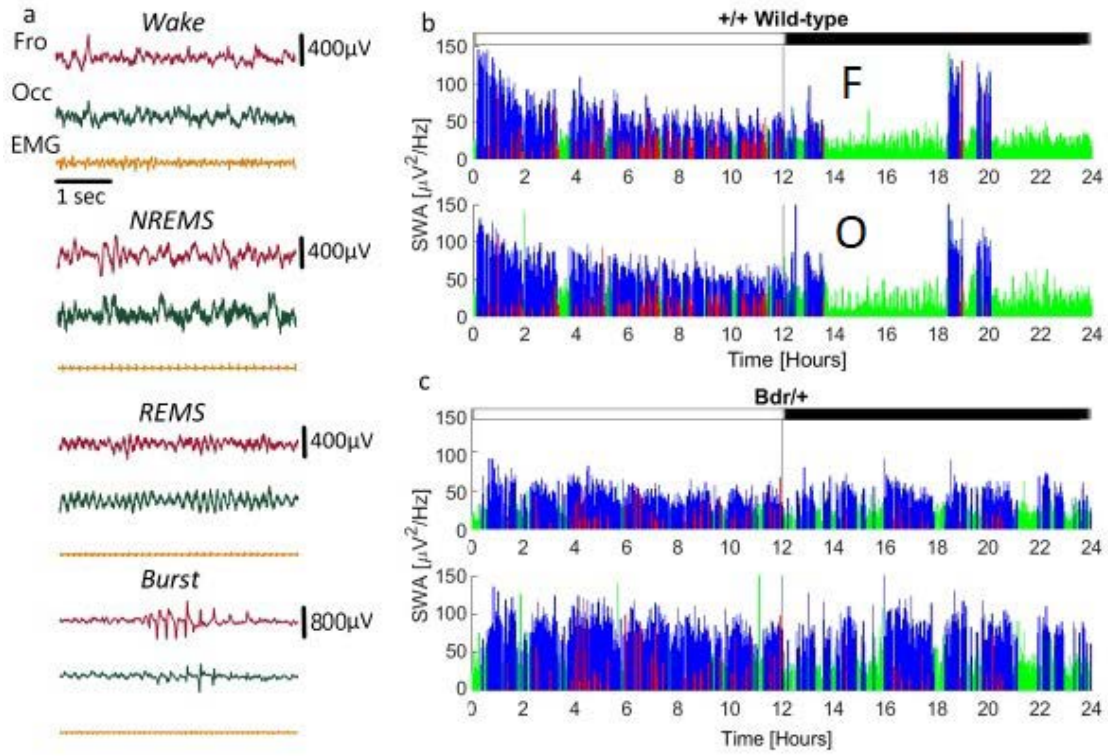


Figure 5.2, *a) Representative raw EEG traces from a Bdr/+ mouse of each vigilance state and a burst event. Bdr/+ and +/+ mice have similar raw EEG traces except Burst events. b,c) Representative 24 – hour Slow Wave Activity in +/+ wild-type mouse and Bdr/+ mouse. Upper panel shows the frontal derivation, and lower panel shows occipital derivation. NREM sleep were shown in blue; Wake in green; REM sleep in red.*

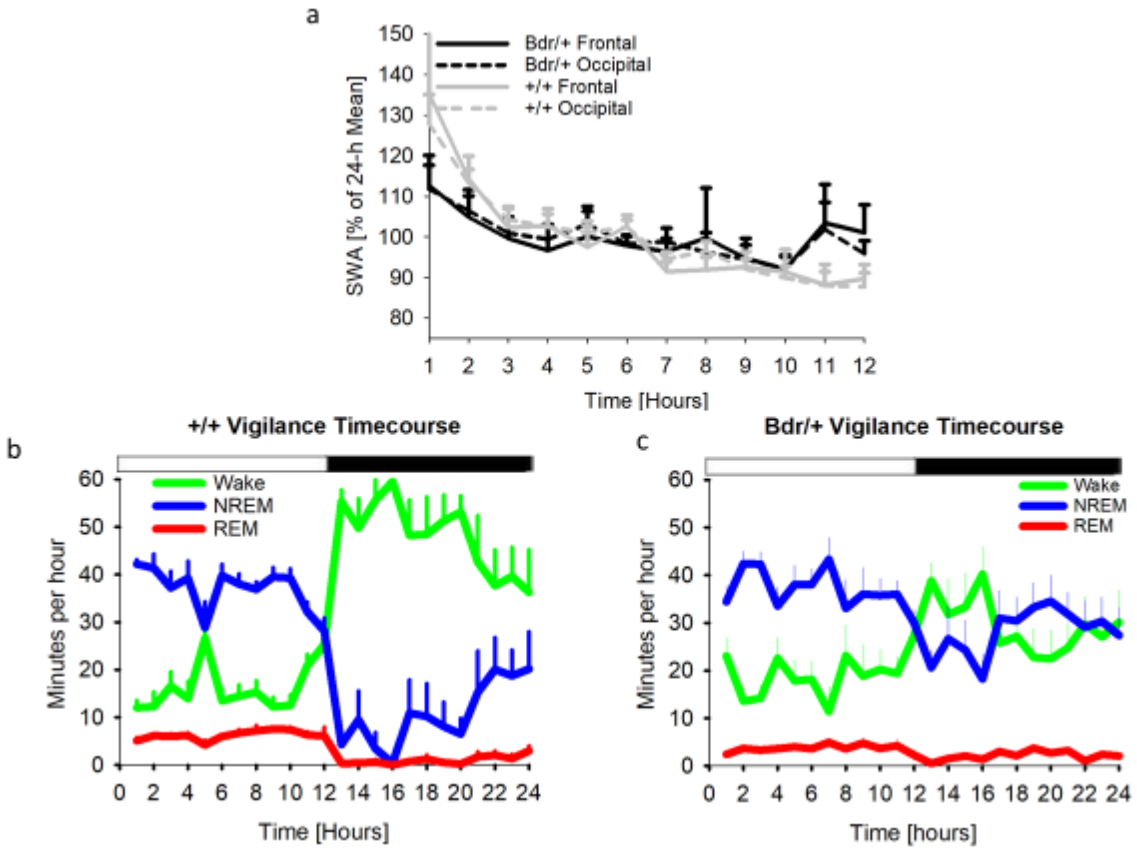


Figure 5.3, *a) Mean values of SWA of Bdr/+ (n = 8) and +/+ (n = 6) across 12-hour Baseline day shown as percentages of 12 – hour mean of each animal. b, c) Mean values of minutes spent in each vigilance state (Wake, NREM sleep and REM sleep) by Bdr/+ and +/+ animals. All error bars are S.E.M.*

To investigate if there is any difference in the electrophysiology in the neocortex due to genotypical variation that gave rise to disruption in the overall sleep/wake distribution structure, first I compared mean EEG power density between +/+ and Bdr/+ mice in each vigilance state (Fig. 5.4). 4-second epoch's EEG power density plots show reduced power in the higher EEG frequency Beta band (15 – 30 Hz) in NREM sleep and in REM sleep in the frontal and occipital derivations. Wake and REM sleep are widely reported to be dominated by theta activity as exemplified by +/+ mice, whose EEG power density peaked in EEG Theta band (5 – 10 Hz). Bdr/+ mice showed decreased peaks in the Theta range in Wake and REM sleep (reached statistical significance in the occipital derivation

between 7.5 – 10 Hz during REM sleep; between 8 – 10 Hz during Wake, P < 0.05, unpaired two-tailed t-test on log-transformed values). Total EEG power densities in the frequency range (7 - 30 Hz) between Bdr/+ and +/+ mice (Fig. 5.5) were not significantly different, but reached p-value of 0.06 (unpaired two-tailed t-test) in the occipital derivation.

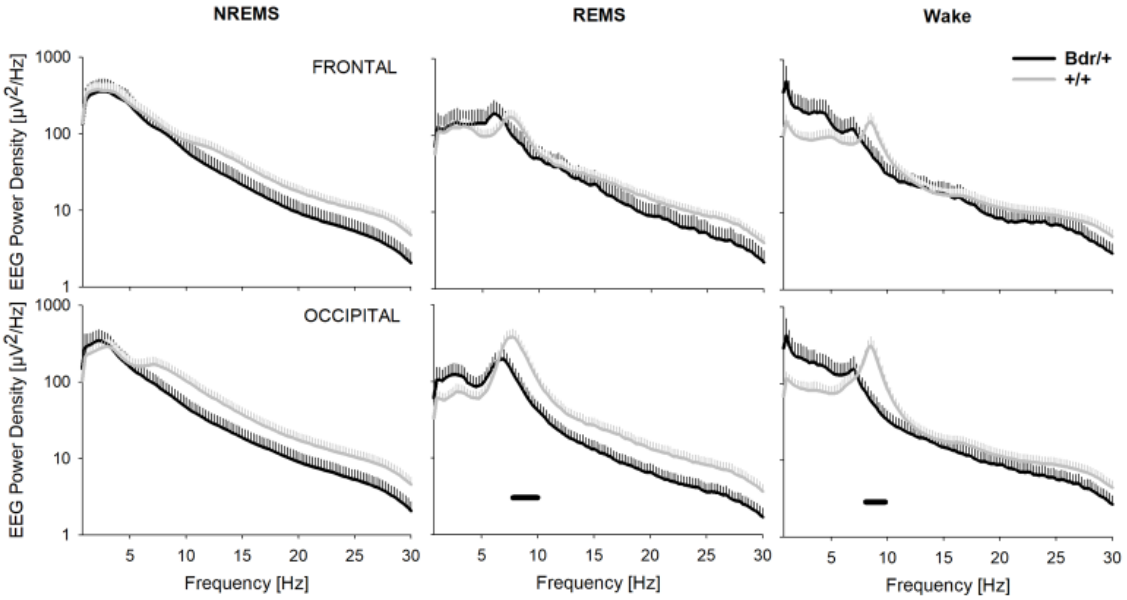


Figure 5.4, *EEG power density spectra of Bdr/+ mice and wild-type mice in NREMS and REMS for the 24 – hour baseline day. Mean values (Bdr/+ mice, n = 8; +/+ mice, n = 6) in $\mu V^2/Hz$ are plotted on a logarithmic scale, for frontal (top panels) and occipital (bottom panels) derivations. Horizontal lines represent mean values of EEG power density of Bdr/+ and +/+ mice are significantly different for the corresponding frequency bins (7.5 – 10 Hz for occipital derivation during REM sleep; 8 – 10 Hz for occipital derivation during Wake, P < 0.05, unpaired two-tailed t-test on log-transformed values).*

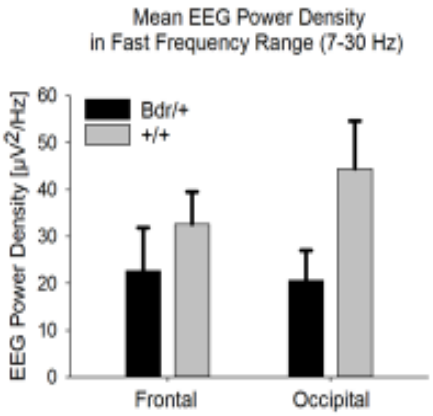


Figure 5.5, *Barplot shows the means of EEG power density in all vigilance states in the fast frequency range (7 – 30 Hz).*

5.3.2 Characterising 'Burst' activity

In Fig. 5.6 & 5.7, I summarised the characteristics of 'burst' activities observed in Bdr/+ mice. Burst activities occurred in all vigilance states, and Fig. 5.6a showed slight differences in the amplitudes of bursts observed in Wake, NREM sleep and REM sleep states in both frontal and occipital derivations. Comparatively speaking, bursts occurred most in the Wake state, then in REM sleep and least in NREM sleep (Fig. 5.6c). I also observed bursts during quiet wakefulness (Fig. 5.6a) and during active wakefulness e.g. during wheel running (Supp. Figure 1). EEG spectral analysis of 4-sec epochs containing EEG burst activity showed a slower peak frequency at 4.5 Hz in Wake and NREM sleep and faster peak frequency at 5.2 Hz in REM sleep in the frontal derivation. Although very similar peak frequencies were observed in the occipital derivation in all states, peaks in EEG power density were less prominent and showed smaller amplitudes in occipital derivation (Fig. 5.7b). The absence of peaks in EEG spectrogram between 9 - 16 Hz also illustrates that when identifying burst epochs spindles were not mistaken with bursts.

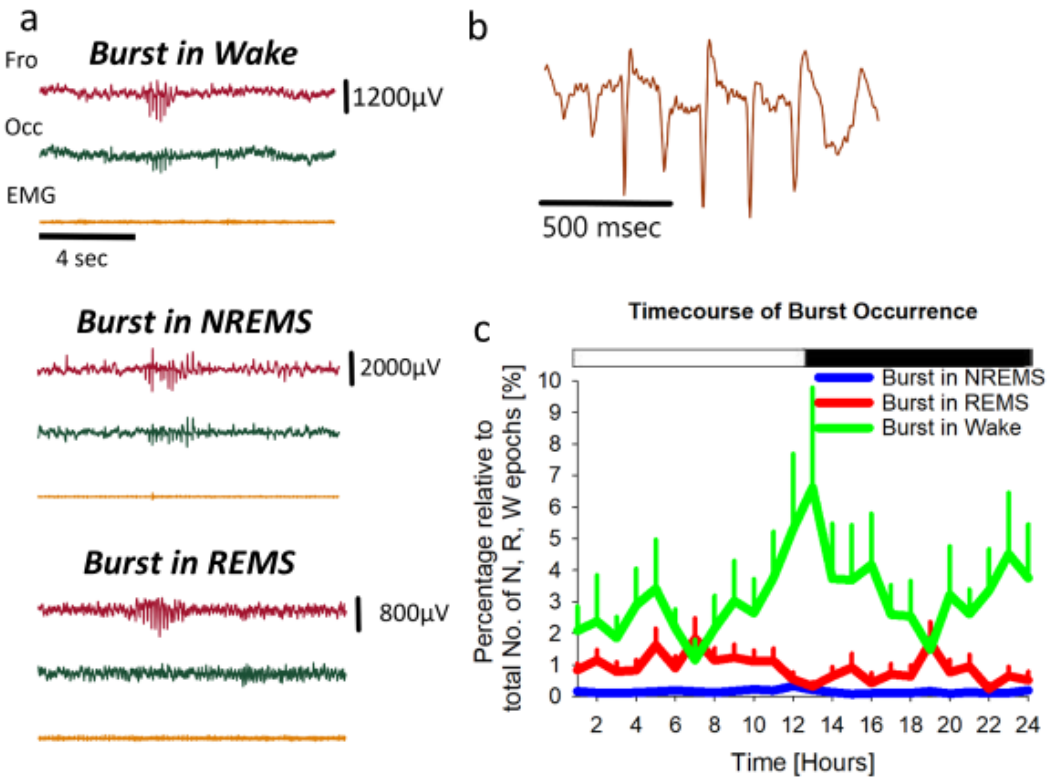


Figure 5.6, *a) Example 12-sec raw traces of EEG and EMG capturing a 'burst' event in each vigilance state. b) The same 'burst' activity in a) 'Burst in Wake' from frontal derivation plotted on a smaller scale. c) Mean number of 4-second epochs capturing a Burst event in Bdr/+ mice (n = 8) plotted in each vigilance state (NREM sleep, REM sleep and Wake) across 24-hour Baseline day (total number of Burst epochs per animal in 24 hours = 1946 ± 289.7, mean ± S.E.M.). Each value point represents sums of number of epochs per hour. Note different EEG amplitude scales.*

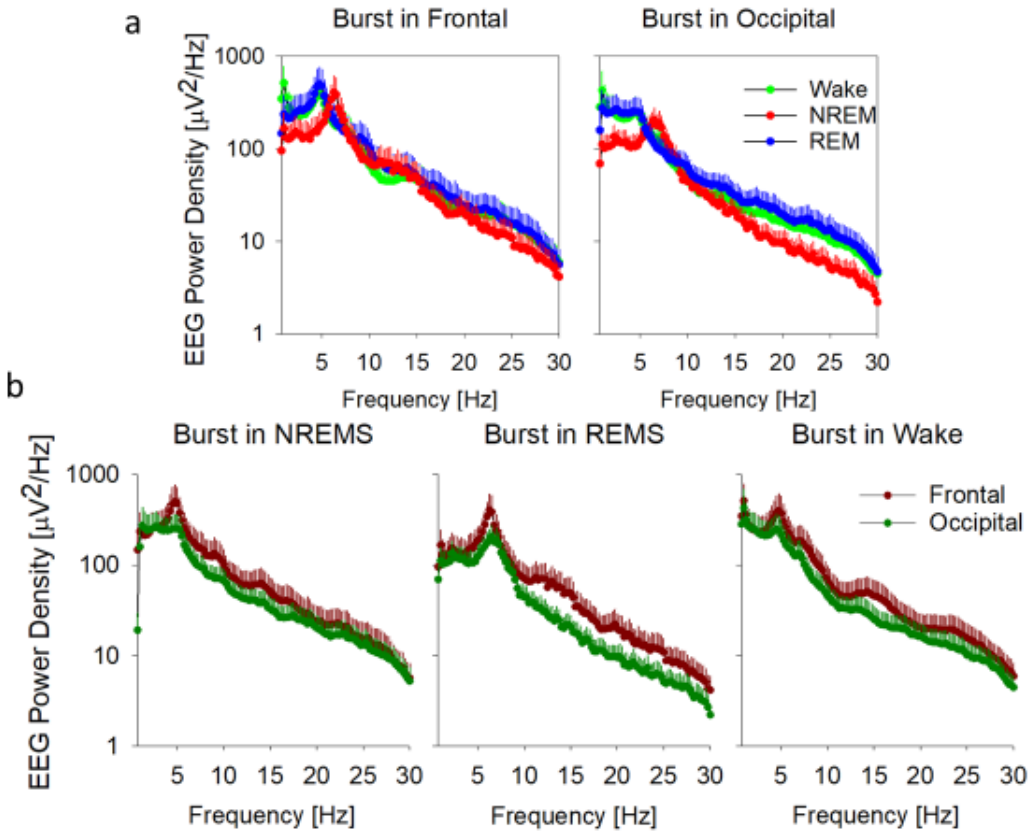


Figure 5.7, *a) Mean EEG power density of 4-second epochs capturing a Burst event in 24 hours (NREM sleep, REM sleep and Wake). Left panel shows frontal EEG derivation, right panel shows occipital EEG derivation. b) Mean EEG power density of 4-second epochs capturing a Burst event in each vigilance state (total number of epochs per animal in each vigilance state: NREMS = 380.6 ± 64.9; REMS = 153.9 ± 24.2; Wake = 1411.5 ± 304.4, mean ± S.E.M.). All error bars are S.E.M.*

To find out if burst events are homogeneous within each state, I plotted a histogram of number of epochs containing burst activity (probability density plot) with respect to their peak frequencies (Fig. 5.8). In both NREM sleep and Wake states, peak frequencies formed a Gaussian distribution, whereas in REM sleep the distribution seems to be bimodal. These data illustrate the 'burst' events in EEG as one of the electrophysiological phenotypes of Bdr mutants, and furthermore show subtle variations in the characteristics of 'burst' events between vigilance states.

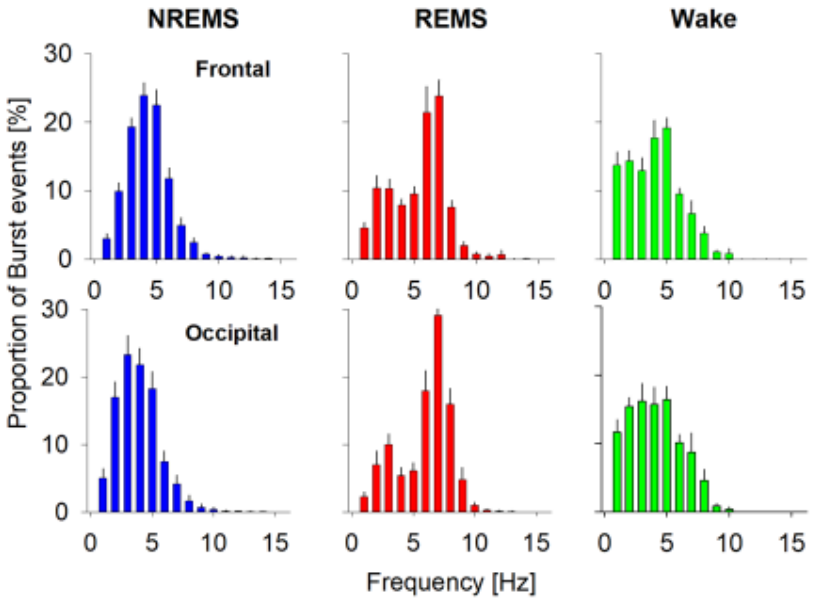


Figure 5.8, *histograms of peak EEG power frequencies of Burst events relative to total number of burst events (shown in percentage) in a Bdr/+ mouse in each vigilance state. Top panel shows frontal derivation, and bottom panel shows occipital derivation. All error bars are S.E.M.*

5.3.3 Sleep Deprivation experiments on Bdr/+ and wild-type mice

I performed sleep deprivation (SD) experiments on Bdr/+ and wild-type mice lasting 6 hours from light onset. As shown in Table 1, both genotypes were able to be kept awake throughout the SD period (Wake duration larger than 99% of total SD duration in both genotypes). In Fig. 5.9, I examined the EEG power density of Recovery sleep (six hours) in two-hour intervals with respect to the average EEG power density of Baseline day light period (Table 2, shown as percentages). Expectedly, the largest increases in power were in the EEG delta band and were most prominent in the first two-hour interval for both genotypes. As recovery sleep went on, the peak in EEG power gradually decreased, and by the third interval the EEG power spectrograms of Bdr/+ and +/+ mice were almost level with those on Baseline day light period. Another observation is that in wild-type mice, the

maximum increase in the amplitude of delta waves was 37.3% higher and 24.4% higher in the frontal and occipital derivation respectively than Bdr/+ mice in the first interval. The gap in percentage increases between two genotypes seen in the first interval gradually closed down towards the end of recovery sleep. Notably, the amount of REM sleep during six-hour Recovery sleep showed again shorter duration in Bdr/+ mice than in wild-type mice (Table 1, Bdr vs wild-type SD day 7^{th} – 12^{th} h light phase, mean values of REMS time as percentage of total recording time. Difference = - 5.476 %, t = - 5.872, $P < 0.001$, unpaired two-tailed t-test). Following the six hours of recovery sleep in the light period all mice were left undisturbed to be continuously monitored during the following dark period. The Bdr/+ mice showed, consistent with Baseline day, longer durations of NREM sleep than wild-type mice in the first half of dark period (Table 1, Bdr vs wild-type SD day 13^{th} – 18^{th} h light phase, mean values of NREMS time as percentage of total recording time. Difference = 24.863 %, t = - 3.277, $P < 0.01$, unpaired two-tailed t-test). Together these data show that there is a profound difference in cortical activity of Bdr/+ mice from wild-type mice after a prolonged wakefulness, which suggests there is an underlying mechanistic difference that is manifested here

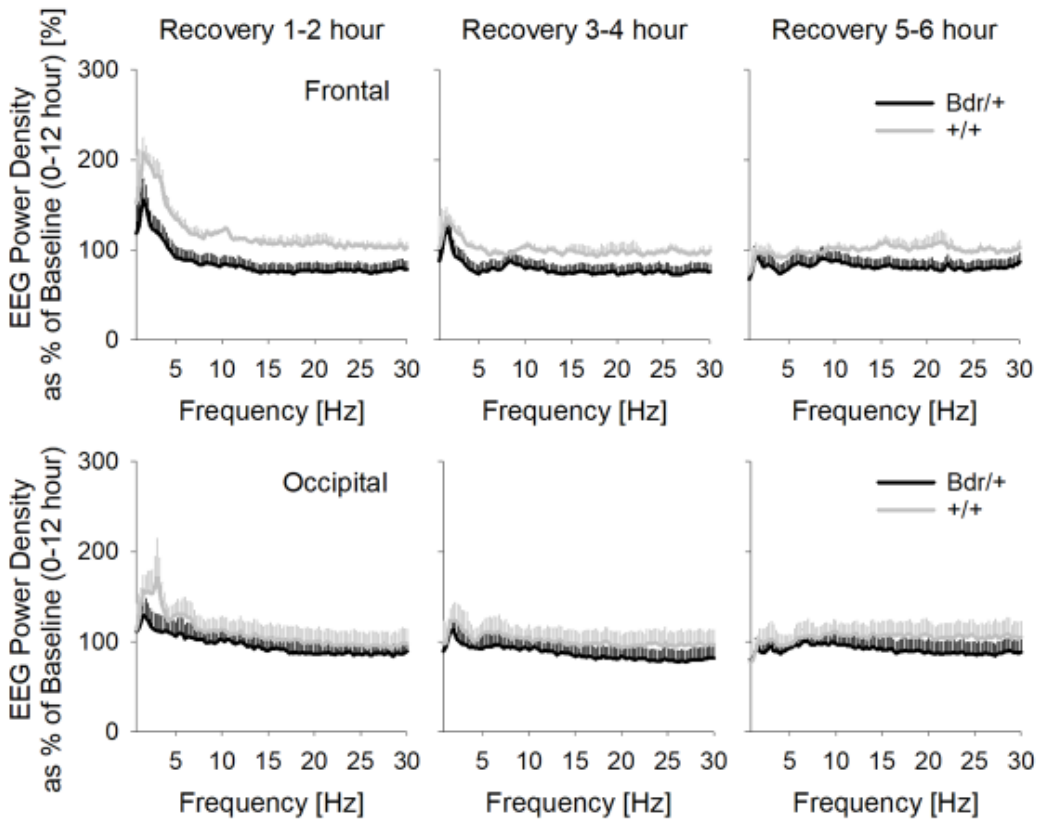


Figure 5.9, *EEG power density of Bdr/+ (n = 8) and +/+ mice (n = 5, 1 outlier removed from analysis) during the recovery sleep (Sleep Deprivation day 7th - 12th hour) after 6 hours of sleep deprivation, shown as the percentage of the mean EEG power density of Baseline day's light period (mean of 1st – 12th hour). Mean recovery sleep EEG power density is shown in three two-hour intervals. Mean Baseline day EEG power density was computed including wake, NREM sleep and REM sleep, and recovery sleep EEG power density was computed for only NREM sleep. Top panels and bottom panels show frontal and occipital derivations respectively. All error bars are S.E.M.*

Table 2, Percentage change in the EEG delta power during Recovery sleep compared to Baseline day light period EEG delta power.

	+/+			**Bdr/+**		
	1-2 hours	3-4 hours	5-6 hours	1-2 hours	3-4 hours	5-6 hours
F [%]	207.5±17.0*****	135.8±11.3	98.2 ± 9.2	155.4 ±23.2	123.7±19.7	92.5±14.1
O [%]	170.8±44.0*****	123.4±17.6	102.8±19.5	129.5 ±21.7	113.0±18.6	94.8±13.5

Table 2, *mean values ± S.E.M. of maximum percentage change in the EEG delta band power density. Asterisk (*) indicate $P < 0.05$ for unpaired two-tailed t-test between corresponding value of Bdr/+ and wild-type mice.*

5.4 Discussion

The basic activity profiles of blind-drunk mice show reduced activity measured by wheel running in the dark phase compared to wild-type littermates; worse entrainment to circadian light-dark cycle due to Bdr mice's activeness in the light phase and overall reduced activity within 24 hours. Although Bdr/+ mice in this study were backcrossed to C57BL/6 as a new genetic background compared to the Bdr mice* study in (Oliver et al. 2012), they both showed very similar activity profiles. Another similarity between the Bdr mice* in (Oliver et al. 2012) and Bdr mice in this study is heterogeneity in rest and activity patterns that ranged from robust and entrained rhythms to highly irregular circadian profiles. This type of individual variation can also be seen in schizophrenic patients, and is ascribed to genetic variability (Wulff et al. 2009), and it was suggested that a predisposing gene for a neuropsychiatric disorder could produce either heterogeneity alone or be altered by subtle environmental factors.

Receiving input from subcortical regions: EEG power spectrogram during REM sleep followed similar patterns, except Bdr/+ mice were not able to produce peaks in theta band compared with wild-type mice. During REM sleep, the hippocampal theta rhythm that characterises REM sleep is driven by septo-hippocampal projections from GABAergic neurons (Gerashchenko, Salin-Pascual, and Shiromani 2001). Lu and colleagues found, by using retrograde labelling method, that neurons that project to medial septum during REM sleep initiation were found in the precoeruleus region and are primarily glutamatergic (Lu et al. 2006). The same study also reported, by lesioning the precoeruleus region, EEG theta rhythm was abolished during sleep. Even though EEG theta activity persisted in Blind-drunk

mice, less predominant peaks were observed in mutants compared to wild-type mice in the frontal and occipital EEG derivations. This suggests that the strength of inputs received by cortical neurons from efferent hippocampal GABAergic and/or glutamatergic (Ujfalussy and Kiss 2006) projections was weakened by the defects in the synaptic vesicle release mechanisms in Bdr/+ mice. In support of this, Jeans *et al.* showed in an electrophysiological study that layer II/III neurons of somatosensory cortical acute slices of Bdr mutant mice showed less frequent miniature excitatory post-synaptic currents compared with wild-type littermates (Jeans et al. 2007). Furthermore, I reported a significant reduction in the total time spent in REM sleep in Bdr/+ mice compared to wild-type mice (Table 1 and Results section) during light period of Baseline day. This may link to reduced level of input from the precoeruleus, which is involved in REM sleep initiation circuitry (Lu et al. 2006; Saper et al. 2010). The average duration of each REM sleep episode of Bdr/+ mice did not differ from wild-type mice ($P > 0.05$, unpaired t-test). One study previously found that optogenetic activation of cholinergic neurons in the pons increased the frequency of REM periods, but did not affect their duration (Van Dort et al. 2015). Grosmark and colleagues showed that during an episode of NREM-REM-NREM sleep, the firing rates of hippocampal pyramidal neurons and interneurons in the septal region during NREM sleep had least correlation with hippocampal LFP power density in the theta band during REM sleep (Grosmark et al. 2012). Reduced correlation seemingly enforces the argument that neuronal activities in the hippocampus during REM sleep are strongly influenced by afferent projections from other brain regions most likely the brain stem. Interestingly, the same study reported the latter NREM sleep episode showed significant decrease in the hippocampal LFP spectral power than the former NREM sleep episode in the delta and theta frequency range (Grosmark et al. 2012), suggesting a reorganisation role of REM

sleep on hippocampal firing rate and a functional role of REM sleep on NREM sleep homeostasis.

Effects of reduced REM sleep duration and REM sleep theta power on general sleep/wake architecture in Bdr/+ mice. Previously, a model of REM sleep homeostasis was proposed (Benington and Heller 1994a, 1994b) that homeostatic pressure - or need for REM sleep - drives the expression of REM periods. While asleep, REM pressure accumulates during NREM sleep and triggers a REM period. Although this model has been criticised, it is difficult to validate experimentally because to date no directly quantifiable measure of homeostatic REM pressure has been identified. But results in this chapter may be relevant to the REM sleep homeostasis hypothesis. Since total REM sleep time is reduced in Bdr/+ mice, it could have been caused by ill-functioning subcortical circuit that sends disrupted input from the precoeruleus to and relayed by the hippocampus onto the cortex. As REM sleep pressure was not dissipated in Bdr/+ mice during the light phase, in order to normalise REM sleep pressure in the dark period, Bdr/+ mice continuously fall in to NREM sleep, from which the animals can enter into REM sleep (Saper et al. 2010). Furthermore, this may provide a possible explanation as to why Bdr/+ mice exhibited shorter Wake duration and greater NREMS duration than wild-type mice in the dark period, that the need to dissipate homeostatic REM sleep pressure may have overridden the circadian drive in effort to rebalance the amount of REM sleep. The results from SD experiment were in line with this view that after six hours of SD, with significantly more REM sleep in the first six hours of recovery period, wild-type mice quickly recovered and showed 81.2 % of Wake

duration compared to 54.3 % of Bdr/+ mice in the first half of the following dark period (Table 1, SD day 13^{th} – 18^{th} hours).

Extended NREM sleep in the dark period by Bdr/+ mice. The total amount of NREM sleep (Table 1, Baseline day 1-12 hours) and the amplitude of EEG power density in delta band (Fig. 5.3 left panels) of Bdr/+ and wild-type mice, however, showed comparable levels. This observation suggests that Bdr/+ mice were able to maintain characteristic high SWA during NREM sleep despite the reported synaptic dysfunction related to the mutation in the *Snap-25* gene. Several studies argued that generations of slow waves and slow oscillations in the cortex can be achieved *in vitro* by cortical slices (Sanchez-Vives and Mattia 2014; Mann, Kohl, and Paulsen 2009), and some (Sanchez-Vives and Mattia 2014) argued that slow wave sleep is the default state in the cortex. The Bdr/+ mice were able to sustain NREM sleep in the light period and extending NREM sleep throughout most of the dark period. A reduced subcortical influence may cause a slight functional deafferentation of cortex from the hypothalamus and the brainstem nuclei, which form a mutual inhibition relationship that regulates neuromodulation at sleep-wake transitions (Saper et al. 2010). A previous Bdr/+ study also showed that there was a phase advance in the circadian rhythm (Oliver et al. 2012), which may link to weakened suprachiasmatic nuclei and ventral lateral preoptic nuclei outputs. The observed reduction in theta band EEG power density in Bdr/+ during Wake (Fig. 5.5) of Baseline day may suggest that Bdr/+ mice were in a lower state of arousal and attentive wakefulness than wild-type mice, potentially caused by reduced connectivity with the subcortical arousal-promoting nuclei. Summarising the arguments above I posit

that there is a general dysconnectivity from subcortical regions due to synaptic transmission defects in the Bdr mutant.

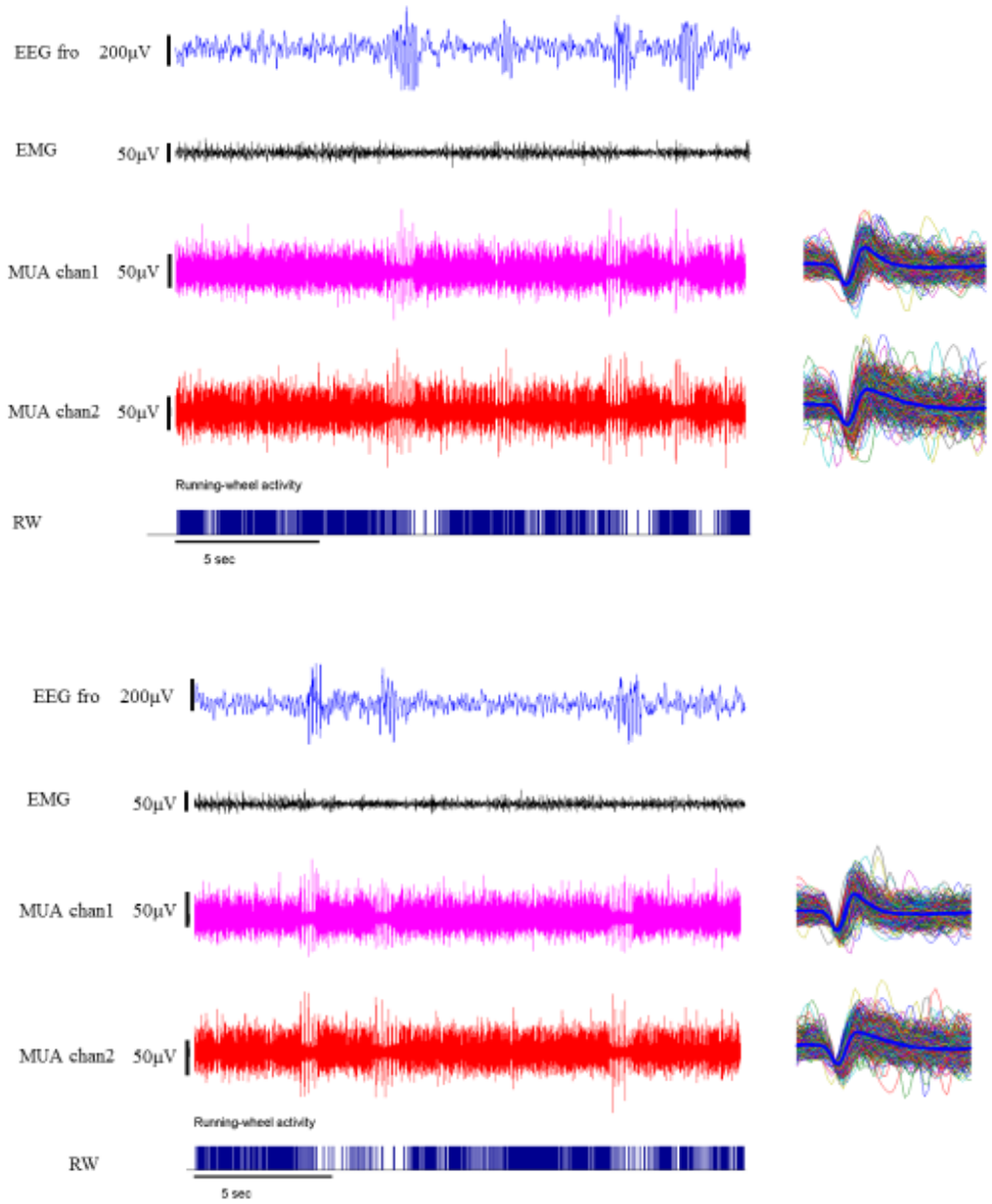
From a homeostatic process prospective, the cortical neurons build up homeostatic pressure during wake episodes, during which cellular metabolic pressure accumulates (Kleim et al. 2003), more dendritic spines form (Maret et al. 2011) and net synaptic potentiation occurs (Vyazovskiy et al. 2008). All of these require slow wave sleep for renormalisation of synaptic strengths and net reduction in spine number hypothesised by the Sleep Homeostasis Hypothesis (Tononi and Cirelli 2014). Given the defects in vesicle trafficking in Bdr/+ mice, it would be supposedly more difficult for neurons in these mice to generate the necessary rebalance of synaptic potentiation and cleansing of accumulated cellular waste in for the same duration of slow wave sleep. Therefore, the prolonged NREM sleep was possibly to compensate for the exocytosis inefficiencies caused by *Snap-25* mutation.

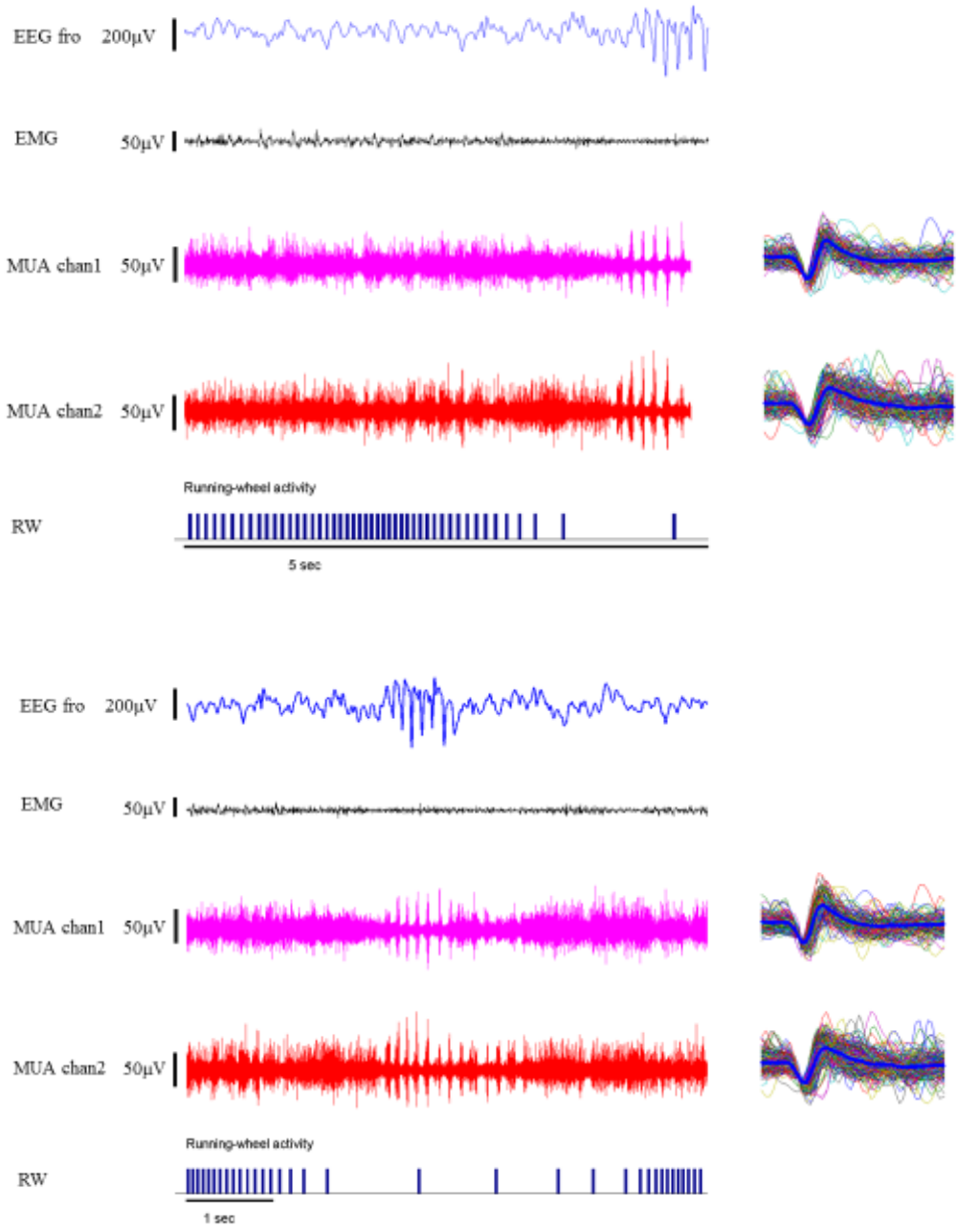
'Burst' activities in Bdr/+ mice.

EEG burst activities were observed across all vigilance state and from distant cortical areas, making it difficult to dissect if these cortical events were associated with any specific cortical state or area. However, from describing and characterising these burst activities, it may be possible to extract some hints as to the origin of burst activity. 'Burst' activity observed in Bdr/+ mice resembled features of spike-wave discharges (SWD) that have been extensively studied previously in Sprague-Dawley rats (Buzsáki et al. 1990). Spike-wave

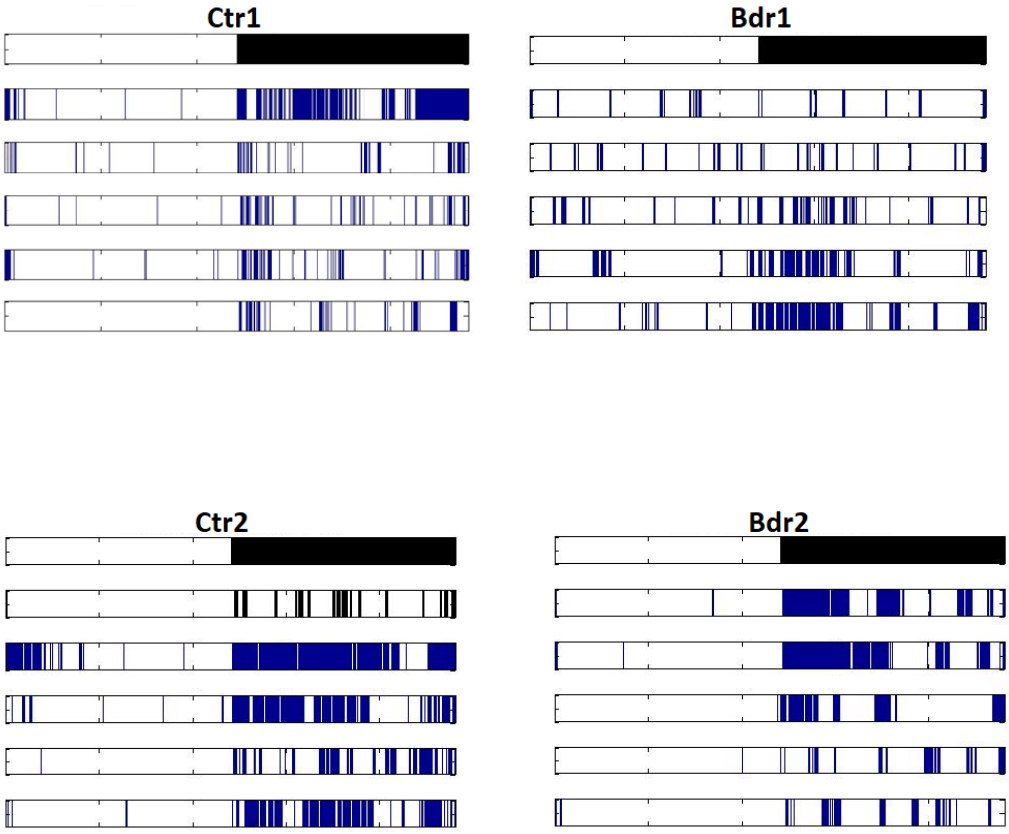
discharges refers to the EEG pattern that occur at a frequency around 2 - 6 Hz in rats (Pearce et al. 2014). Another common observation is that during SWD or 'burst' activity, both phenomena were accompanied by behavioural arrest (Supp. Figure 1) (Pearce et al. 2014). Both the cortex (Destexhe, Contreras, and Steriade 1998; Steriade and Contreras 1998) and the thalamus (Kim et al. 2001) were posited to be necessary in the generation of SWDs. From analysis of calcium current amplitude in the thalamocortical neurons in *coloboma* (*Cm+*) mice, a deletion mutant encompassing the *Snap-25* locus (Hess, Collins, and Wilson 1996), voltage-gated calcium channels are also implicated to be involved in increase in peak current density of low voltage-activated currents preceded the onset of SWDs (Zhang et al. 2011). Interestingly, administration of calcium antagonist, nimodipine, largely normalised SWDs in heterozygous *Snap-25* knockout mice (Corradini et al. 2014). The hippocampus is also shown to be involved in the generation of SWD. One study showed selective silencing of hippocampal parvalbumin positive interneurons induced development of seizures in mice (Drexel et al. 2017). However, the biggest distinction between SWDs reported elsewhere and 'burst' events observed here is that SWD duration lasted much longer than 'burst' (SWD duration > 12 sec (Buzsáki et al. 1990; Corradini et al. 2014); 'burst' duration < 12 sec) with much smaller amplitude (SWD amplitude < 400µV (Pearce et al. 2014); 'burst' amplitude > 800µV). In a recent study on *Snap-25* knock-in mice, very similar bursts were also recorded in cortical, thalamic and hippocampal EEG as in Bdr mice, with very comparable burst amplitude and temporal duration (Watanabe et al. 2015). *Snap-25* knock-in mice (*Snap25*$^{S187A/S187A}$) were generated by replacing exon 7 of *Snap-25* gene with a mutated minigene in which Ala codon was substituted for Ser^{187} in the targeting vector, and these mice express 50% SNAP-25 protein compared to WT. The main reported phenotypes were behavioural anxiety and abnormal inconsistency of behaviour,

e.g. impulsiveness on elevated platform and sudden stop and movement in open fields. The same authors also showed temporal synchronisation between cortical, thalamic and hippocampal burst events (Watanabe et al. 2015). Furthermore, burst activities showed rhythmic oscillations in closely synchronised manner with extracellular multi-unit recordings (Supp. Figure 1) as SWDs did (Buzsaki et al. 1988). The close temporal relationship between EEG burst and rhythmic MUA spikes recorded from contralateral hemisphere in Bdr/+, and synchronised cortical, thalamic and hippocampal EEG burst events, suggests that dysfunction of synaptic transmission in a circuit involving neocortex, thalamus and hippocampus manifested as behavioural arrest. The burst activities represent an abnormally hyperactive network, in which inhibition from parvalbumin interneurons were weakened due to defective synaptic exocytosis, such that post-synaptic excitatory potentials would have a higher probability of passing firing threshold. The excitation-inhibition imbalance would cause the population to enter avalanche of spiking activities across the cortex. Further electrophysiological experiments are needed to study the underlying mechanisms of the generation of burst activities, and recording from the thalamus, hippocampus and the SCN may shed some light on the molecular and network mechanisms and how the hyperexcitability in Bdr cortical network is related to perturbed sleep-wake architecture and possibly schizophrenia.


EEG fro 200µV
EMG 50µV
MUA chan1 50µV
MUA chan2 50µV
Running-wheel activity
RW
5 sec
EEG fro 200µV
EMG 50µV
MUA chan1 50µV
MUA chan2 50µV
Running-wheel activity
RW
5 sec



Supp. Figure 1, *showing segments of raw data illustrating the recordings of 'burst' events in EEG and MUA (contralateral regions), and the corresponding EMG and running behaviours.*



Supp. Figure 2, *showing 5-day wheel running activities of two wild-type mice and Bdr/+ mice. Wildtype mice show good entrainment to circadian rhythm, while Bdr/+ mice display variability in the ability to entrain to Light-Dark cycle, as illustrated in mouse Bdr1 showing poor entrainment and in mouse Bdr2 showing relatively better entrainment.*

Chapter 6: General Discussion and Conclusion

6.1 Summary of Findings

The key findings in this thesis are:

1. Individual NREM sleep episodes with increased number of EEG slow waves with higher amplitude and steeper slope accounts for the changes of EEG spectral power in the slow wave activity on a global scale across 24 hours. Parameters of individual slow waves within minutes of NREM sleep onset varied depending on what were the immediate preceding states in C57BL/6 mice. This suggests that NREM sleep initiated in a more local and desynchronised fashion following REM sleep than compared to following waking.
2. Neuronal firing patterns within the motor and somatosensory cortices vary during voluntary wheel running in C57BL/6 mice. Firing rates of a portion of recorded cortical neurons were modulated by stereotypic wheel running leading to an overall reduction in neuronal activity. Furthermore, in all recorded neurons, firing rates were increased during acceleration or deceleration, whereas firing rates were lowest during steady speed running.
3. Activity profiles of Blind-drunk mice, a mouse model of schizophrenia, show reduced amplitude of circadian rhythmicity compared to wild-type mice, but no phase change in the circadian rhythm was observed. EEG-EMG based sleep scoring in these mice showed increased total NREM sleep time and decreased total REM sleep time during the dark period. EEG 'burst' activities, similar to spike-wave discharges, were observed with peak frequency in the theta band.

These findings characterise the sleep and electrophysiological phenotypes of a mouse model of schizophrenia. Furthermore, EEG `burst` activities could be a manifestation of synaptic dysfunction, and imply a possible disruption in the hippocampo-cortical circuits.

Below, I will briefly discuss the validity and limitations of these key findings and suggest how they can be drawn together to contribute towards understanding of sleep in general and its relevance in health and disease.

Comparing sleep deprivation methods. To study role of sleep and the effects of sleep loss in various fields, a variety of methods have been employed to deprive animals to their sleep for various durations. I will briefly compare these methods, and explain the pros and cons of sleep deprivation method adopted in my experiments. The earliest sleep deprivation method reported was the disk-over-water method, which involves putting the animal on a small platform within a tank of water (Jouvet et al. 1964). Since the animal has to maintain wakefulness in order to stay balanced on top of the disk, otherwise falling into the water, this method can achieve specific deprivation of REM sleep, a state with a complete loss of muscle tone, thus allowing animals to maintain certain amount of slow-wave sleep. This method, despite being highly efficient in unsupervised sleep deprivation, is associated with high levels of stress and not suitable for electrophysiological investigations. Motorised treadmills or wheels are common procedures to keep the animals wake (Guzman-Marin et al. 2003). This method is thought to be less stressful than the previous one, but the forced exercise may confound the effects of sleep loss. A widely adopted sleep deprivation method is gentle handling, which involves monitoring sleep-wake activity and interfering by tapping the cage or gentle handling the animal as soon as

sleep is detected (Rechtschaffen et al. 1983). This method is considered one of the least stressful ways of sleep deprivation with minimal increases in stress hormones such as glucocorticoids (van der Borght et al. 2006). The last is novel object presentation method, which is a supervised method and involves introduction of novel objects to the animal when the animal shows loss of interest in the object or returning to nest. This method utilises the natural tendency in rodents to explore environment, which is the main advantage because sleep is prevented due to an endogenous drive to explore a novel environment rather than an external perturbation of the animal. The active exploration during sleep deprivation also accommodates the purpose of testing the effects of prolonged wakefulness, as the nature of novel object exploration is most comparable to normal waking in animals. This further allows experiments designed to compare effects of build-up of cellular processes in situations of spontaneous and prolonged waking duration. Another benefit is, in tether mice, novel object presentation avoids interfering with quality of recorded data, and avoid possible injuries of the animals by handling them. One caveat of using this method that requires caution is that gene expression following a period of sleep deprivation by exposure of novel objects will compound the effects of exploration with the effects of sleep loss per se.

Animal behaviours in home cages with running wheels. Wheels are widely used in laboratories to measure circadian activity rhythms in rodents. In some subsets of rodent species, the circadian rhythms were altered. For example, the murid rodent *Arvicanthis niloticus,* a diurnal species in the wild, appears to be nocturnal when given access to wheels in a laboratory setting (Blanchong et al. 1999). Similar change in the phase preference was observed in *Octodon degus*, and the shift in circadian phase immediately reverted when wheels were removed (Kas and Edgar 1999). Evidence above suggests that wheel running

activity is distinctly different from general waking activity. These changes in the circadian phase due to wheel running might be linked to epigenetic mechanisms as well as the underlying neural systems. Another aspect of wheel running is that the running behaviour is involved in the reward systems in the brain. The implication of common mechanisms underlying wheel running and reward system can be found in the similarities of responses to running and dopaminergic drugs (Ferreira et al. 2006; Meeusen and De Meirleir 1995). In addition, chronic wheel running decreases the analgesic properties of morphine (D'Anci, Gerstein, and Kanarek 2000; Kanarek et al. 1998). Dopamine and opioid systems in the basal forebrain as well as cFos, known to be involved in drug reward, increased following voluntary wheel running (Greenwood et al. 2011). This suggests that wheel running is activated by the reward system with possible connection to genetic background, and thus distinct neurocircuitry activation in different transgenic lines of rodents may contribute to different behavioural respond to voluntary wheel running.

Relevance of Bdr/+ mice's electrophysiological and sleep phenotypes to human disease. Diagnosis of epilepsy and detection of seizure activity commonly relies on EEG recordings in both humans and animal models. Interestingly, a link was suggested to exist between epileptic seizures and different vigilance states. Spectral analysis of EEG theta band showed high correlation between theta power and epileptic discharge occurrence during REM sleep in partial epileptic patients, and high levels of acetylcholine during REM sleep suppresses epileptic events with reduced number of inter-ictal epileptic discharges (Ferrillo, Beelke, and Nobili 2000). The hippocampal-cortical network is extremely sensitive to low concentrations of cholinergic stimulation, and responds with network synchronisation of hippocampal theta oscillations (Friedman, Behrens, and Heinemann 2007), and hypersynchronised theta activity in the hippocampus has been described in

epileptic patients during REM sleep (Wieser 1991). 'Burst' activity of Bdr/+ mice described in **Chapter 5** shows global synchronisation with cortical multiunit activity despite showing less theta power than wild-type mice. Similarities in epileptic discharges and burst activities suggests that investigating the cellular and network mechanisms of 'burst' activities in the Blind-drunk mouse model may provide some insights into the cause of epileptic seizures during REM sleep in human patients. Conversely, during NREM sleep, hypersynchronisation of thalamocortical delta oscillations and spindles can trigger seizures in human epileptic patients possibly related to changes in the GABAergic cortical tone (Osorio et al. 2015). In addition, the intrinsically bursting slow oscillating cortical neurons tend to transform evoked response into self-sustained paroxysmal barrages of action potentials at a similar frequency to that of slow oscillation (Steriade, Contreras, and Amzica 1994). As stated by Steriade and colleagues, such paroxysmal neural activity might also take place with extensive lesion of thalamic nuclei, suggesting cortical networks of interconnected bursting neurons leads to recurrent volleys of currents eventually lead to epileptic-like activity. Spectral analysis of EEG in Bdr/+ mice showed that the peak frequency of burst activity is higher in NREM sleep than in REM sleep. This may suggest that the differences in burst activity's oscillating frequencies in different vigilance states is the manifestation of the same underlying synaptic disruption but on different pathways.

Sleep-wake pattern disruptions have been reported in a variety of psychiatric diseases including Alzheimers's disease, Parkinson's disease, bipolar disorder, depression and schizophrenia (Wulff et al. 2010). It was proposed that brain disorders and abnormal sleep patterns have a common mechanistic origin, and the destabilisation of sleep mechanisms may give rise to many co-morbid pathologies. In schizophrenic patients, characterised by the dysfunction of inhibitory neuronal circuits and reduced number of

neurons in the hippocampus (Hendler, Bleich-Cohen, and Sharon 2009), were reported to show reductions in REM sleep latency and REM sleep duration, increases in sleep latency and duration of stage 4 NREM sleep (Cohrs 2008). A range of circadian abnormalities, such as phase delay, phase advancements and irregular sleep timing (Wulff et al. 2012), are also associated with schizophrenic symptoms. The disruptions of sleep patterns observed in schizophrenic patients are very similar to that of Bdr/+ mice reported here which showed reductions in REM sleep duration and EEG theta power and increase in the NREM sleep duration during dark period. In addition, a genetic association study showed that levels of SNAP-25 are reduced in the hippocampus of patients with schizophrenia (Young et al. 1998). Abnormalities in SNAP-25 in mice induced psychiatric-like endophenotypes (Oliver and Davies 2009). Such commonalities in sleep pattern disruption and observations from the hippocampus support what has been hypothesised here that synaptic dysfunctions, particularly in the subcortical neuromodulation circuits and hippocampo-cortical circuits, lead to abnormal sleep phenotypes in schizophrenic patients and mouse models of schizophrenia. Furthermore, it strengthens the blind-drunk mouse model as a viable model to further investigate the underlying cellular and genetic causes of schizophrenia and test possible treatments for schizophrenia and other psychiatric diseases.

6.2 Concluding Remarks

Sleep is ubiquitously observed among diurnal and nocturnal mammalian species. The timing, duration and intensity is determined by the circadian process and by the local use-dependent homeostatic process. The roles of subcortical regulation of sleep and wake distribution has been extensively explored, yet, how the regional mechanisms of sleep regulation contribute towards global sleep regulation remains unanswered. In the first

study, I recorded EEG and multi-unit activity from the mouse cortex, and investigated local dynamics of cortical activities at the onset of non-rapid eye movement sleep. While effects of neuromodulation undoubtedly play an important role at the transitions of vigilance states, my results show that immediate preceding sleep-wake history also affects the parameters of EEG slow waves and neuronal firing rates at the onset of transitioning into NREM sleep. If technology allows, recording simultaneously from different subcortical sleep regulating regions and from different regions of cortex would provide great insight to the details of reaction of global neuronal responses to preceding history leading up to sleep, and shed light on how global and local drives for sleep initiation are interlinked. Next, I went on to investigate whether specific waking behaviours would have differences in the effects on cortical activities, comparing between sleep deprivation and wheel running activities. My results showed that the cortical activities differed depending on behavioural contents during waking, and showed that during wheel running neuronal activities displayed reduced firing rates and incidence of synchronised silence among subpopulation of neurons. These characteristics shared common features with quiet wakefulness, suggesting stereotypic repetitive locomotion may represent a 'low cost' behaviour possibly a result of adaptive flexibility with respect to evolution. The next step would be to investigate any metabolic and/or synaptic changes at cellular level after wheel running that could possibly link to the reduction in neuronal activities. Finally, with the aim of investigating underlying causes for sleep disruption symptoms in schizophrenic patients, I characterised sleep and electrophysiological phenotypes in Blind-drunk mice, a mouse model of schizophrenia achieved with point mutation in synaptosomal-associated protein of 25 kDa (SNAP-25). Consistent with previous studies (Oliver et al. 2012; Corradini et al. 2014), my results showed that Blind-drunk mice displayed disruption in sleep-wake

patterns and abnormal epileptic seizure-like cortical discharges. Many studies have implicated the role of the hippocampus and the septic complex in the genesis of such discharges. Therefore, for future experiments, testing *Snap-25* expression promoting drugs on the effect of sleep disruption, as well as the effect of antiepileptic drugs while recording from the hippocampus and septic region may prove to be insightful to the circuit mechanisms underlying seizure activity and sleep pattern disruption.

References

Achermann, P., and A. A. Borbely. 2003. 'Mathematical models of sleep regulation', *Front Biosci*, 8: s683-93.

Achermann, P., D. J. Dijk, D. P. Brunner, and A. A. Borbely. 1993. 'A model of human sleep homeostasis based on EEG slow-wave activity: quantitative comparison of data and simulations', *Brain Res Bull*, 31: 97-113.

Adamantidis, A. R., F. Zhang, A. M. Aravanis, K. Deisseroth, and L. de Lecea. 2007. 'Neural substrates of awakening probed with optogenetic control of hypocretin neurons', *Nature*, 450: 420-4.

Aeschbach, D., C. Cajochen, H. Landolt, and A. A. Borbely. 1996. 'Homeostatic sleep regulation in habitual short sleepers and long sleepers', *Am J Physiol*, 270: R41-53.

Amzica, F., and M. Steriade. 1995. 'Short- and long-range neuronal synchronization of the slow (< 1 Hz) cortical oscillation', *J Neurophysiol*, 73: 20-38.

———. 1998a. 'Cellular substrates and laminar profile of sleep K-complex', *Neuroscience*, 82: 671-86.

———. 1998b. 'Electrophysiological correlates of sleep delta waves', *Electroencephalogr Clin Neurophysiol*, 107: 69-83.

———. 1998c. 'Electrophysiological correlates of sleep delta waves1Correspondence and reprint requests may be addressed to either author.1', *Electroencephalography and Clinical Neurophysiology*, 107: 69-83.

Aserinsky, E., and N. Kleitman. 1953. 'Regularly occurring periods of eye motility, and concomitant phenomena, during sleep', *Science*, 118: 273-4.

Aton, S. J., J. Seibt, M. Dumoulin, S. K. Jha, N. Steinmetz, T. Coleman, N. Naidoo, and M. G. Frank. 2009. 'Mechanisms of sleep-dependent consolidation of cortical plasticity', *Neuron*, 61: 454-66.

Aton, S. J., A. Suresh, C. Broussard, and M. G. Frank. 2014. 'Sleep promotes cortical response potentiation following visual experience', *Sleep*, 37: 1163-70.

Baker, R., T. C. Gent, Q. Yang, S. Parker, A. L. Vyssotski, W. Wisden, S. G. Brickley, and N. P. Franks. 2014. 'Altered activity in the central medial thalamus precedes changes in the neocortex during transitions into both sleep and propofol anesthesia', *J Neurosci*, 34: 13326-35.

Bang, Sun Jung, Patricia Jensen, Susan M. Dymecki, and Kathryn G. Commons. 2012. 'Projections and interconnections of genetically defined serotonin neurons in mice', *European Journal of Neuroscience*, 35: 85-96.

Bao, W., and J. Y. Wu. 2003. 'Propagating wave and irregular dynamics: spatiotemporal patterns of cholinergic theta oscillations in neocortex in vitro', *J Neurophysiol*, 90: 333-41.

Bark, I. Christina. 1993. 'Structure of the Chicken Gene for SNAP-25 Reveals Duplicated Exons Encoding Distinct Isoforms of the Protein', *Journal of Molecular Biology*, 233: 67-76.

Belke, T. W., and W. D. Pierce. 2014. 'Effect of sucrose availability and pre-running on the intrinsic value of wheel running as an operant and a reinforcing consequence', *Behav Processes*, 103: 35-42.

Belke, T. W., and J. P. Wagner. 2005. 'The reinforcing property and the rewarding aftereffect of wheel running in rats: a combination of two paradigms', *Behav Processes*, 68: 165-72.

Beltramo, R., G. D'Urso, M. Dal Maschio, P. Farisello, S. Bovetti, Y. Clovis, G. Lassi, V. Tucci, D. De Pietri Tonelli, and T. Fellin. 2013. 'Layer-specific excitatory circuits differentially control recurrent network dynamics in the neocortex', *Nat Neurosci*, 16: 227-34.

Benington, J. H., and H. C. Heller. 1994a. 'Does the function of REM sleep concern non-REM sleep or waking?', *Prog Neurobiol*, 44: 433-49.

———. 1994b. 'REM-sleep timing is controlled homeostatically by accumulation of REM-sleep propensity in non-REM sleep', *Am J Physiol*, 266: R1992-2000.
Blanchong, J. A., T. L. McElhinny, M. M. Mahoney, and L. Smale. 1999. 'Nocturnal and diurnal rhythms in the unstriped Nile rat, Arvicanthis niloticus', *J Biol Rhythms*, 14: 364-77.
Borbely, A. A. 1982. 'A two process model of sleep regulation', *Hum Neurobiol*, 1: 195-204.
Bramness, J. G., O. H. Gundersen, J. Guterstam, E. B. Rognli, M. Konstenius, E. M. Loberg, S. Medhus, L. Tanum, and J. Franck. 2012. 'Amphetamine-induced psychosis--a separate diagnostic entity or primary psychosis triggered in the vulnerable?', *BMC Psychiatry*, 12: 221.
Brankack, J., M. Stewart, and S. E. Fox. 1993. 'Current source density analysis of the hippocampal theta rhythm: associated sustained potentials and candidate synaptic generators', *Brain Res*, 615: 310-27.
Bromberg-Martin, E. S., M. Matsumoto, and O. Hikosaka. 2010. 'Dopamine in motivational control: rewarding, aversive, and alerting', *Neuron*, 68: 815-34.
Brown, P., and J. F. Marsden. 2001. 'Cortical network resonance and motor activity in humans', *Neuroscientist*, 7: 518-27.
Buchsbaum, M. S., W. B. Mendelson, W. C. Duncan, R. Coppola, J. Kelsoe, and J. C. Gillin. 1982. 'Topographic cortical mapping of EEG sleep stages during daytime naps in normal subjects', *Sleep*, 5: 248-55.
Buzsaki, G., C. A. Anastassiou, and C. Koch. 2012. 'The origin of extracellular fields and currents--EEG, ECoG, LFP and spikes', *Nat Rev Neurosci*, 13: 407-20.
Buzsaki, G., R. G. Bickford, D. M. Armstrong, G. Ponomareff, K. S. Chen, R. Ruiz, L. J. Thal, and F. H. Gage. 1988. 'Electric activity in the neocortex of freely moving young and aged rats', *Neuroscience*, 26: 735-44.
Buzsáki, G., I. Laszlovszky, A. Lajtha, and C. Vadász. 1990. 'Spike-and-wave neocortical patterns in rats: Genetic and aminergic control', *Neuroscience*, 38: 323-33.
Caplan, J. B., J. R. Madsen, A. Schulze-Bonhage, R. Aschenbrenner-Scheibe, E. L. Newman, and M. J. Kahana. 2003. 'Human theta oscillations related to sensorimotor integration and spatial learning', *J Neurosci*, 23: 4726-36.
Carter, M. E., O. Yizhar, S. Chikahisa, H. Nguyen, A. Adamantidis, S. Nishino, K. Deisseroth, and L. de Lecea. 2010. 'Tuning arousal with optogenetic modulation of locus coeruleus neurons', *Nat Neurosci*, 13: 1526-33.
Caton, R. 1875. 'Electrical currents of the brain', *British Medical Journal*, 2: 278.
Cenquizca, L. A., and L. W. Swanson. 2007. 'Spatial organization of direct hippocampal field CA1 axonal projections to the rest of the cerebral cortex', *Brain Res Rev*, 56: 1-26.
Chandler, D. J., W. J. Gao, and B. D. Waterhouse. 2014. 'Heterogeneous organization of the locus coeruleus projections to prefrontal and motor cortices', *Proc Natl Acad Sci U S A*, 111: 6816-21.
Chauvette, S., J. Seigneur, and I. Timofeev. 2012. 'Sleep oscillations in the thalamocortical system induce long-term neuronal plasticity', *Neuron*, 75: 1105-13.
Chauvette, S., M. Volgushev, and I. Timofeev. 2010a. 'Origin of active states in local neocortical networks during slow sleep oscillation', *Cereb Cortex*, 20: 2660-74.
———. 2010b. 'Origin of Active States in Local Neocortical Networks during Slow Sleep Oscillation', *Cereb Cortex*.
Cirillo, M. A., and L. J. Seidman. 2003. 'Verbal declarative memory dysfunction in schizophrenia: from clinical assessment to genetics and brain mechanisms', *Neuropsychol Rev*, 13: 43-77.
Cohrs, S. 2008. 'Sleep disturbances in patients with schizophrenia : impact and effect of antipsychotics', *CNS Drugs*, 22: 939-62.
Connors, B. W., and M. J. Gutnick. 1990. 'Intrinsic firing patterns of diverse neocortical neurons', *Trends Neurosci*, 13: 99-104.

Constantinople, C. M., and R. M. Bruno. 2011. 'Effects and mechanisms of wakefulness on local cortical networks', *Neuron*, 69: 1061-8.
Contreras, D., and M. Steriade. 1995. 'Cellular basis of EEG slow rhythms: a study of dynamic corticothalamic relationships', *J Neurosci*, 15: 604-22.
Contreras, D., I. Timofeev, and M. Steriade. 1996. 'Mechanisms of long-lasting hyperpolarizations underlying slow sleep oscillations in cat corticothalamic networks', *J Physiol*, 494 (Pt 1): 251-64.
Corner, M. A. 2013. 'From neural plate to cortical arousal-a neuronal network theory of sleep derived from in vitro "model" systems for primordial patterns of spontaneous bioelectric activity in the vertebrate central nervous system', *Brain Sci*, 3: 800-20.
Corradini, I., A. Donzelli, F. Antonucci, H. Welzl, M. Loos, R. Martucci, S. De Astis, L. Pattini, F. Inverardi, D. Wolfer, M. Caleo, Y. Bozzi, C. Verderio, C. Frassoni, D. Braida, M. Clerici, H. P. Lipp, M. Sala, and M. Matteoli. 2014. 'Epileptiform activity and cognitive deficits in SNAP-25(+/-) mice are normalized by antiepileptic drugs', *Cereb Cortex*, 24: 364-76.
Correa, M., M. Pardo, P. Bayarri, L. Lopez-Cruz, N. San Miguel, O. Valverde, C. Ledent, and J. D. Salamone. 2015. 'Choosing voluntary exercise over sucrose consumption depends upon dopamine transmission: effects of haloperidol in wild type and adenosine AKO mice', *Psychopharmacology (Berl)*.
Crunelli, V., and S. W. Hughes. 2009. 'The slow (<1 Hz) rhythm of non-REM sleep: a dialogue between three cardinal oscillators', *Nat Neurosci*, 13: 9-17.
———. 2010. 'The slow (<1 Hz) rhythm of non-REM sleep: a dialogue between three cardinal oscillators', *Nat Neurosci*, 13: 9-17.
Cui, N., L. E. McKillop, S. P. Fisher, P. L. Oliver, and V. V. Vyazovskiy. 2014. 'Long-term history and immediate preceding state affect EEG slow wave characteristics at NREM sleep onset in C57BL/6 mice', *Arch Ital Biol*, 152: 156-68.
D'Anci, K. E., A. V. Gerstein, and R. B. Kanarek. 2000. 'Long-term voluntary access to running wheels decreases kappa-opioid antinociception', *Pharmacol Biochem Behav*, 66: 343-6.
Daan, S., D. G. Beersma, and A. A. Borbely. 1984. 'Timing of human sleep: recovery process gated by a circadian pacemaker', *Am J Physiol*, 246: R161-83.
Davis, H., P. A. Davis, A. L. Loomis, E. N. Harvey, and G. Hobart. 1937. 'Changes in Human Brain Potentials during the Onset of Sleep', *Science*, 86: 448-50.
De Gennaro, L., M. Ferrara, G. Curcio, and R. Cristiani. 2001. 'Antero-posterior EEG changes during the wakefulness-sleep transition', *Clin Neurophysiol*, 112: 1901-11.
Destexhe, A., D. Contreras, and M. Steriade. 1998. 'Mechanisms underlying the synchronizing action of corticothalamic feedback through inhibition of thalamic relay cells', *J Neurophysiol*, 79: 999-1016.
———. 1999. 'Spatiotemporal analysis of local field potentials and unit discharges in cat cerebral cortex during natural wake and sleep states', *J Neurosci*, 19: 4595-608.
Dijk, D. J., D. G. Beersma, and S. Daan. 1987. 'EEG power density during nap sleep: reflection of an hourglass measuring the duration of prior wakefulness', *J Biol Rhythms*, 2: 207-19.
Dijk, D. J., D. G. Beersma, S. Daan, G. M. Bloem, and R. H. Van den Hoofdakker. 1987. 'Quantitative analysis of the effects of slow wave sleep deprivation during the first 3 h of sleep on subsequent EEG power density', *Eur Arch Psychiatry Neurol Sci*, 236: 323-8.
Drexel, Meinrad, Roman A. Romanov, James Wood, Stefan Weger, Regine Heilbronn, Peer Wulff, Ramon O. Tasan, Tibor Harkany, and Günther Sperk. 2017. 'Selective Silencing of Hippocampal Parvalbumin Interneurons Induces Development of Recurrent Spontaneous Limbic Seizures in Mice', *The Journal of Neuroscience*, 37: 8166-79.
Dugovic, C., A. Wauquier, and P. A. Janssen. 1989. 'Differential effects of the new antipsychotic risperidone on sleep and wakefulness in the rat', *Neuropharmacology*, 28: 1431-3.
Durkin, J., and S. J. Aton. 2015. 'Sleep-Dependent Potentiation in the Visual System Is at Odds with the Synaptic Homeostasis Hypothesis', *Sleep*.

Edgar, D. M., T. S. Kilduff, C. E. Martin, and W. C. Dement. 1991. 'Influence of running wheel activity on free-running sleep/wake and drinking circadian rhythms in mice', *Physiol Behav*, 50: 373-8.

Fatt, P., and B. Katz. 1952. 'Spontaneous subthreshold activity at motor nerve endings', *J Physiol*, 117: 109-28.

Ferreira, A., S. Lamarque, P. Boyer, F. Perez-Diaz, R. Jouvent, and C. Cohen-Salmon. 2006. 'Spontaneous appetence for wheel-running: a model of dependency on physical activity in rat', *Eur Psychiatry*, 21: 580-8.

Ferrillo, F., M. Beelke, and L. Nobili. 2000. 'Sleep EEG synchronization mechanisms and activation of interictal epileptic spikes', *Clin Neurophysiol*, 111 Suppl 2: S65-73.

Fogerson, P. M., and J. R. Huguenard. 2016. 'Tapping the Brakes: Cellular and Synaptic Mechanisms that Regulate Thalamic Oscillations', *Neuron*, 92: 687-704.

Fort, P., C. L. Bassetti, and P. H. Luppi. 2009. 'Alternating vigilance states: new insights regarding neuronal networks and mechanisms', *Eur J Neurosci*, 29: 1741-53.

Franken, P., D. Chollet, and M. Tafti. 2001. 'The homeostatic regulation of sleep need is under genetic control', *J Neurosci*, 21: 2610-21.

Franks, N. P. 2008. 'General anaesthesia: from molecular targets to neuronal pathways of sleep and arousal', *Nat Rev Neurosci*, 9: 370-86.

Friedman, A., C. J. Behrens, and U. Heinemann. 2007. 'Cholinergic dysfunction in temporal lobe epilepsy', *Epilepsia*, 48 Suppl 5: 126-30.

Fusar-Poli, P., S. Borgwardt, A. Bechdolf, J. Addington, A. Riecher-Rossler, F. Schultze-Lutter, M. Keshavan, S. Wood, S. Ruhrmann, L. J. Seidman, L. Valmaggia, T. Cannon, E. Velthorst, L. De Haan, B. Cornblatt, I. Bonoldi, M. Birchwood, T. McGlashan, W. Carpenter, P. McGorry, J. Klosterkotter, P. McGuire, and A. Yung. 2013. 'The psychosis high-risk state: a comprehensive state-of-the-art review', *JAMA Psychiatry*, 70: 107-20.

Geering, B. A., P. Achermann, F. Eggimann, and A. A. Borbely. 1993. 'Period-amplitude analysis and power spectral analysis: a comparison based on all-night sleep EEG recordings', *J Sleep Res*, 2: 121-29.

Gerashchenko, D., R. Salin-Pascual, and P. J. Shiromani. 2001. 'Effects of hypocretin-saporin injections into the medial septum on sleep and hippocampal theta', *Brain Res*, 913: 106-15.

Glynn, D., R. A. Bortnick, and A. J. Morton. 2003. 'Complexin II is essential for normal neurological function in mice', *Hum Mol Genet*, 12: 2431-48.

Glynn, D., C. J. Drew, K. Reim, N. Brose, and A. J. Morton. 2005. 'Profound ataxia in complexin I knockout mice masks a complex phenotype that includes exploratory and habituation deficits', *Hum Mol Genet*, 14: 2369-85.

Goldberg, T. E., R. S. Keefe, R. S. Goldman, D. G. Robinson, and P. D. Harvey. 2010. 'Circumstances under which practice does not make perfect: a review of the practice effect literature in schizophrenia and its relevance to clinical treatment studies', *Neuropsychopharmacology*, 35: 1053-62.

Golmayo, L., A. Nunez, and L. Zaborszky. 2003. 'Electrophysiological evidence for the existence of a posterior cortical-prefrontal-basal forebrain circuitry in modulating sensory responses in visual and somatosensory rat cortical areas', *Neuroscience*, 119: 597-609.

Greenwood, B. N., T. E. Foley, T. V. Le, P. V. Strong, A. B. Loughridge, H. E. Day, and M. Fleshner. 2011. 'Long-term voluntary wheel running is rewarding and produces plasticity in the mesolimbic reward pathway', *Behav Brain Res*, 217: 354-62.

Gritti, I., L. Mainville, and B. E. Jones. 1994. 'Projections of GABAergic and cholinergic basal forebrain and GABAergic preoptic-anterior hypothalamic neurons to the posterior lateral hypothalamus of the rat', *J Comp Neurol*, 339: 251-68.

Groenewegen, H. J., and H. B. Uylings. 2000. 'The prefrontal cortex and the integration of sensory, limbic and autonomic information', *Prog Brain Res*, 126: 3-28.

Grosmark, A. D., K. Mizuseki, E. Pastalkova, K. Diba, and G. Buzsaki. 2012. 'REM Sleep Reorganizes Hippocampal Excitability', *Neuron*, 75: 1001-7.

Gu, C., C. P. Coomans, K. Hu, F. A. Scheer, H. E. Stanley, and J. H. Meijer. 2015. 'Lack of exercise leads to significant and reversible loss of scale invariance in both aged and young mice', *Proc Natl Acad Sci U S A*, 112: 2320-4.

Guzman-Marin, R., N. Suntsova, D. R. Stewart, H. Gong, R. Szymusiak, and D. McGinty. 2003. 'Sleep deprivation reduces proliferation of cells in the dentate gyrus of the hippocampus in rats', *J Physiol*, 549: 563-71.

Hahn, T. T., J. M. McFarland, S. Berberich, B. Sakmann, and M. R. Mehta. 2012. 'Spontaneous persistent activity in entorhinal cortex modulates cortico-hippocampal interaction in vivo', *Nat Neurosci*, 15: 1531-8.

Haider, B., A. Duque, A. R. Hasenstaub, and D. A. McCormick. 2006. 'Neocortical network activity in vivo is generated through a dynamic balance of excitation and inhibition', *J Neurosci*, 26: 4535-45.

Hajnik, T., A. Toth, and L. Detari. 2013. 'Characteristic changes in the slow cortical waves after a 6-h sleep deprivation in rat', *Brain Res*, 1501: 1-11.

Halassa, M. M., Z. Chen, R. D. Wimmer, P. M. Brunetti, S. Zhao, B. Zikopoulos, F. Wang, E. N. Brown, and M. A. Wilson. 2014. 'State-dependent architecture of thalamic reticular subnetworks', *Cell*, 158: 808-21.

Harris, K. D., and A. Thiele. 2011. 'Cortical state and attention', *Nat Rev Neurosci*, 12: 509-23.

Hartigan, John A. 1975. *Clustering algorithms* (Wiley: New York,).

Hassani, Oum Kaltoum, Maan Gee Lee, Pablo Henny, and Barbara E. Jones. 2009. 'Discharge Profiles of Identified GABAergic in Comparison to Cholinergic and Putative Glutamatergic Basal Forebrain Neurons across the Sleep–Wake Cycle', *The Journal of Neuroscience*, 29: 11828-40.

Hendler, T., M. Bleich-Cohen, and H. Sharon. 2009. 'Neurofunctional view of psychiatry: clinical brain imaging revisited', *Curr Opin Psychiatry*, 22: 300-5.

Hengen, K. B., M. E. Lambo, S. D. Van Hooser, D. B. Katz, and G. G. Turrigiano. 2013. 'Firing rate homeostasis in visual cortex of freely behaving rodents', *Neuron*, 80: 335-42.

Henny, P., and B. E. Jones. 2008. 'Projections from basal forebrain to prefrontal cortex comprise cholinergic, GABAergic and glutamatergic inputs to pyramidal cells or interneurons', *Eur J Neurosci*, 27: 654-70.

Herrera, C. G., M. C. Cadavieco, S. Jego, A. Ponomarenko, T. Korotkova, and A. Adamantidis. 2016. 'Hypothalamic feedforward inhibition of thalamocortical network controls arousal and consciousness', *Nat Neurosci*, 19: 290-8.

Hess, E. J., K. A. Collins, and M. C. Wilson. 1996. 'Mouse model of hyperkinesis implicates SNAP-25 in behavioral regulation', *J Neurosci*, 16: 3104-11.

Hinard, V., C. Mikhail, S. Pradervand, T. Curie, R. H. Houtkooper, J. Auwerx, P. Franken, and M. Tafti. 2012. 'Key electrophysiological, molecular, and metabolic signatures of sleep and wakefulness revealed in primary cortical cultures', *J Neurosci*, 32: 12506-17.

Huber, R., T. Deboer, and I. Tobler. 2000. 'Topography of EEG dynamics after sleep deprivation in mice', *J Neurophysiol*, 84: 1888-93.

Huber, R., M. F. Ghilardi, M. Massimini, F. Ferrarelli, B. A. Riedner, M. J. Peterson, and G. Tononi. 2006. 'Arm immobilization causes cortical plastic changes and locally decreases sleep slow wave activity', *Nat Neurosci*, 9: 1169-76.

Hughes, A. T., B. Fahey, D. J. Cutler, A. N. Coogan, and H. D. Piggins. 2004. 'Aberrant gating of photic input to the suprachiasmatic circadian pacemaker of mice lacking the VPAC2 receptor', *J Neurosci*, 24: 3522-6.

Hughes, A. T., and H. D. Piggins. 2008. 'Behavioral responses of Vipr2-/- mice to light', *J Biol Rhythms*, 23: 211-9.

Jablensky, A. 2000. 'Prevalence and incidence of schizophrenia spectrum disorders: implications for prevention', *Aust N Z J Psychiatry*, 34 Suppl: S26-34; discussion S35-8.
Jeans, A. F., P. L. Oliver, R. Johnson, M. Capogna, J. Vikman, Z. Molnar, A. Babbs, C. J. Partridge, A. Salehi, M. Bengtsson, L. Eliasson, P. Rorsman, and K. E. Davies. 2007. 'A dominant mutation in Snap25 causes impaired vesicle trafficking, sensorimotor gating, and ataxia in the blind-drunk mouse', *Proc Natl Acad Sci U S A*, 104: 2431-6.
Ji, D., and M. A. Wilson. 2007. 'Coordinated memory replay in the visual cortex and hippocampus during sleep', *Nat Neurosci*, 10: 100-7.
Jodo, E., and G. Aston-Jones. 1997. 'Activation of locus coeruleus by prefrontal cortex is mediated by excitatory amino acid inputs', *Brain Res*, 768: 327-32.
Johnson, R. D., P. L. Oliver, and K. E. Davies. 2008. 'SNARE proteins and schizophrenia: linking synaptic and neurodevelopmental hypotheses', *Acta Biochim Pol*, 55: 619-28.
Jolliffe, I. T. 2002. *Principal component analysis* (Springer: New York).
Jones, B. E., and A. C. Cuello. 1989. 'Afferents to the basal forebrain cholinergic cell area from pontomesencephalic--catecholamine, serotonin, and acetylcholine--neurons', *Neuroscience*, 31: 37-61.
Jones, B. E., and T. Z. Yang. 1985. 'The efferent projections from the reticular formation and the locus coeruleus studied by anterograde and retrograde axonal transport in the rat', *J Comp Neurol*, 242: 56-92.
Jones, M. W., and M. A. Wilson. 2005. 'Theta rhythms coordinate hippocampal-prefrontal interactions in a spatial memory task', *PLoS Biol*, 3: e402.
Jouvet, D., P. Vimont, F. Delorme, and M. Jouvet. 1964. '[Study of Selective Deprivation of the Paradoxal Sleep Phase in the Cat]', *C R Seances Soc Biol Fil*, 158: 756-9.
Kahana, M. J., R. Sekuler, J. B. Caplan, M. Kirschen, and J. R. Madsen. 1999. 'Human theta oscillations exhibit task dependence during virtual maze navigation', *Nature*, 399: 781-4.
Kanarek, R. B., A. V. Gerstein, R. P. Wildman, W. F. Mathes, and K. E. D'Anci. 1998. 'Chronic running-wheel activity decreases sensitivity to morphine-induced analgesia in male and female rats', *Pharmacol Biochem Behav*, 61: 19-27.
Kas, M. J., and D. M. Edgar. 1999. 'A nonphotic stimulus inverts the diurnal-nocturnal phase preference in Octodon degus', *J Neurosci*, 19: 328-33.
Kattler, H., D. J. Dijk, and A. A. Borbely. 1994. 'Effect of unilateral somatosensory stimulation prior to sleep on the sleep EEG in humans', *J Sleep Res*, 3: 159-64.
Kim, D., I. Song, S. Keum, T. Lee, M. J. Jeong, S. S. Kim, M. W. McEnery, and H. S. Shin. 2001. 'Lack of the burst firing of thalamocortical relay neurons and resistance to absence seizures in mice lacking alpha(1G) T-type Ca(2+) channels', *Neuron*, 31: 35-45.
Kleim, J. A., R. Bruneau, K. Calder, D. Pocock, P. M. VandenBerg, E. MacDonald, M. H. Monfils, R. J. Sutherland, and K. Nader. 2003. 'Functional organization of adult motor cortex is dependent upon continued protein synthesis', *Neuron*, 40: 167-76.
Kropff, E., J. E. Carmichael, M. B. Moser, and E. I. Moser. 2015. 'Speed cells in the medial entorhinal cortex', *Nature*, 523: 419-24.
Krueger, J. M. 2012. 'Translation of Brain Activity into Sleep', *Hirosaki Igaku*, 63: S1-S16.
Krueger, J. M., D. M. Rector, S. Roy, H. P. Van Dongen, G. Belenky, and J. Panksepp. 2008. 'Sleep as a fundamental property of neuronal assemblies', *Nat Rev Neurosci*, 9: 910-9.
Krueger, J. M., and G. Tononi. 2011. 'Local use-dependent sleep; synthesis of the new paradigm', *Curr Top Med Chem*, 11: 2490-2.
Kurtz, M. M., P. J. Moberg, R. C. Gur, and R. E. Gur. 2001. 'Approaches to cognitive remediation of neuropsychological deficits in schizophrenia: a review and meta-analysis', *Neuropsychol Rev*, 11: 197-210.
Lacy, R. T., J. C. Strickland, M. K. Brophy, M. A. Witte, and M. A. Smith. 2014. 'Exercise decreases speedball self-administration', *Life Sci*, 114: 86-92.

Lancel, M., H. van Riezen, and A. Glatt. 1992. 'Enhanced slow-wave activity within NREM sleep in the cortical and subcortical EEG of the cat after sleep deprivation', *Sleep*, 15: 102-18.
Lee, M. G., O. K. Hassani, A. Alonso, and B. E. Jones. 2005. 'Cholinergic basal forebrain neurons burst with theta during waking and paradoxical sleep', *J Neurosci*, 25: 4365-9.
Lee, M. G., O. K. Hassani, and B. E. Jones. 2005. 'Discharge of identified orexin/hypocretin neurons across the sleep-waking cycle', *J Neurosci*, 25: 6716-20.
Lee, S. H., and Y. Dan. 2012. 'Neuromodulation of brain states', *Neuron*, 76: 209-22.
Leemburg, S., V. V. Vyazovskiy, U. Olcese, C. L. Bassetti, G. Tononi, and C. Cirelli. 2010. 'Sleep homeostasis in the rat is preserved during chronic sleep restriction', *Proc Natl Acad Sci U S A*, 107: 15939-44.
Lemieux, M., J. Y. Chen, P. Lonjers, M. Bazhenov, and I. Timofeev. 2014. 'The impact of cortical deafferentation on the neocortical slow oscillation', *J Neurosci*, 34: 5689-703.
Lesku, J. A., N. C. Rattenborg, M. Valcu, A. L. Vyssotski, S. Kuhn, F. Kuemmeth, W. Heidrich, and B. Kempenaers. 2012. 'Adaptive Sleep Loss in Polygynous Pectoral Sandpipers', *Science*.
Lloyd, Stuart P. 1982. 'Least Squares Quantization in PCM', *IEEE Transactions on Information Theory*, 28: 129-37.
Lorincz, M. L., D. Gunner, Y. Bao, W. M. Connelly, J. T. Isaac, S. W. Hughes, and V. Crunelli. 2015. 'A distinct class of slow (~0.2-2 Hz) intrinsically bursting layer 5 pyramidal neurons determines UP/DOWN state dynamics in the neocortex', *J Neurosci*, 35: 5442-58.
Lu, J., D. Sherman, M. Devor, and C. B. Saper. 2006. 'A putative flip-flop switch for control of REM sleep', *Nature*, 441: 589-94.
Lukatch, H. S., and M. B. MacIver. 1997. 'Physiology, pharmacology, and topography of cholinergic neocortical oscillations in vitro', *J Neurophysiol*, 77: 2427-45.
Mackay, A. V., L. L. Iversen, M. Rossor, E. Spokes, E. Bird, A. Arregui, I. Creese, and S. H. Synder. 1982. 'Increased brain dopamine and dopamine receptors in schizophrenia', *Arch Gen Psychiatry*, 39: 991-7.
Magill, P. J., A. Pogosyan, A. Sharott, J. Csicsvari, J. P. Bolam, and P. Brown. 2006. 'Changes in functional connectivity within the rat striatopallidal axis during global brain activation in vivo', *J Neurosci*, 26: 6318-29.
Magnin, M., M. Rey, H. Bastuji, P. Guillemant, F. Mauguiere, and L. Garcia-Larrea. 2010. 'Thalamic deactivation at sleep onset precedes that of the cerebral cortex in humans', *Proc Natl Acad Sci U S A*, 107: 3829-33.
Mann, E. O., M. M. Kohl, and O. Paulsen. 2009. 'Distinct roles of GABA(A) and GABA(B) receptors in balancing and terminating persistent cortical activity', *J Neurosci*, 29: 7513-18.
Marder, E., and D. Bucher. 2001. 'Central pattern generators and the control of rhythmic movements', *Curr Biol*, 11: R986-96.
Maret, S., U. Faraguna, A. B. Nelson, C. Cirelli, and G. Tononi. 2011. 'Sleep and waking modulate spine turnover in the adolescent mouse cortex', *Nat Neurosci*, 14: 1418-20.
Marquez-Ruiz, J., and M. Escudero. 2010. 'Eye movements and abducens motoneuron behavior after cholinergic activation of the nucleus reticularis pontis caudalis', *Sleep*, 33: 1517-27.
Marshall, L., H. Helgadottir, M. Molle, and J. Born. 2006. 'Boosting slow oscillations during sleep potentiates memory', *Nature*, 444: 610-3.
Massimini, M., R. Huber, F. Ferrarelli, S. Hill, and G. Tononi. 2004. 'The sleep slow oscillation as a traveling wave', *J Neurosci*, 24: 6862-70.
McCarley, R. W., and J. A. Hobson. 1975. 'Neuronal excitability modulation over the sleep cycle: a structural and mathematical model', *Science*, 189: 58-60.
McCormick, D. A., and H. C. Pape. 1990. 'Properties of a hyperpolarization-activated cation current and its role in rhythmic oscillation in thalamic relay neurones', *J Physiol*, 431: 291-318.
McGinley, M. J., S. V. David, and D. A. McCormick. 2015. 'Cortical Membrane Potential Signature of Optimal States for Sensory Signal Detection', *Neuron*, 87: 179-92.

Meeusen, R., and K. De Meirleir. 1995. 'Exercise and brain neurotransmission', *Sports Med*, 20: 160-88.
Meijer, J. H., and Y. Robbers. 2014. 'Wheel running in the wild', *Proc Biol Sci*, 281.
Meijer, J. H., J. Schaap, K. Watanabe, and H. Albus. 1997. 'Multiunit activity recordings in the suprachiasmatic nuclei: in vivo versus in vitro models', *Brain Res*, 753: 322-7.
Metherate, R., C. L. Cox, and J. H. Ashe. 1992. 'Cellular bases of neocortical activation: modulation of neural oscillations by the nucleus basalis and endogenous acetylcholine', *J Neurosci*, 12: 4701-11.
Mignot, E. 2008. 'Why we sleep: the temporal organization of recovery', *PLoS Biol*, 6: e106.
Mileykovskiy, B. Y., L. I. Kiyashchenko, and J. M. Siegel. 2005. 'Behavioral correlates of activity in identified hypocretin/orexin neurons', *Neuron*, 46: 787-98.
Mistlberger, R., B. Bergmann, and A. Rechtschaffen. 1987. 'Period-amplitude analysis of rat electroencephalogram: effects of sleep deprivation and exercise', *Sleep*, 10: 508-22.
Mistlberger, R. E. 2005. 'Circadian regulation of sleep in mammals: role of the suprachiasmatic nucleus', *Brain Res Brain Res Rev*, 49: 429-54.
Mitler, M. M., and W. C. Dement. 1974. 'Cataplectic-like behavior in cats after micro-injections of carbachol in pontine reticular formation', *Brain Res*, 68: 335-43.
Montgomery, Sean M., Martha I. Betancur, and György Buzsáki. 2009. 'Behavior-Dependent Coordination of Multiple Theta Dipoles in the Hippocampus', *The Journal of Neuroscience*, 29: 1381-94.
Monti, J. M. 1993. 'Involvement of histamine in the control of the waking state', *Life Sci*, 53: 1331-8.
Morgan, C. J., and H. V. Curran. 2006. 'Acute and chronic effects of ketamine upon human memory: a review', *Psychopharmacology (Berl)*, 188: 408-24.
Moruzzi, G., and H. W. Magoun. 1949. 'Brain stem reticular formation and activation of the EEG', *Electroencephalogr Clin Neurophysiol*, 1: 455-73.
Murphy, M., M. A. Bruno, B. A. Riedner, P. Boveroux, Q. Noirhomme, E. C. Landsness, J. F. Brichant, C. Phillips, M. Massimini, S. Laureys, G. Tononi, and M. Boly. 2011. 'Propofol anesthesia and sleep: a high-density EEG study', *Sleep*, 34: 283-91A.
Nakamura, K., I. Inoue, S. Takahashi, T. Komoda, and S. Katayama. 2008. 'Cryptochrome and Period Proteins Are Regulated by the CLOCK/BMAL1 Gene: Crosstalk between the PPARs/RXRalpha-Regulated and CLOCK/BMAL1-Regulated Systems', *PPAR Res*, 2008: 348610.
Neske, Garrett T. 2016. 'The Slow Oscillation in Cortical and Thalamic Networks: Mechanisms and Functions', *Frontiers in Neural Circuits*, 9.
Niell, C. M., and M. P. Stryker. 2010. 'Modulation of visual responses by behavioral state in mouse visual cortex', *Neuron*, 65: 472-9.
Nir, Y., R. J. Staba, T. Andrillon, V. V. Vyazovskiy, C. Cirelli, I. Fried, and G. Tononi. 2011. 'Regional slow waves and spindles in human sleep', *Neuron*, 70: 153-69.
Okun, M., N. Steinmetz, L. Cossell, M. F. Iacaruso, H. Ko, P. Bartho, T. Moore, S. B. Hofer, T. D. Mrsic-Flogel, M. Carandini, and K. D. Harris. 2015. 'Diverse coupling of neurons to populations in sensory cortex', *Nature*, 521: 511-15.
Oliver, P. L., and K. E. Davies. 2009. 'Interaction between environmental and genetic factors modulates schizophrenic endophenotypes in the Snap-25 mouse mutant blind-drunk', *Hum Mol Genet*, 18: 4576-89.
Oliver, P. L., M. V. Sobczyk, E. S. Maywood, B. Edwards, S. Lee, A. Livieratos, H. Oster, R. Butler, S. I. Godinho, K. Wulff, S. N. Peirson, S. P. Fisher, J. E. Chesham, J. W. Smith, M. H. Hastings, K. E. Davies, and R. G. Foster. 2012. 'Disrupted circadian rhythms in a mouse model of schizophrenia', *Curr Biol*, 22: 314-9.

Osorio, Ivan, Mark G. Frei, Andres M. Lozano, and Richard Wennberg. 2015. 'Subcortical (thalamic) automated seizure detection: A new option for contingent therapy delivery', *Epilepsia*, 56: e156-e60.
Palchykova, S., R. Winsky-Sommerer, P. Meerlo, R. Durr, and I. Tobler. 2006. 'Sleep deprivation impairs object recognition in mice', *Neurobiol Learn Mem*, 85: 263-71.
Pearce, Patrice S., Daniel Friedman, John J. LaFrancois, Sloka S. Iyengar, André A. Fenton, Neil J. MacLusky, and Helen E. Scharfman. 2014. 'Spike–wave discharges in adult Sprague–Dawley rats and their implications for animal models of temporal lobe epilepsy', *Epilepsy & Behavior*, 32: 121-31.
Peever, J. 2011. 'Control of motoneuron function and muscle tone during REM sleep, REM sleep behavior disorder and cataplexy/narcolepsy', *Arch Ital Biol*, 149: 454-66.
Petsche, H., and C. Stumpf. 1962. '[The origin of theta-rhytm in the rabbit hippocampus]', *Wien Klin Wochenschr*, 74: 696-700.
Polack, P. O., J. Friedman, and P. Golshani. 2013. 'Cellular mechanisms of brain state-dependent gain modulation in visual cortex', *Nat Neurosci*, 16: 1331-9.
Pomarol-Clotet, E., T. M. Oh, K. R. Laws, and P. J. McKenna. 2008. 'Semantic priming in schizophrenia: systematic review and meta-analysis', *Br J Psychiatry*, 192: 92-7.
Power, A., A. T. Hughes, R. E. Samuels, and H. D. Piggins. 2010. 'Rhythm-promoting actions of exercise in mice with deficient neuropeptide signaling', *J Biol Rhythms*, 25: 235-46.
Pritchett, D., A. Jagannath, L. A. Brown, S. K. Tam, S. Hasan, S. Gatti, P. J. Harrison, D. M. Bannerman, R. G. Foster, and S. N. Peirson. 2015. 'Deletion of Metabotropic Glutamate Receptors 2 and 3 (mGlu2 & mGlu3) in Mice Disrupts Sleep and Wheel-Running Activity, and Increases the Sensitivity of the Circadian System to Light', *PLoS One*, 10: e0125523.
Qiu, M. H., M. C. Chen, and J. Lu. 2015. 'Cortical neuronal activity does not regulate sleep homeostasis', *Neuroscience*, 297: 211-8.
Ramos-Miguel, A., C. L. Beasley, A. J. Dwork, J. J. Mann, G. Rosoklija, A. M. Barr, and W. G. Honer. 2015a. 'Increased SNARE Protein-Protein Interactions in Orbitofrontal and Anterior Cingulate Cortices in Schizophrenia', *Biol Psychiatry*, 78: 361-73.
Ramos-Miguel, Alfredo, Clare L. Beasley, Andrew J. Dwork, J. John Mann, Gorazd Rosoklija, Alasdair M. Barr, and William G. Honer. 2015b. 'Increased SNARE Protein-Protein Interactions in Orbitofrontal and Anterior Cingulate Cortices in Schizophrenia', *Biological Psychiatry*, 78: 361-73.
Rasch, B., and J. Born. 2013. 'About Sleep's Role in Memory', *Physiol Rev*, 93: 681-766.
Rechtschaffen, A., M. A. Gilliland, B. M. Bergmann, and J. B. Winter. 1983. 'Physiological correlates of prolonged sleep deprivation in rats', *Science*, 221: 182-4.
Reim, K., M. Mansour, F. Varoqueaux, H. T. McMahon, T. C. Sudhof, N. Brose, and C. Rosenmund. 2001. 'Complexins regulate a late step in Ca2+-dependent neurotransmitter release', *Cell*, 104: 71-81.
Rhodes, J. S., T. Garland, Jr., and S. C. Gammie. 2003. 'Patterns of brain activity associated with variation in voluntary wheel-running behavior', *Behav Neurosci*, 117: 1243-56.
Riedner, B. A., V. V. Vyazovskiy, R. Huber, M. Massimini, S. Esser, M. Murphy, and G. Tononi. 2007. 'Sleep homeostasis and cortical synchronization: III. A high-density EEG study of sleep slow waves in humans', *Sleep*, 30: 1643-57.
Ros, H., R. N. Sachdev, Y. Yu, N. Sestan, and D. A. McCormick. 2009. 'Neocortical networks entrain neuronal circuits in cerebellar cortex', *J Neurosci*, 29: 10309-20.
Ruderfer, D. M., A. H. Fanous, S. Ripke, A. McQuillin, R. L. Amdur, Consortium Schizophrenia Working Group of the Psychiatric Genomics, Consortium Bipolar Disorder Working Group of the Psychiatric Genomics, Consortium Cross-Disorder Working Group of the Psychiatric Genomics, P. V. Gejman, M. C. O'Donovan, O. A. Andreassen, S. Djurovic, C. M. Hultman, J. R. Kelsoe, S. Jamain, M. Landen, M. Leboyer, V. Nimgaonkar, J. Nurnberger, J. W. Smoller, N. Craddock, A. Corvin, P. F. Sullivan, P. Holmans, P. Sklar, and K. S. Kendler.

2014. 'Polygenic dissection of diagnosis and clinical dimensions of bipolar disorder and schizophrenia', *Mol Psychiatry*, 19: 1017-24.
Rudolph, M., M. Pospischil, I. Timofeev, and A. Destexhe. 2007. 'Inhibition determines membrane potential dynamics and controls action potential generation in awake and sleeping cat cortex', *J Neurosci*, 27: 5280-90.
Rusterholz, T., and P. Achermann. 2011. 'Topographical aspects in the dynamics of sleep homeostasis in young men: individual patterns', *BMC Neurosci*, 12: 84.
Saleem, A. B., A. Ayaz, K. J. Jeffery, K. D. Harris, and M. Carandini. 2013. 'Integration of visual motion and locomotion in mouse visual cortex', *Nat Neurosci*, 16: 1864-9.
Sanchez-Vives, M. V., and M. Mattia. 2014. 'Slow wave activity as the default mode of the cerebral cortex', *Arch Ital Biol*, 152: 147-55.
Sanchez-Vives, M. V., and D. A. McCormick. 2000. 'Cellular and network mechanisms of rhythmic recurrent activity in neocortex', *Nat Neurosci*, 3: 1027-34.
Sanchez-Vives, M. V., L. G. Nowak, and D. A. McCormick. 2000. 'Cellular mechanisms of long-lasting adaptation in visual cortical neurons in vitro', *J Neurosci*, 20: 4286-99.
Saper, C. B., P. M. Fuller, N. P. Pedersen, J. Lu, and T. E. Scammell. 2010. 'Sleep state switching', *Neuron*, 68: 1023-42.
Saper, C. B., T. E. Scammell, and J. Lu. 2005. 'Hypothalamic regulation of sleep and circadian rhythms', *Nature*, 437: 1257-63.
Sarasso, S., P. Proserpio, A. Pigorini, F. Moroni, M. Ferrara, L. De Gennaro, F. De Carli, G. Lo Russo, M. Massimini, and L. Nobili. 2014. 'Hippocampal sleep spindles preceding neocortical sleep onset in humans', *Neuroimage*, 86: 425-32.
Schoch, S., F. Deak, A. Konigstorfer, M. Mozhayeva, Y. Sara, T. C. Sudhof, and E. T. Kavalali. 2001. 'SNARE function analyzed in synaptobrevin/VAMP knockout mice', *Science*, 294: 1117-22.
Schroeder, A. M., D. Truong, D. H. Loh, M. C. Jordan, K. P. Roos, and C. S. Colwell. 2012. 'Voluntary scheduled exercise alters diurnal rhythms of behaviour, physiology and gene expression in wild-type and vasoactive intestinal peptide-deficient mice', *J Physiol*, 590: 6213-26.
Schwierin, B., P. Achermann, T. Deboer, A. Oleksenko, A. A. Borbely, and I. Tobler. 1999. 'Regional differences in the dynamics of the cortical EEG in the rat after sleep deprivation', *Clin Neurophysiol*, 110: 869-75.
Sellers, K. K., D. V. Bennett, A. Hutt, J. H. Williams, and F. Frohlich. 2015. 'Awake vs. anesthetized: layer-specific sensory processing in visual cortex and functional connectivity between cortical areas', *J Neurophysiol*, 113: 3798-815.
Shen, X. M., D. Selcen, J. Brengman, and A. G. Engel. 2014. 'Mutant SNAP25B causes myasthenia, cortical hyperexcitability, ataxia, and intellectual disability', *Neurology*, 83: 2247-55.
Sherin, J. E., P. J. Shiromani, R. W. McCarley, and C. B. Saper. 1996. 'Activation of ventrolateral preoptic neurons during sleep', *Science*, 271: 216-9.
Shu, Y., A. Hasenstaub, and D. A. McCormick. 2003. 'Turning on and off recurrent balanced cortical activity', *Nature*, 423: 288-93.
Siapas, A. G., E. V. Lubenov, and M. A. Wilson. 2005. 'Prefrontal phase locking to hippocampal theta oscillations', *Neuron*, 46: 141-51.
Siclari, F., G. Bernardi, B. A. Riedner, J. J. LaRocque, R. M. Benca, and G. Tononi. 2014. 'Two distinct synchronization processes in the transition to sleep: a high-density electroencephalographic study', *Sleep*, 37: 1621-37.
Siegel, J. M. 2008. 'Do all animals sleep?', *Trends Neurosci*, 31: 208-13.
Silva, L. R., Y. Amitai, and B. W. Connors. 1991. 'Intrinsic oscillations of neocortex generated by layer 5 pyramidal neurons', *Science*, 251: 432-5.
Sirota, A., and G. Buzsaki. 2005. 'Interaction between neocortical and hippocampal networks via slow oscillations', *Thalamus Relat Syst*, 3: 245-59.

Sirota, A., S. Montgomery, S. Fujisawa, Y. Isomura, M. Zugaro, and G. Buzsaki. 2008. 'Entrainment of neocortical neurons and gamma oscillations by the hippocampal theta rhythm', *Neuron*, 60: 683-97.

Slezia, A., B. Hangya, I. Ulbert, and L. Acsady. 2011. 'Phase advancement and nucleus-specific timing of thalamocortical activity during slow cortical oscillation', *J Neurosci*, 31: 607-17.

Sokolov, B. P. 1998. 'Expression of NMDAR1, GluR1, GluR7, and KA1 glutamate receptor mRNAs is decreased in frontal cortex of "neuroleptic-free" schizophrenics: evidence on reversible up-regulation by typical neuroleptics', *J Neurochem*, 71: 2454-64.

Sørensen, Jakob B., Gábor Nagy, Frederique Varoqueaux, Ralf B. Nehring, Nils Brose, Michael C. Wilson, and Erwin Neher. 2003. 'Differential Control of the Releasable Vesicle Pools by SNAP-25 Splice Variants and SNAP-23', *Cell*, 114: 75-86.

Steriade, M., F. Amzica, and A. Nunez. 1993. 'Cholinergic and noradrenergic modulation of the slow (approximately 0.3 Hz) oscillation in neocortical cells', *J Neurophysiol*, 70: 1385-400.

Steriade, M., and D. Contreras. 1998. 'Spike-wave complexes and fast components of cortically generated seizures. I. Role of neocortex and thalamus', *J Neurophysiol*, 80: 1439-55.

Steriade, M., D. Contreras, and F. Amzica. 1994. 'Synchronized sleep oscillations and their paroxysmal developments', *Trends Neurosci*, 17: 199-208.

Steriade, M., S. Datta, D. Pare, G. Oakson, and R. C. Curro Dossi. 1990. 'Neuronal activities in brain-stem cholinergic nuclei related to tonic activation processes in thalamocortical systems', *J Neurosci*, 10: 2541-59.

Steriade, M., A. Nunez, and F. Amzica. 1993a. 'Intracellular analysis of relations between the slow (< 1 Hz) neocortical oscillation and other sleep rhythms of the electroencephalogram', *J Neurosci*, 13: 3266-83.

———. 1993b. 'A novel slow (< 1 Hz) oscillation of neocortical neurons in vivo: depolarizing and hyperpolarizing components', *J Neurosci*, 13: 3252-65.

Steriade, M., D. Pare, A. Parent, and Y. Smith. 1988. 'Projections of cholinergic and non-cholinergic neurons of the brainstem core to relay and associational thalamic nuclei in the cat and macaque monkey', *Neuroscience*, 25: 47-67.

Steriade, M., I. Timofeev, and F. Grenier. 2001. 'Natural waking and sleep states: a view from inside neocortical neurons', *J Neurophysiol*, 85: 1969-85.

Sudhof, T. C. 2013. 'Neurotransmitter release: the last millisecond in the life of a synaptic vesicle', *Neuron*, 80: 675-90.

Sudhof, T. C., and J. E. Rothman. 2009. 'Membrane fusion: grappling with SNARE and SM proteins', *Science*, 323: 474-7.

Sutton, R. Bryan, Dirk Fasshauer, Reinhard Jahn, and Axel T. Brunger. 1998. 'Crystal structure of a SNARE complex involved in synaptic exocytosis at 2.4 Å resolution', *Nature*, 395: 347.

Takahashi, J. S., H. K. Hong, C. H. Ko, and E. L. McDearmon. 2008. 'The genetics of mammalian circadian order and disorder: implications for physiology and disease', *Nat Rev Genet*, 9: 764-75.

Thierry, A. M., Y. Gioanni, E. Degenetais, and J. Glowinski. 2000. 'Hippocampo-prefrontal cortex pathway: anatomical and electrophysiological characteristics', *Hippocampus*, 10: 411-9.

Thompson, P. M., S. Egbufoama, and M. P. Vawter. 2003. 'SNAP-25 reduction in the hippocampus of patients with schizophrenia', *Prog Neuropsychopharmacol Biol Psychiatry*, 27: 411-7.

Thomson, A. M., and J. Deuchars. 1994. 'Temporal and spatial properties of local circuits in neocortex', *Trends Neurosci*, 17: 119-26.

Timofeev, I. 2013. 'Local origin of slow EEG waves during sleep', *Zh Vyssh Nerv Deiat Im I P Pavlova*, 63: 105-12.

Tobler, I. 2005. 'Phylogeny of sleep regulation.' in, *Principles and Practice of Sleep Medicine* (W. B. Saunders Philadelphia).

Tobler, I., and A. A. Borbely. 1986. 'Sleep EEG in the rat as a function of prior waking', *Electroencephalogr Clin Neurophysiol*, 64: 74-6.

Tononi, G., and C. Cirelli. 2006. 'Sleep function and synaptic homeostasis', *Sleep Med Rev*, 10: 49-62.
———. 2014. 'Sleep and the price of plasticity: from synaptic and cellular homeostasis to memory consolidation and integration', *Neuron*, 81: 12-34.
Trachsel, L., I. Tobler, and A. A. Borbely. 1988. 'Electroencephalogram analysis of non-rapid eye movement sleep in rats', *Am J Physiol*, 255: R27-37.
———. 1989. 'Effect of sleep deprivation on EEG slow wave activity within non-REM sleep episodes in the rat', *Electroencephalogr Clin Neurophysiol*, 73: 167-71.
Turrigiano, G. G. 1999. 'Homeostatic plasticity in neuronal networks: the more things change, the more they stay the same', *Trends Neurosci*, 22: 221-7.
Ujfalussy, B., and T. Kiss. 2006. 'How do glutamatergic and GABAergic cells contribute to synchronization in the medial septum?', *J Comput Neurosci*, 21: 343-57.
Vacic, V., S. McCarthy, D. Malhotra, F. Murray, H. H. Chou, A. Peoples, V. Makarov, S. Yoon, A. Bhandari, R. Corominas, L. M. Iakoucheva, O. Krastoshevsky, V. Krause, V. Larach-Walters, D. K. Welsh, D. Craig, J. R. Kelsoe, E. S. Gershon, S. M. Leal, M. Dell Aquila, D. W. Morris, M. Gill, A. Corvin, P. A. Insel, J. McClellan, M. C. King, M. Karayiorgou, D. L. Levy, L. E. DeLisi, and J. Sebat. 2011. 'Duplications of the neuropeptide receptor gene VIPR2 confer significant risk for schizophrenia', *Nature*, 471: 499-503.
van der Borght, K., F. Ferrari, K. Klauke, V. Roman, R. Havekes, A. Sgoifo, E. A. van der Zee, and P. Meerlo. 2006. 'Hippocampal cell proliferation across the day: increase by running wheel activity, but no effect of sleep and wakefulness', *Behav Brain Res*, 167: 36-41.
Van Dort, C. J., D. P. Zachs, J. D. Kenny, S. Zheng, R. R. Goldblum, N. A. Gelwan, D. M. Ramos, M. A. Nolan, K. Wang, F. J. Weng, Y. Lin, M. A. Wilson, and E. N. Brown. 2015. 'Optogenetic activation of cholinergic neurons in the PPT or LDT induces REM sleep', *Proc Natl Acad Sci U S A*, 112: 584-9.
Vienne, J., B. Bettler, P. Franken, and M. Tafti. 2010. 'Differential effects of GABAB receptor subtypes, {gamma}-hydroxybutyric Acid, and Baclofen on EEG activity and sleep regulation', *J Neurosci*, 30: 14194-204.
Vinck, M., R. Batista-Brito, U. Knoblich, and J. A. Cardin. 2015. 'Arousal and Locomotion Make Distinct Contributions to Cortical Activity Patterns and Visual Encoding', *Neuron*.
Vyazovskiy, V., A. A. Borbely, and I. Tobler. 2000. 'Unilateral vibrissae stimulation during waking induces interhemispheric EEG asymmetry during subsequent sleep in the rat', *J Sleep Res*, 9: 367-71.
Vyazovskiy, V. V., P. Achermann, A. A. Borbely, and I. Tobler. 2004. 'The dynamics of spindles and EEG slow-wave activity in NREM sleep in mice', *Arch Ital Biol*, 142: 511-23.
Vyazovskiy, V. V., A. A. Borbely, and I. Tobler. 2002. 'Interhemispheric sleep EEG asymmetry in the rat is enhanced by sleep deprivation', *J Neurophysiol*, 88: 2280-6.
Vyazovskiy, V. V., C. Cirelli, M. Pfister-Genskow, U. Faraguna, and G. Tononi. 2008. 'Molecular and electrophysiological evidence for net synaptic potentiation in wake and depression in sleep', *Nat Neurosci*, 11: 200-8.
Vyazovskiy, V. V., T. Deboer, B. Rudy, D. Lau, A. A. Borbely, and I. Tobler. 2002. 'Sleep EEG in mice that are deficient in the potassium channel subunit K.v.3.2', *Brain Res*, 947: 204-11.
Vyazovskiy, V. V., and A. Delogu. 2014. 'NREM and REM Sleep: Complementary Roles in Recovery after Wakefulness', *Neuroscientist*, 20: 203-19.
Vyazovskiy, V. V., and K. D. Harris. 2013. 'Sleep and the single neuron: the role of global slow oscillations in individual cell rest', *Nat Rev Neurosci*, 14: 443-51.
Vyazovskiy, V. V., U. Olcese, C. Cirelli, and G. Tononi. 2013. 'Prolonged wakefulness alters neuronal responsiveness to local electrical stimulation of the neocortex in awake rats', *J Sleep Res*, 22: 264-71.
Vyazovskiy, V. V., U. Olcese, E. C. Hanlon, Y. Nir, C. Cirelli, and G. Tononi. 2011. 'Local sleep in awake rats', *Nature*, 472: 443-7.

Vyazovskiy, V. V., U. Olcese, Y. M. Lazimy, U. Faraguna, S. K. Esser, J. C. Williams, C. Cirelli, and G. Tononi. 2009. 'Cortical firing and sleep homeostasis', *Neuron*, 63: 865-78.

Vyazovskiy, V. V., S. Palchykova, P. Achermann, I. Tobler, and T. Deboer. 2017. 'Different Effects of Sleep Deprivation and Torpor on EEG Slow-Wave Characteristics in Djungarian Hamsters', *Cereb Cortex*, 27: 950-61.

Vyazovskiy, V. V., B. A. Riedner, C. Cirelli, and G. Tononi. 2007. 'Sleep homeostasis and cortical synchronization: II. A local field potential study of sleep slow waves in the rat', *Sleep*, 30: 1631-42.

Vyazovskiy, V. V., G. Ruijgrok, T. Deboer, and I. Tobler. 2006. 'Running wheel accessibility affects the regional electroencephalogram during sleep in mice', *Cereb Cortex*, 16: 328-36.

Vyazovskiy, V. V., and I. Tobler. 2005. 'Theta activity in the waking EEG is a marker of sleep propensity in the rat', *Brain Res*, 1050: 64-71.

———. 2008. 'Handedness leads to interhemispheric EEG asymmetry during sleep in the rat', *J Neurophysiol*, 99: 969-75.

———. 2012. 'The temporal structure of behaviour and sleep homeostasis', *PLoS One*, 7: e50677.

Vyazovskiy, V. V., I. Tobler, and R. Winsky-Sommerer. 2007. 'Alteration of behavior in mice by muscimol is associated with regional electroencephalogram synchronization', *Neuroscience*, 147: 833-41.

Vyazovskiy, V. V., E. Welker, J. M. Fritschy, and I. Tobler. 2004. 'Regional pattern of metabolic activation is reflected in the sleep EEG after sleep deprivation combined with unilateral whisker stimulation in mice', *Eur J Neurosci*, 20: 1363-70.

Walinder, J., A. Skott, A. Carlsson, and B. E. Roos. 1976. 'Potentiation by metyrosine of thioridazine effects in chronic schizophrenics. A long-term trial using double-blind crossover technique', *Arch Gen Psychiatry*, 33: 501-5.

Washbourne, Philip, Peter M. Thompson, Mario Carta, Edmar T. Costa, James R. Mathews, Guillermina Lopez-Benditó, Zoltán Molnár, Mark W. Becher, C. Fernando Valenzuela, L. Donald Partridge, and Michael C. Wilson. 2001. 'Genetic ablation of the t-SNARE SNAP-25 distinguishes mechanisms of neuroexocytosis', *Nature Neuroscience*, 5: 19.

Watanabe, S., S. Yamamori, S. Otsuka, M. Saito, E. Suzuki, M. Kataoka, H. Miyaoka, and M. Takahashi. 2015. 'Epileptogenesis and epileptic maturation in phosphorylation site-specific SNAP-25 mutant mice', *Epilepsy Res*, 115: 30-44.

Welch, P. 1967. 'The use of fast Fourier transform for the estimation of power spectra: A method based on time averaging over short, modified periodograms', *IEEE Transactions on Audio and Electroacoustics*, 15: 70-73.

Werth, E., P. Achermann, and A. A. Borbely. 1996. 'Brain topography of the human sleep EEG: antero-posterior shifts of spectral power', *Neuroreport*, 8: 123-7.

Whiteford, H. A., L. Degenhardt, J. Rehm, A. J. Baxter, A. J. Ferrari, H. E. Erskine, F. J. Charlson, R. E. Norman, A. D. Flaxman, N. Johns, R. Burstein, C. J. Murray, and T. Vos. 2013. 'Global burden of disease attributable to mental and substance use disorders: findings from the Global Burden of Disease Study 2010', *Lancet*, 382: 1575-86.

Wieser, H. G. 1991. 'Temporal lobe epilepsy, sleep and arousal: stereo-EEG findings', *Epilepsy Res Suppl*, 2: 97-119.

Wright, K. P., Jr., P. Badia, and A. Wauquier. 1995. 'Topographical and temporal patterns of brain activity during the transition from wakefulness to sleep', *Sleep*, 18: 880-9.

Wulff, K., D. J. Dijk, B. Middleton, R. G. Foster, and E. M. Joyce. 2012. 'Sleep and circadian rhythm disruption in schizophrenia', *Br J Psychiatry*, 200: 308-16.

Wulff, K., S. Gatti, J. G. Wettstein, and R. G. Foster. 2010. 'Sleep and circadian rhythm disruption in psychiatric and neurodegenerative disease', *Nat Rev Neurosci*, 11: 589-99.

Wulff, K., K. Porcheret, E. Cussans, and R. G. Foster. 2009. 'Sleep and circadian rhythm disturbances: multiple genes and multiple phenotypes', *Curr Opin Genet Dev*, 19: 237-46.

Xu, J., F. Luo, Z. Zhang, L. Xue, X. S. Wu, H. C. Chiang, W. Shin, and L. G. Wu. 2013. 'SNARE proteins synaptobrevin, SNAP-25, and syntaxin are involved in rapid and slow endocytosis at synapses', *Cell Rep*, 3: 1414-21.

Yamazaki, S., M. C. Kerbeshian, C. G. Hocker, G. D. Block, and M. Menaker. 1998. 'Rhythmic properties of the hamster suprachiasmatic nucleus in vivo', *J Neurosci*, 18: 10709-23.

Yang, K., C. H. Trepanier, H. Li, M. A. Beazely, E. A. Lerner, M. F. Jackson, and J. F. MacDonald. 2009. 'Vasoactive intestinal peptide acts via multiple signal pathways to regulate hippocampal NMDA receptors and synaptic transmission', *Hippocampus*, 19: 779-89.

Young, C. E., K. Arima, J. Xie, L. Hu, T. G. Beach, P. Falkai, and W. G. Honer. 1998. 'SNAP-25 deficit and hippocampal connectivity in schizophrenia', *Cereb Cortex*, 8: 261-8.

Zaborszky, L., K. Pang, J. Somogyi, Z. Nadasdy, and I. Kallo. 1999. 'The basal forebrain corticopetal system revisited', *Ann N Y Acad Sci*, 877: 339-67.

Zaborszky, Laszlo, Attila Csordas, Kevin Mosca, Joseph Kim, Matthew R. Gielow, Csaba Vadasz, and Zoltan Nadasdy. 2015. 'Neurons in the Basal Forebrain Project to the Cortex in a Complex Topographic Organization that Reflects Corticocortical Connectivity Patterns: An Experimental Study Based on Retrograde Tracing and 3D Reconstruction', *Cerebral Cortex*, 25: 118-37.

Zagha, E., A. E. Casale, R. N. Sachdev, M. J. McGinley, and D. A. McCormick. 2013. 'Motor cortex feedback influences sensory processing by modulating network state', *Neuron*, 79: 567-78.

Zagha, E., and D. A. McCormick. 2014. 'Neural control of brain state', *Curr Opin Neurobiol*, 29: 178-86.

Zhang, H., S. Zhu, Y. Zhu, J. Chen, G. Zhang, and H. Chang. 2011. 'An association study between SNAP-25 gene and attention-deficit hyperactivity disorder', *Eur J Paediatr Neurol*, 15: 48-52.

Zlebnik, N. E., V. L. Hedges, M. E. Carroll, and R. L. Meisel. 2014. 'Chronic wheel running affects cocaine-induced c-Fos expression in brain reward areas in rats', *Behav Brain Res*, 261: 71-8.